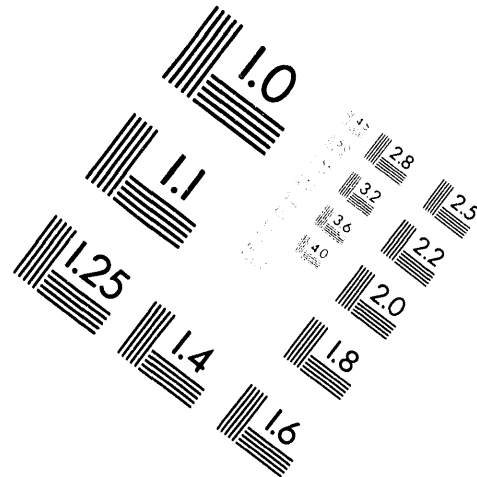
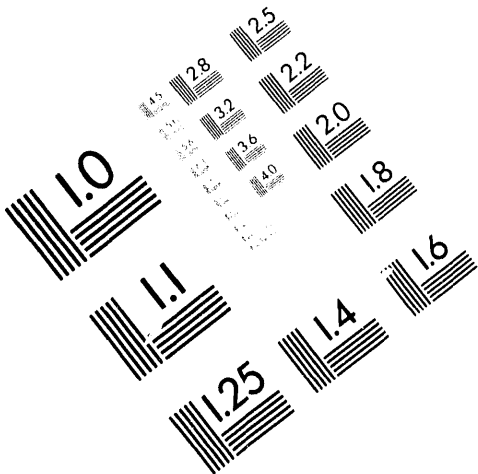




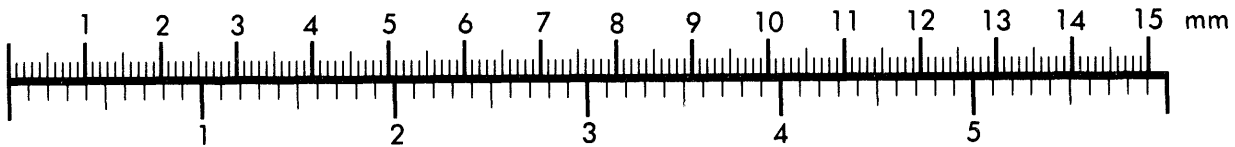
**AIM**

**Association for Information and Image Management**

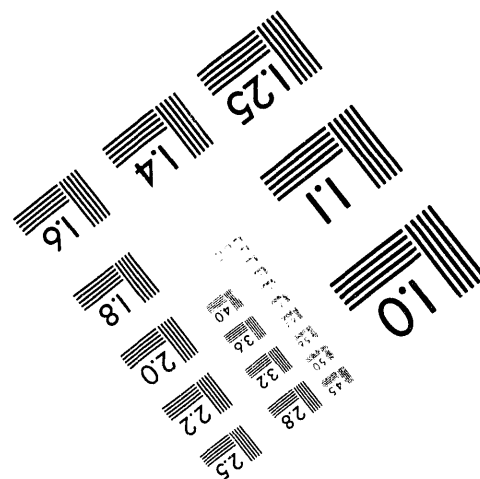
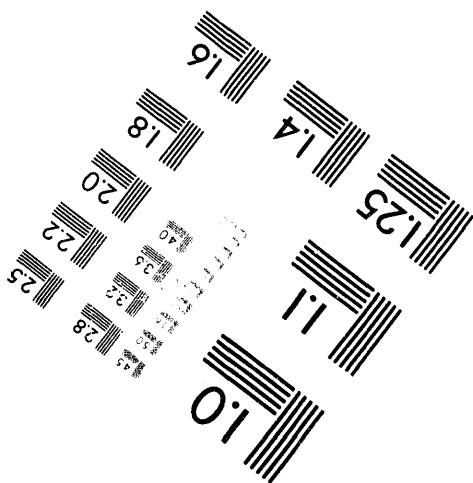
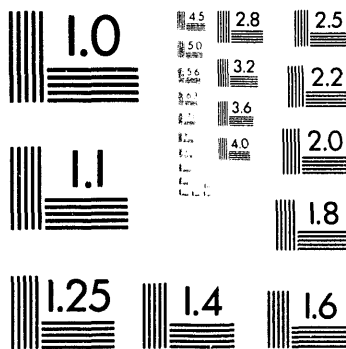
1100 Wayne Avenue, Suite 1100  
Silver Spring, Maryland 20910  
301/587-8202



Centimeter



Inches



MANUFACTURED TO AIM STANDARDS  
BY APPLIED IMAGE, INC.

**1 of 2**

GA-A21645  
UC-420

**DIII-D RESEARCH OPERATIONS**  
**ANNUAL REPORT TO THE**  
**U.S. DEPARTMENT OF ENERGY**

**OCTOBER 1, 1992 THROUGH SEPTEMBER 30, 1993**

by  
**PROJECT STAFF**  
**R.J. LA HAYE, Editor**

Work supported by  
U.S. Department of Energy  
under Contract Nos. DE-AC03-89ER51114  
W-7405-ENG-48 and DE-AC05-84OR21400

**GENERAL ATOMICS PROJECT 3466, 3467, 3470, 3473**  
**DATE PUBLISHED: MAY 1994**

**MASTER**  
DISTRIBUTION OF THIS DOCUMENT IS UNLIMITED *zp*



## CONTENTS

1.	DIII-D PROGRAM OVERVIEW .....	1-1
1.1.	Introduction .....	1-1
1.2.	Highlights of the FY93 DIII-D Research Program .....	1-4
1.2.1.	Divertor Radiation by D <sub>2</sub> or Ne Injection .....	1-6
1.2.2.	Divertor Cryopumping and Particle Control .....	1-7
1.2.3.	Helium Exhaust on DIII-D Using the Cryopump .....	1-8
1.2.4.	Improved Understanding of VH-Mode .....	1-8
2.	DIVERTOR AND BOUNDARY RESEARCH PROGRAM .....	2-1
2.1.	Boundary Physics and Technology Overview .....	2-1
2.2.	Divertor Physics .....	2-2
2.3.	Boundary Physics Modeling .....	2-5
2.4.	Impurity Transport and Control in DIII-D .....	2-5
2.4.1.	Spectroscopy and Modeling .....	2-6
2.4.2.	Helium Transport/Exhaust .....	2-6
2.4.3.	DiMES .....	2-6
2.4.4.	Wall Conditioning .....	2-7
2.5.	Divertor Cryopumping and Density Control .....	2-8
3.	ADVANCED TOKAMAK STUDIES .....	3-1
3.1.	Overview .....	3-1
3.2.	Beta-Limiting Instabilities in DIII-D Very High Performance Discharges ....	3-3
3.3.	Noninductive Current Drive .....	3-5
3.4.	High $\beta_p$ Improved Confinement .....	3-7
4.	TOKAMAK PHYSICS .....	4-1
4.1.	Overview .....	4-1
4.2.	H-Mode Confinement .....	4-1
4.3.	VH-Mode Experiments .....	4-3
4.4.	Plasma Shape Experiments .....	4-5
4.5.	Wall Stabilization of Ideal Kink Modes .....	4-6

## CONTENTS (CONTINUED)

5.	OPERATIONS .....	5-1
5.1.	Tokamak Operations .....	5-1
5.1.1.	Introduction .....	5-1
5.1.2.	Vent Recovery .....	5-1
5.1.3.	Tokamak Operation .....	5-1
5.2.	Neutral Beam Operations .....	5-3
5.2.1.	Operations Summary .....	5-3
5.2.2.	System Improvement, Maintenance and Testing .....	5-3
5.2.3.	System Availability .....	5-4
5.3.	Electron Cyclotron and Ion Cyclotron Heating Operations .....	5-4
5.3.1.	ECH 60 GHz .....	5-4
5.3.2.	ICH Operations .....	5-5
5.4.	Disruption Studies and Plasma Control .....	5-6
5.4.1.	Introduction .....	5-6
5.4.2.	Disruption Studies .....	5-6
5.4.3.	Plasma Control .....	5-7
5.5.	Diagnostics .....	5-7
5.5.1.	Overview .....	5-7
5.5.2.	New or upgraded diagnostics .....	5-7
5.5.3.	Diagnostics under development .....	5-14
5.6.	Reliability & Availability .....	5-14
5.6.1.	Integrated Preventive Maintenance Program .....	5-14
5.6.2.	Significant Event Reviews .....	5-15
5.7.	Radiation Management .....	5-16
5.8.	Electrical Engineering .....	5-18
5.8.1.	Overview .....	5-18
5.8.2.	Operation Support .....	5-18
5.8.3.	Coil and Neutral Beam Power Systems .....	5-18
5.8.4.	Instrumentation and Control Systems .....	5-19
5.9.	Mechanical Engineering .....	5-19
5.9.1.	Tokamak Systems .....	5-19
5.9.2.	Diagnostic Support Activities .....	5-20
5.9.3.	Fluid Systems .....	5-21
5.9.4.	ADP Cryogenic Operation .....	5-22
5.10	Computer Data Systems .....	5-22

## CONTENTS (CONTINUED)

6.	PROGRAM DEVELOPMENT .....	6-1
6.1.	Fast Wave Current Drive Upgrade.....	6-1
6.2.	Radiative Divertor Program .....	6-6
6.3.	110 GHz ECH System .....	6-9
7.	SUPPORT SERVICES .....	7-1
7.1.	Quality Assurance .....	7-1
7.1.1.	Design Support.....	7-1
7.1.2.	Inspection Support .....	7-1
7.1.3.	Tooling/Layout/Alignment Support.....	7-2
7.1.4.	QA System Improvements .....	7-2
7.1.5.	Other Support .....	7-2
7.2.	Planning and Control .....	7-3
7.3.	Environment Safety and Health .....	7-3
7.3.1.	Fusion and DIII-D Safety .....	7-3
7.3.2.	FY93 Safety .....	7-4
7.3.2.1.	Training .....	7-4
7.3.2.2.	Inspections .....	7-5
7.3.2.3.	Other Activities .....	7-6
7.3.3.	Radiation Safety .....	7-6
7.4.	Visitor and Public Information Program.....	7-7
8.	CONTRIBUTION TO ITER PHYSICS R&D .....	8-1
9.	TPX SUPPORT.....	9-1
10.	COLLABORATIVE EFFORTS .....	10-1
10.1.	DIII-D Collaboration Programs Overview .....	10-1
10.2.	Japan Atomic Energy Research Institute .....	10-1
10.3.	Lawrence Livermore National Laboratory .....	10-2
10.4.	Oak Ridge National Laboratory .....	10-7
10.4.1.	Advanced Divertor and Boundary Physics Program .....	10-7
10.4.2.	ORNL Fast Wave Current Drive Program.....	10-9
10.4.3.	Pellet Injector Program .....	10-10

## CONTENTS (CONTINUED)

10.5.	UCLA/SANDIA.....	10-11
10.5.1.	Edge Turbulence and L-H Transition Physics .....	10-12
10.5.2.	Core Turbulence Measurements .....	10-14
10.5.3.	SOL Characterization and Scaling .....	10-14
10.5.4.	Density Profile Measurements .....	10-14
10.5.5.	ICRF Wave Measurements .....	10-14
10.6.	INTERNATIONAL COLLABORATIONS .....	10-15
10.6.1.	JET .....	10-17
10.6.2.	ASDEX-U/W7 Stellarator.....	10-17
10.6.3.	TORE SUPRA .....	10-17
10.6.4.	JT-60U .....	10-18
10.6.5.	GAMMA-10.....	10-18
10.6.6.	T-10.....	10-18
10.6.7.	TRINITY .....	10-19
10.6.8.	TEXTOR.....	10-19
11.	FY93 PUBLICATIONS.....	11-1

## LIST OF FIGURES

Fig. 1.1-1.	Cross section of DIII-D with flux surfaces of a double-null divertor discharge superimposed. ....	1-2
Fig. 1.2-1.	DIII-D fusion performance has doubled every two years .....	1-5
Fig. 1.2-2.	Comparison of IRTV heat flux profiles on divertor with and without neon puffing/enhanced edge and divertor radiation .....	1-6
Fig. 1.2-3.	The cryopump allows control of $n_e$ during ELMing H-mode so that, for example, $n_e$ can be reduced at constant $I_p$ and beam power or kept constant at different $I_p$ . ....	1-7
Fig. 1.2-4.	First He exhaust experiments on DIII-D using the cryopump .....	1-8
Fig. 1.2-5.	Comparison of (a) $E_r$ , (b) $E_r \times B$ shear and (c) $\chi_{eff}$ with and without magnetic braking of VH-mode plasmas .....	1-9
Fig. 2.2-1.	A "natural" radiative divertor reduces inner strikepoint heat flux in DIII-D .....	2-3
Fig. 2.2-2.	Divertor heat flux is reduced with deuterium gas puffing .....	2-4
Fig. 2.4-1.	A DIMES sample is shown inserted into the DIII-D divertor floor .....	2-7
Fig. 2.4-2.	UV impurity line radiation is reduced with the all-graphite wall .....	2-9
Fig. 3.2-1.	Time evolution of the MHD event ending the ELM-free VH-mode phase of discharge 73203 .....	3-4
Fig. 3.3-1.	The current drive efficiency as a function of central electron temperature.....	3-6
Fig. 3.4-1.	Time history for discharge 77676 .....	3-8
Fig. 3.4-2.	Comparison of density profiles at 3.36 s .....	3-9
Fig. 4.2-1.	Use of cryopumping to keep $n_e$ fixed at two different values of $I_p$ .....	4-2
Fig. 4.2-2.	Use of cryopumping to vary $n_e$ at fixed $I_p$ and beam power. ....	4-3

## LIST OF FIGURES (Continued)

Fig. 4.4-1.	Performance figure-of-merit $\beta\tau$ versus shape parameter $S^2R^2/\kappa$ .....	4-7
Fig. 4.5-1.	Growth rate versus wall distance normalized to the DIII-D wall position for DIII-D discharge 75828 at 2700 ms .....	4-10
Fig. 4.5-2.	Growth rate versus wall distance normalized to the DIII-D wall position for DIII-D discharge 67700 at 1750 ms .....	4-11
Fig. 5.2-1.	Neutral beam availability by month.....	5-4
Fig. 5.3-1.	ICRF decoupler .....	5-5
Fig. 5.5-1.	Views of new imaging arrays of bolometers .....	5-12
Fig. 5.5-2.	Contour plot of radiation during $n_e$ injection from divertor region .....	5-13
Fig. 6.1-1.	Overall schematic of new FWCD system .....	6-2
Fig. 6.1-2.	Photograph of FWCD transmitter units .....	6-4
Fig. 6.1-3.	New FWCD antennas.....	6-5
Fig. 6.2-1.	$D_2$ puffing reduces divertor heat flux while increasing core density .....	6-6
Fig. 6.2-2.	Neon puffing reduces divertor heat flux with only small effect on confinement but increases core $Z_{eff}$ .....	6-7
Fig. 6.2-3.	Shape studies show that confinement and plasma performance increase with triangularity.....	6-8
Fig. 6.2-4.	Preliminary conceptual design of a plasma radiative divertor and operational features .....	6-9
Fig. 10.3-1.	Divertor interferometer views.....	10-2
Fig. 10.3-2.	Divertor Thomson scattering. ....	10-3
Fig. 10.3-3.	High $\beta_p$ discharge evolution showing a) the radial and temporal dependence of integral $q$ surfaces and b) the enhancement of core density, correlated with turnoff of MHD fluctuations at 3360 ms.....	10-6
Fig. 10.3-4.	Layout of 16 channel MSE instrument, showing eight new edge channels and eight reconfigured central channels.....	10-7
Fig. 10.4-1.	Variation of $D_{He}/\lambda_{eff}$ with plasma current.....	10-8
Fig. 10.4-2.	Variation of $D_{He}/\lambda_{eff}$ with ELM frequency .....	10-8
Fig. 10.4-3.	ORNL fast wave current drive antenna.....	10-10
Fig. 10.4-4.	ORNL pellet injector to be installed on DIII-D .....	10-11

## LIST OF FIGURES (Continued)

Fig. 10.5-1.	Comparison of the radial electric field measured by the reciprocating Langmuir probe using the measured floating potential and $T_e$ profiles for ohmic and ohmic-sustained H-modes .....	10-12
Fig. 10.5-2.	Radial profiles of the turbulent particle and convective heat fluxes in the DIII-D boundary for OH and OH-sustained H-modes .....	10-13
Fig. 10.5-3.	Comparison of SOL density profiles for lower single-null and double-null divertor L-mode discharges with $I_p = 1.3$ MA .....	10-15
Fig. 10.5-4.	H-mode density profile .....	10-16
Fig. 10.5-5.	ICH power versus time and detected power via reflectometer .....	10-16

## LIST OF TABLES

1.1-1. DIII-D Capabilities.....	1-2
1.1-2. DIII-D Achieved Parameters.....	1-3
1.1-3. Collaborators Participating at DIII-D.....	1-4
1.2-1. Technical DIII-D Highlights of 1993.....	1-5
4.4-1. Best Performance in Different Configurations.....	4-8
5.5-1. Plasma Diagnostics.....	5-8
8.1-1. ITER Physics R&D Needs.....	8-1
8.1-2. ITER Physics R&D Contributors.....	8-3

# 1. DIII-D PROGRAM OVERVIEW

## 1.1. INTRODUCTION

The DIII-D tokamak research program is carried out by General Atomics (GA) for the U.S. Department of Energy (DOE). The DIII-D is the most flexible tokamak in the world. The primary goal of the DIII-D tokamak research program is to provide data to develop a conceptual physics blueprint for a commercially attractive electrical demonstration plant (DEMO) that would open a path to fusion power commercialization. In doing so, the DIII-D program provides physics and technology R&D outputs to aid the Tokamak Physics Experiment (TPX) and the International Thermonuclear Experimental Reactor (ITER). Specific DIII-D objectives include the steady-state sustainment of plasma current as well as demonstrating techniques for microwave heating, divertor heat removal, fuel exhaust and tokamak plasma control. The DIII-D program is addressing these objectives in an integrated fashion with high beta and with good confinement. The long-range plan is organized into two major thrusts; the development of an advanced divertor and the development of advanced tokamak concepts. These two thrusts have a common goal: an improved DEMO reactor with lower cost and smaller size than the present DEMO which can be extrapolated from the conventional ITER operational scenario. In order to prepare for the long-range program, in FY93 the DIII-D research program concentrated on three major areas: Divertor and Boundary Physics, Advanced Tokamak Studies, and Tokamak Physics.

The major goals of the Divertor and Boundary Physics studies are the control of impurities, efficient heat removal and understanding the strong role that the edge plasma plays in the global energy confinement of the plasma. The advanced tokamak studies initiated the investigation into new techniques for improving energy confinement, controlling particle fueling and increasing plasma beta. The major goal of the Tokamak Physics Studies is the understanding of energy and particle transport in a reactor relevant plasma.

A cross sectional view of DIII-D (Fig. 1.1-1) shows a diverted configuration in which magnetic equilibrium forms a so-called double-null geometry. Several of the major machine components are also called out in this figure. This equilibrium configuration is only one of many available in DIII-D. Because of this flexibility in shaping and positioning of the magnetic equilibrium, a broad range of plasma parameters are available for experimentation. The DIII-D tokamak characteristics, maximum plasma parameters and experimental results are summarized in Tables 1.1-1 and 1.1-2.

To carry out the DIII-D program, GA provides a combination of extensive institutional experience in the field, a skilled and experienced staff of international repute, and a uniquely flexible facility — the DIII-D tokamak. GA has had an active fusion research program for more than three decades. It is the only industrial participant in the U.S. program with a major, integrated effort in all aspects of plasma physics and fusion research, from basic plasma theory, magnetic fusion device design, engineering, construction, and operation, to fusion reactor technology.

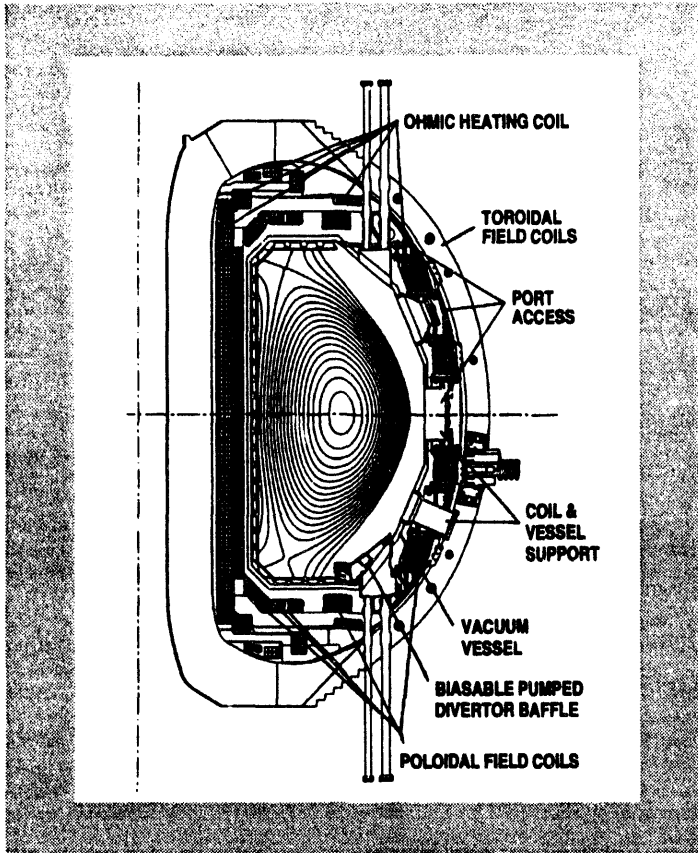


Fig. 1.1-1. Cross sections of DIII-D with flux surfaces of a double-null divertor discharge superimposed

<b>TABLE 1.1-1 DIII-D CAPABILITIES</b>	
	Present
Vacuum vessel volume	37 m <sup>3</sup>
Major radius	1.67 m
Minor radius	0.67 m
Maximum toroidal field	2.2 T
Vertical elongation ratio	2.6
Available OH flux	12 V-s
Maximum plasma current	3.0 MA
Neutral beam power	20 MW
RF power (ECH)	1.4 MW
RF power (ICRF)	2.0 MW
Current flattop (divertor at 2 MA)	5 s
Current flattop (divertor at 1 MA)	10 s

In addition, collaborations with other U.S. and international fusion programs are an essential feature of the DIII-D program. These collaborations assist and bring expertise to DIII-D. Principal among these efforts are the ongoing cooperative efforts with the Japan Atomic Energy Research Institute (JAERI), the Lawrence Livermore National Laboratory (LLNL), Oak Ridge National Laboratory (ORNL), Sandia National Laboratory (SNL), and the University of California at Los Angeles (UCLA). A list of collaborations at DIII-D is given in Table 1.1-3. In addition to hosting scientists and engineers to participate in DIII-D experiments, GA scientists and engineers participate on the experiments at other national and international laboratories and universities. We are active participants on the ITER and TPX programs and participate in the development of a physics database for the national Transport Task Force (TTF).

The Fusion Energy Advisory Committee (FEAC) was charged by the DOE to develop recommendations on how best to pursue the goal of a practical magnetic fusion reactor in the context of several budget scenarios covering the period FY94-FY98. FEAC identified DIII-D as one of the high priority U.S. Fusion program elements. In its report of September 1992, FEAC noted that the DIII-D program supports both ITER and the development of an optimized tokamak. DIII-D will be the largest operating U.S. tokamak in the post-Princeton Tokamak Fusion Test Reactor (TFTR) era. The DIII-D divertor and advanced tokamak upgrades together with the strong national collaborative program will provide the U.S. with an internationally competitive magnetic fusion tokamak facility until the operation of TPX and ITER.

$I/aB$	3.3 MA/m/T
$\beta_T(0)$	44% (second stability)
$\langle\beta_T\rangle$	12.5%
$\beta_N$	6.0
$\beta_p$	5.2
$\epsilon\beta_p$	2.
$\bar{n}_e$	$1.7 \times 10^{20} \text{ m}^{-3}$
$T_e(0)$	7 keV
$T_i(0)$	22 keV
W	3.7 MJ
$\tau_E$	0.48 s, ( $P_{HEAT} = 4 \text{ MW}$ )
$\bar{n}_e(0) \tau_E$	$0.39 \times 10^{20} \text{ m}^{-3} \text{ s}$
$n_D(0) T_i \tau_E$	$5 \times 10^{20} \text{ m}^{-3} \text{ keV s}$
H-mode duration	10.3 sec

**TABLE 1.1-3  
COLLABORATORS PARTICIPATING AT DIII-D**

<b>International Laboratories</b>	<b>National Laboratories</b>	<b>Universities</b>
Cadarache (France)	LLNL	UCLA
CCFM (Canada)	ORNL	UCSD
Culham (England)	SNLA	UC Irvine
FOM (Netherlands)	SNLL	UC Berkeley
Ioffe (Russia)	ANL	MIT
IPP (Germany)	PPPL	RPI
JAERI (Japan)	INEL	Cal Tech
JET (EC)		Johns Hopkins Un.
KFA (Germany)		N. Carolina State Un.
Kurchatov (Russia)		Univ. of Maryland
Lausanne (Switzerland)		Univ. of Illinois
Troitsk (Russia)		Univ. of New Mexico
		Univ. of Paris
		Univ. of Washington
		Univ. of Wisconsin

## 1.2. HIGHLIGHTS OF THE FY93 DIII-D RESEARCH PROGRAM

Progress on achieving higher fusion performance on Doublet III and DIII-D has been steady as shown in the triple product  $nTt_i$  achieved versus calendar year (shown in Fig. 1.2-1) which has doubled every two years and is comparable to that obtained in larger tokamaks. Successes on DIII-D during fiscal year 1993 include: the installation of an all carbon wall which allowed VH-mode without boronization and a rapid recovery from vents, cryopumping of the divertor which for the first time in any tokamak made the density in H-mode controllable and allowed pumping of injected helium giving promise of alpha ash control, deuterium or neon puffing at the divertor with concomitant divertor radiation greatly reducing the divertor heat flux while little affecting global confinement and in the case of the neon puffing also producing an edge region of high radiation which encircles the plasma. (See cover illustration.)  $n_D(0) T_i(0) \tau_E$  was more than doubled to  $5 \times 10^{20} \text{ m}^{-3} \text{ keV s}$ , the ratio of plasma pressure to magnetic field pressure  $\beta$  was increased to 12.5%, a new quiescent high  $\beta_p$  (ratio of plasma pressure to poloidal magnetic field pressure) high performance regime was identified and advances were made in fast wave current drive current and efficiency. In addition to controlling the plasma shape, the digital control system was successful in controlling (1) the plasma density by feedback on the cryopumping and gas fueling rate, (2) the radio frequency ion cyclotron power loading by adjusting the gap between the plasma and antennas, and (3) in maintaining constant beta (stored plasma energy) by feedback control of the neutral beam power. A more complete list of DIII-D highlights is given in Table 1.2-1 and selected highlights with more detail follow.

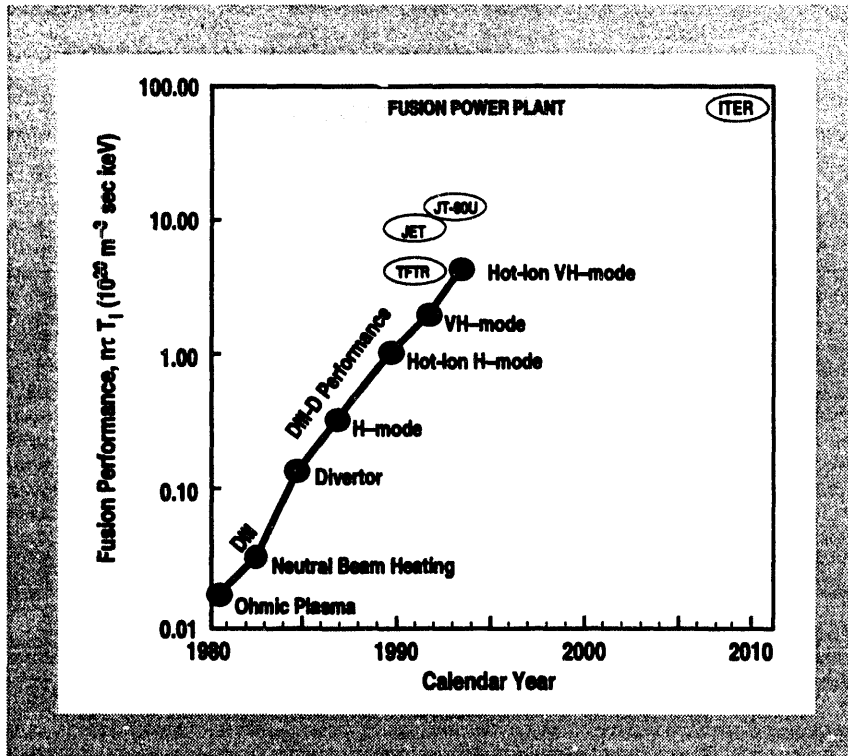


Fig. 1.2-1 DIII-D fusion performance has doubled every two years

TABLE 1.2-1  
TECHNICAL DIII-D HIGHLIGHTS of 1993

- Demonstrated density control with divertor pumping
- Measured helium transport  $\tau_{He}/\tau_E \sim 10$  to 15
- Demonstrated radiative divertor power dispersal
- Initiated DIMES divertor material studies
- Achieved 21 keV hot ion VH-mode  $n_D(0) \tau_E T_i(0) = 5 \times 10^{20} \text{ m}^{-3} \text{ s keV}$
- Increased beta from 11 to 12.5%
- Increased  $\beta\tau$  from 1.3 to 1.7% s
- Completed high triangularity plasma shape experiments
- Increased understanding of VH-mode
- Conducted edge fluctuation studies with Li BES, PCI, reflectometer, scattering, and edge probe
- Conducted transport studies with ECH and FW
- Carried out fast wave current drive physics experiments
- Observed quiescent high poloidal beta with peaked density profile

### 1.2.1. DIVERTOR RADIATION BY D<sub>2</sub> OR Ne INJECTION

Power flow from the plasma core through the scrape-off layer (SOL) and into the divertor represents a serious design challenge. A successful means of reducing the peak flux was found in FY93 by radiating the power away before it strikes the divertor plate by use of deuterium and/or neon injection with cryopumping to limit the density rise; peak heat load on the divertor target plate was reduced by as much as a factor of five. The effect of Ne gas puffing, which has only a small effect on global confinement but a large effect on the profile of divertor heat flux as measured by an absolutely calibrated infrared television (IRTV) camera is shown in Fig. 1.2-2.

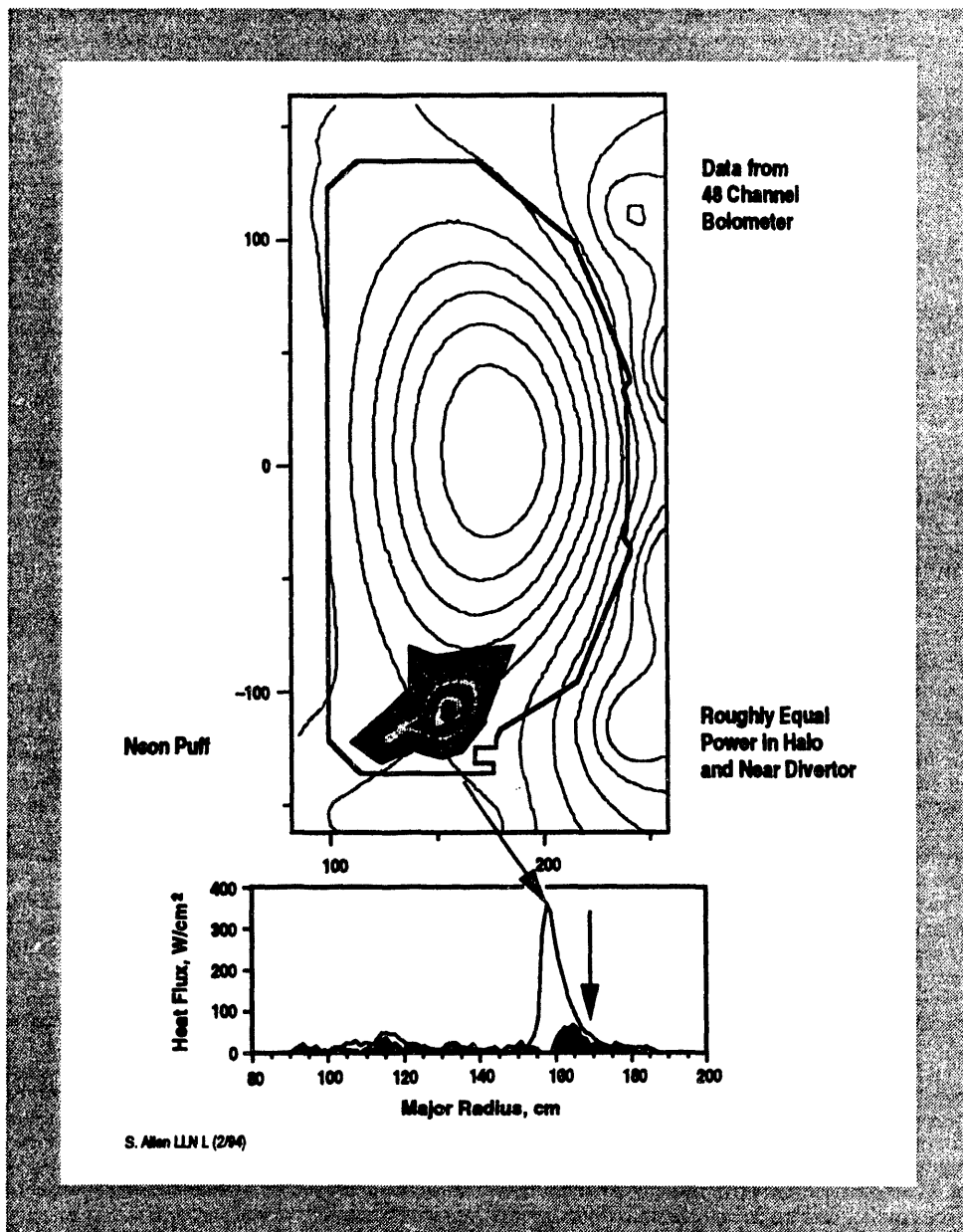


Fig. 1.2-2. Comparison of IRTV heat flux profiles on divertor with and without neon puffing/enhanced edge and divertor radiation

### 1.2.2. DIVERTOR CRYOPUMPING AND PARTICLE CONTROL

For the first time in any tokamak with H-mode, density can now be controlled successfully. The advanced divertor cryopump was effectively brought into operation allowing: density control, observation of helium exhaust and a systematic measurement of the dependence of confinement on density. Plasma density control, for example, is shown in Fig. 1.2-3. Obviating the usual H-mode density rise is of major importance for successful, efficient rf current drive for a steady-state reactor with current profile control.

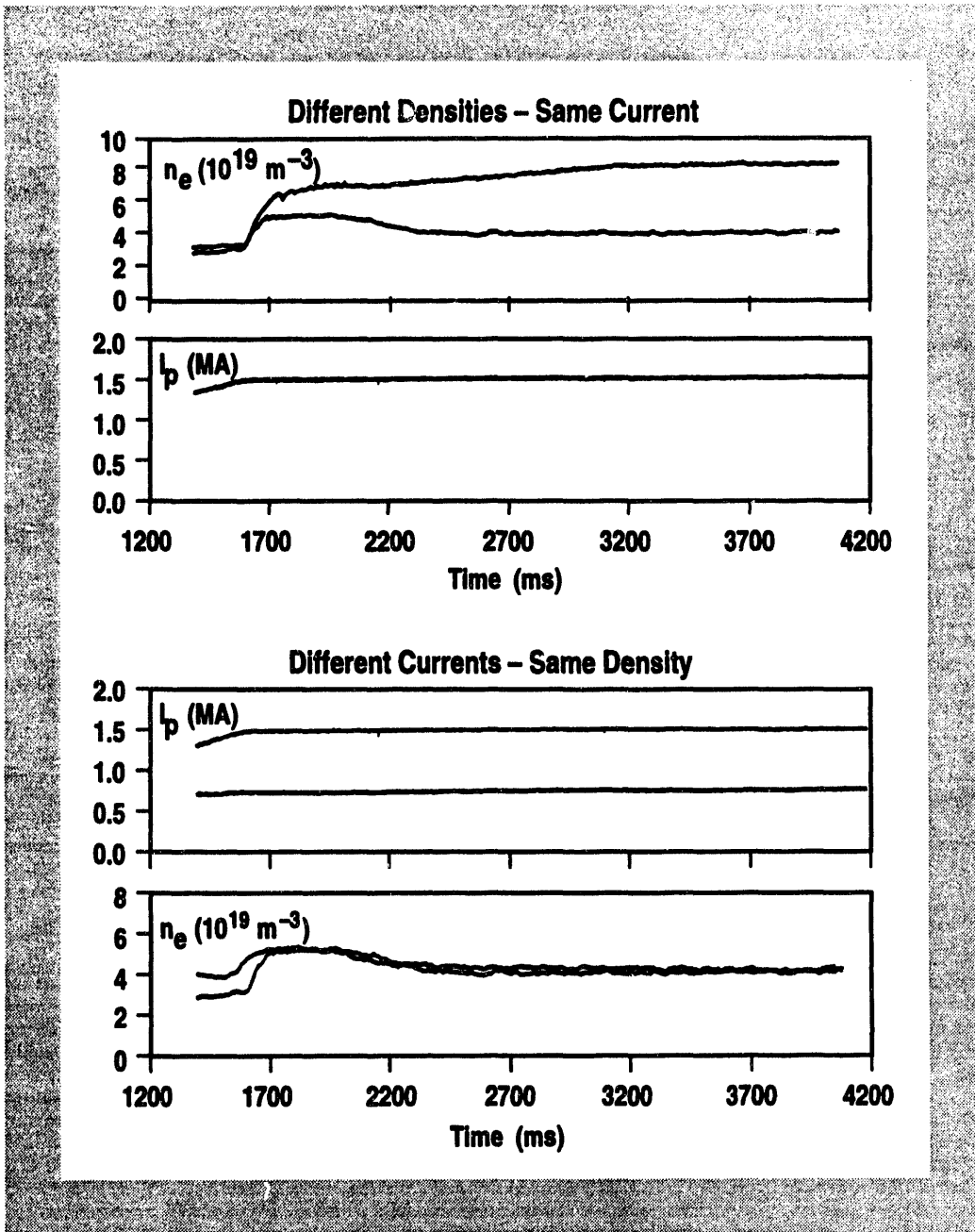


Fig. 1.2-3. The cryopump allows control of  $n_e$  during ELMing H-mode so that, for example,  $n_e$  can be reduced at constant  $I_p$  and beam power or kept constant at different  $I_p$ .

### 1.2.3. HELIUM EXHAUST ON DIII-D USING THE CRYOPUMP

A major potential problem for ITER and fusion reactors in general is buildup of helium ash as a result of alpha particles produced during fusion reactions; too much dilution of the DT plasma by helium will stop the fusion power output. (The sun is now about 28% helium and will eventually become a "red giant" because of a lack of He ash removal.) The use of the new cryopump was successful in pumping away the helium density in DIII-D after a short He gas puff. See Fig. 1.2-4. The decay rate of the He density during the pumping is fast enough to be acceptable for ash control in ITER or a reactor.

### 1.2.4. IMPROVED UNDERSTANDING OF VH-MODE

VH-mode plasmas with confinement up to twice the usual H-mode value were successfully reproduced in an all-carbon vessel without boronization, confirming that clean wall condition is required but the means are not unique. The hypothesis that the VH-mode core confinement improvement is due to entry into a positive feedback loop in which core flow shear increases, particularly deeper inside the core, decreasing turbulence and concomitant transport, increasing flow shear, etc., was confirmed by using "magnetic braking" of core flow as an independent control of toroidal plasma rotation. Where the VH-mode flow shear is decreased by magnetic braking, turbulence and transport increase back to "normal" levels. Comparison of radial electric field  $E_r$ , shear in the flow velocity  $E_r \times B$  and the thermal diffusivity  $\chi_{eff}$  with and without magnetic braking is shown in Fig. 1.2-5.

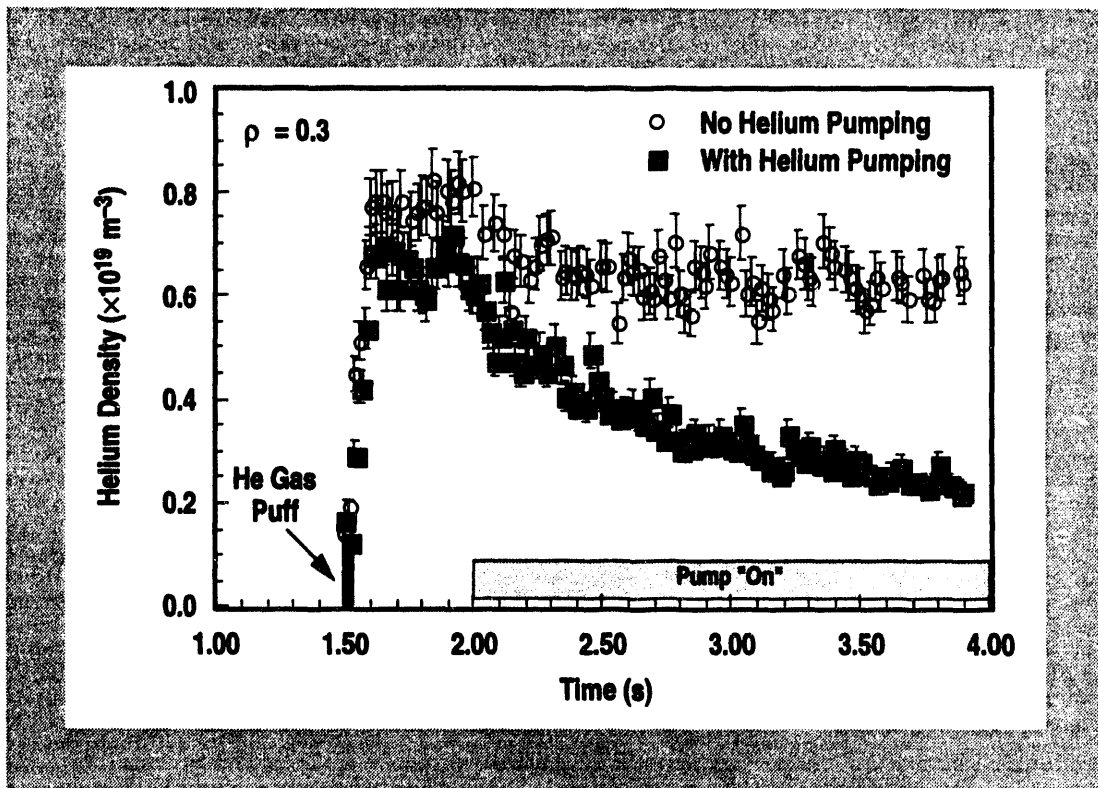


Fig. 1.2-4. First He exhaust experiments on DIII-D using Ar frosting of the ADP cryopump.

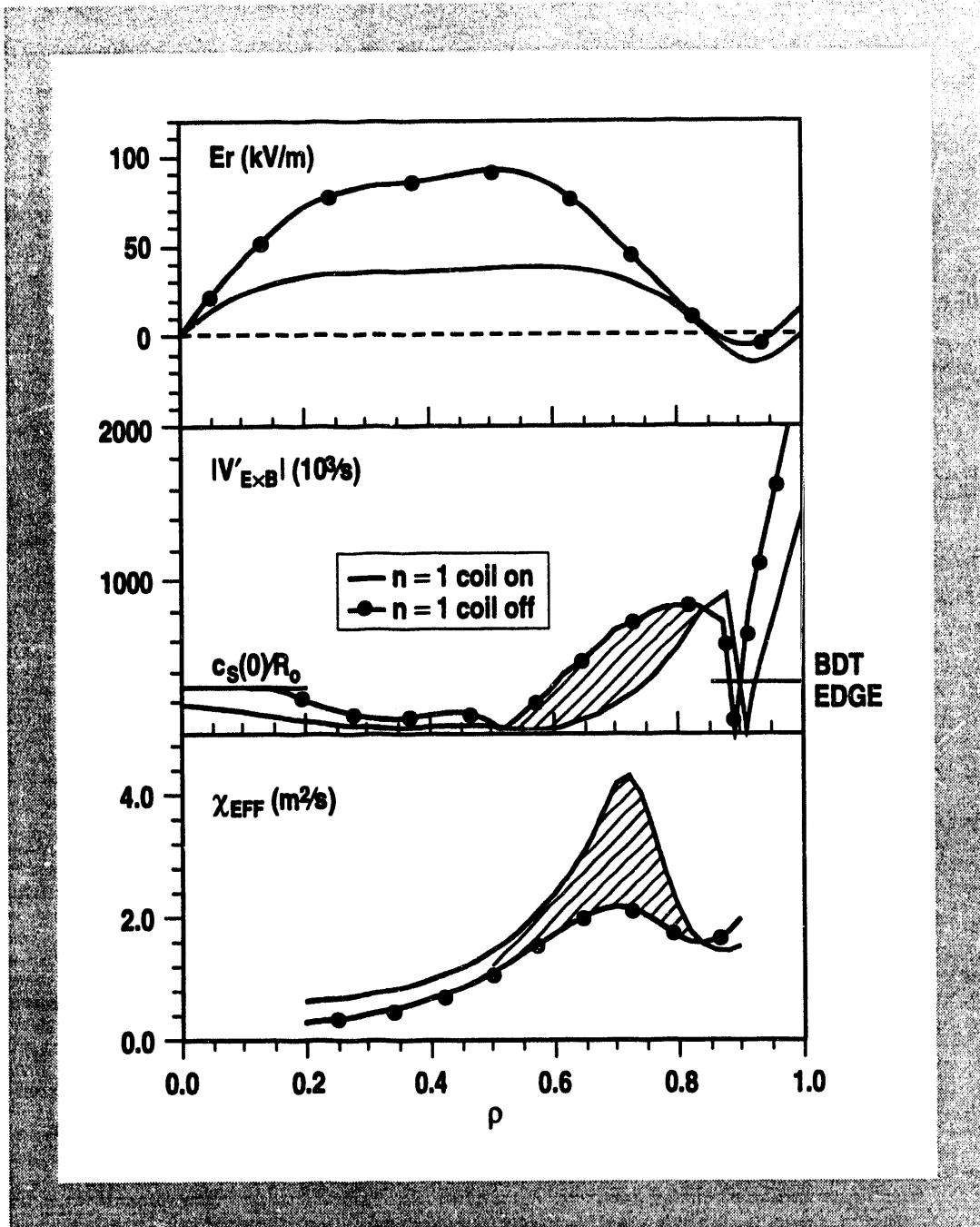


Fig. 1.2-5 Comparison of  $E_r$ ,  $E_r \times B$  shear and  $\chi_{eff}$  with and without magnetic braking of VH-mode plasmas

## 2. DIVERTOR AND BOUNDARY RESEARCH PROGRAM

### 2.1. BOUNDARY PHYSICS AND TECHNOLOGY OVERVIEW

During the past year, intensive efforts for developing an effective particle control technique came to fruition and for the first time since the discovery of the H-mode, density controlled H-mode plasmas were produced. The advanced divertor cryopump project was successfully completed early in the CY94, and following the commissioning of the pump in February several important physics and technology achievements were made. The DIII-D divertor cryopump is the first application of this pumping technology inside a tokamak vessel. The attainment of density controlled H-mode plasmas completed a major DIII-D milestone and in the process significantly enhanced the prospects of a steady-state fusion reactor with rf current drive. Using the cryopump, the first systematic measurement of the dependence of H-mode confinement on plasma density was made. Furthermore, with divertor cryopumping, the first successful demonstration of helium exhaust in an H-mode plasma was performed.

The ability to measure and control impurities in the DIII-D plasma improved steadily during the course of FY93. Spectroscopic measurement and interpretation capabilities in the core plasma were influenced by the improvement of spectral analysis codes and the development of input and output processors for application the MIST code to DIII-D. The application of the multichord divertor spectrometer to the monitoring of divertor impurities was implemented and development of interpretation capabilities using a Monte Carlo impurity transport model continued. The installation of an all carbon wall, coupled with thorough conditioning, dramatically reduced the influx of metallic impurities, and with boronization the influx of carbon and oxygen were also significantly reduced. The study of the transport and exhaust of He ash made major progress on DIII-D during the last year. Preliminary scaling studies and divertor measurements showed favorable trends for a tokamak reactor. The installation of the DIMES (Divertor Materials Erosion Studies) sample exchange system marked the beginning of the capability to use the DIII-D divertor plasma to make direct measurement of material erosion rates, and will provide impurity transport study capability in the future. Each of the above programs will be discussed in more detail below.

Power flow through the scrape-off layer and into the divertor represents a serious design challenge for the next large tokamaks such as ITER. This problem is confronted from three directions. First the process by which power leaves the core plasma was investigated. Second, experiments were continued on the scaling of SOL and divertor plasma transport to gain understanding on how the peak heat flux will scale up to larger tokamaks. Finally, experiments were executed on methods of lessening the heat flux onto the divertor target plates. Power balance experiments this past year have concentrated on single-null plasmas in ELMing H-mode, a configuration and operational scenario envisioned for ITER. IRTV cameras are used to measure direct heat flux to the surfaces of the divertor floor, inner wall and ceiling of the vessel. Two new bolometer arrays measure the magnitude and location of power leaving the plasma as radiation. With these new diagnostic capabilities, there are dramatically increased power balance accountability to 90%. In the SOL, deviations from toroidal symmetry can result in very high heat fluxes in selected areas. This can be especially difficult for the design of future divertors. Irregularities are characterized in the divertor heat flux and currents that flow in the SOL. On the topic of studying means to reduce the peak heat flux

onto the divertor, one possible way is to radiate the power away before it strikes the divertor plate. On DIII-D this is done by injecting gas into the discharge to increase the density of the divertor plasma. In experiments last year the peak heat load on the divertor was reduced target plate by as much as a factor of five.

## 2.2. DIVERTOR PHYSICS

All of the power that is injected into the plasma discharge must exit somewhere. It is this very high power which represents such a problem in the design of the divertor for ITER. Characterizing the location and magnitude of the power leaving the plasma is the first step. Our power balance experiments this past year have concentrated on single-null plasmas in ELMing H-mode, a configuration and operational scenario envisioned for ITER. IRTV cameras are used to measure direct heat flux to the surfaces of the divertor floor, inner wall and ceiling of the vessel. Two new bolometer arrays measure the magnitude and location of power leaving the plasma as radiation. With these two diagnostics  $\geq 90\%$  of the injected power is accounted for. Radiation in the core of the plasma accounts for  $\leq 15\%$  of the power injected. The rest crosses the separatrix and flows through the SOL to the inboard and outboard divertor in roughly equal proportions. IRTV camera measurements show that in the outboard divertor most of the power exits as direct heat flux to the target plate. However in the inboard divertor most of the power is radiated away before striking the inner target plate. This in/out asymmetry is illustrated in Fig. 2.2-1. This result illustrates that the inner strike point cannot be ignored when designing a divertor. Also observed is a minimum separation between the plasma and inner wall before it also collects power. When the inner wall separatrix gap became less than 6 cm significant power flowed to the inner wall with a sharp reduction in peak heat flux to the outer divertor.

Outside the separatrix a thin layer of plasma, the SOL, carries power and particles to the divertor. As this layer becomes narrower the power is concentrated in a thinner layer at the divertor target plate. Variations are measured in the width of this layer and its projected area onto the divertor target plate, with the reciprocating Langmuir probe at the midplane and Langmuir probes in the divertor. In H-mode these SOL widths can be 4 times more narrow than L-mode discharges resulting in a very high peaked heat flux; the SOL width becomes more narrow with increased plasma current. These scaling relations will help predict the heat flux profiles for new large tokamaks such as ITER.

If the magnetic fields in the plasma are not toroidally uniform, the heat flux profile can become distorted, producing very high heat fluxes in selected areas. This can be especially difficult for the design of future divertors. An effort is underway at DIII-D to characterize the tolerance to which magnetic fields must be produced in order to eliminate significant distortion of the heat flux profile. Irregularities were characterized in the divertor heat flux and currents that flow in the SOL. The peak in the heat flux can split during standard operation, but the separation of the peaks appears to decrease with increasing plasma current. This is presumably due to shorter lengths the magnetic field lines must travel before striking the divertor plate at the higher plasma currents. Toroidal variations in the currents in the SOL have also been observed. These currents can distort the magnetic field, in turn distorting the divertor heat flux. These current asymmetries, however, seem to be reduced during H-mode compared to L-mode.

The DIII-D divertor physics group is also involved in studying means to reduce the peak heat flux onto the divertor. One possible way is to radiate the power away before it strikes the divertor plate. On DIII-D this is done by injecting gas into the discharge to increase the density of the divertor plasma. As gas puffing continues a transition occurs where radiation in the divertor abruptly increases and the heat flux drops correspondingly. This effect is illustrated in Fig. 2.2-2. In comparing this to Fig. 2.2-1, the standard operation, the change occurs mostly in the

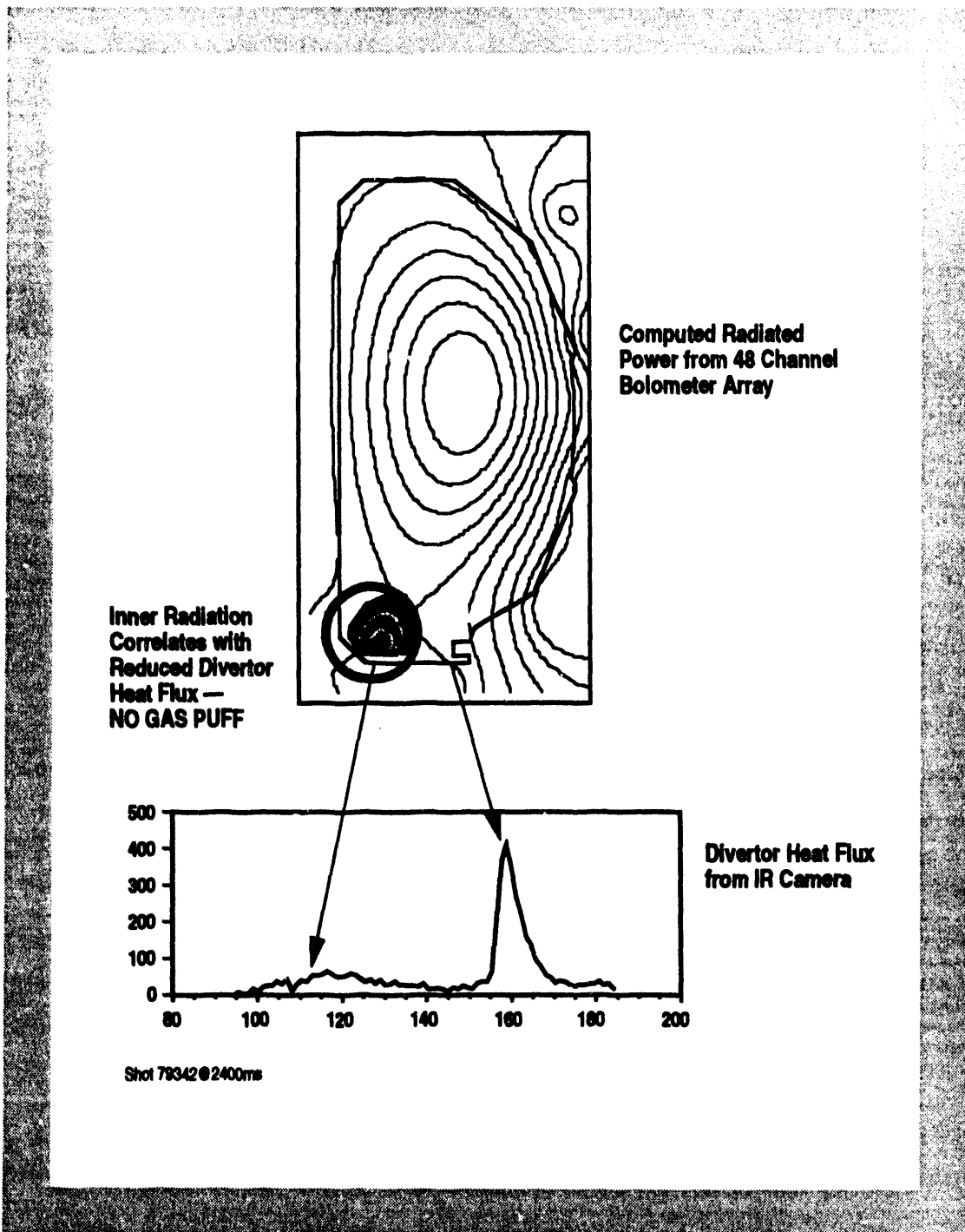
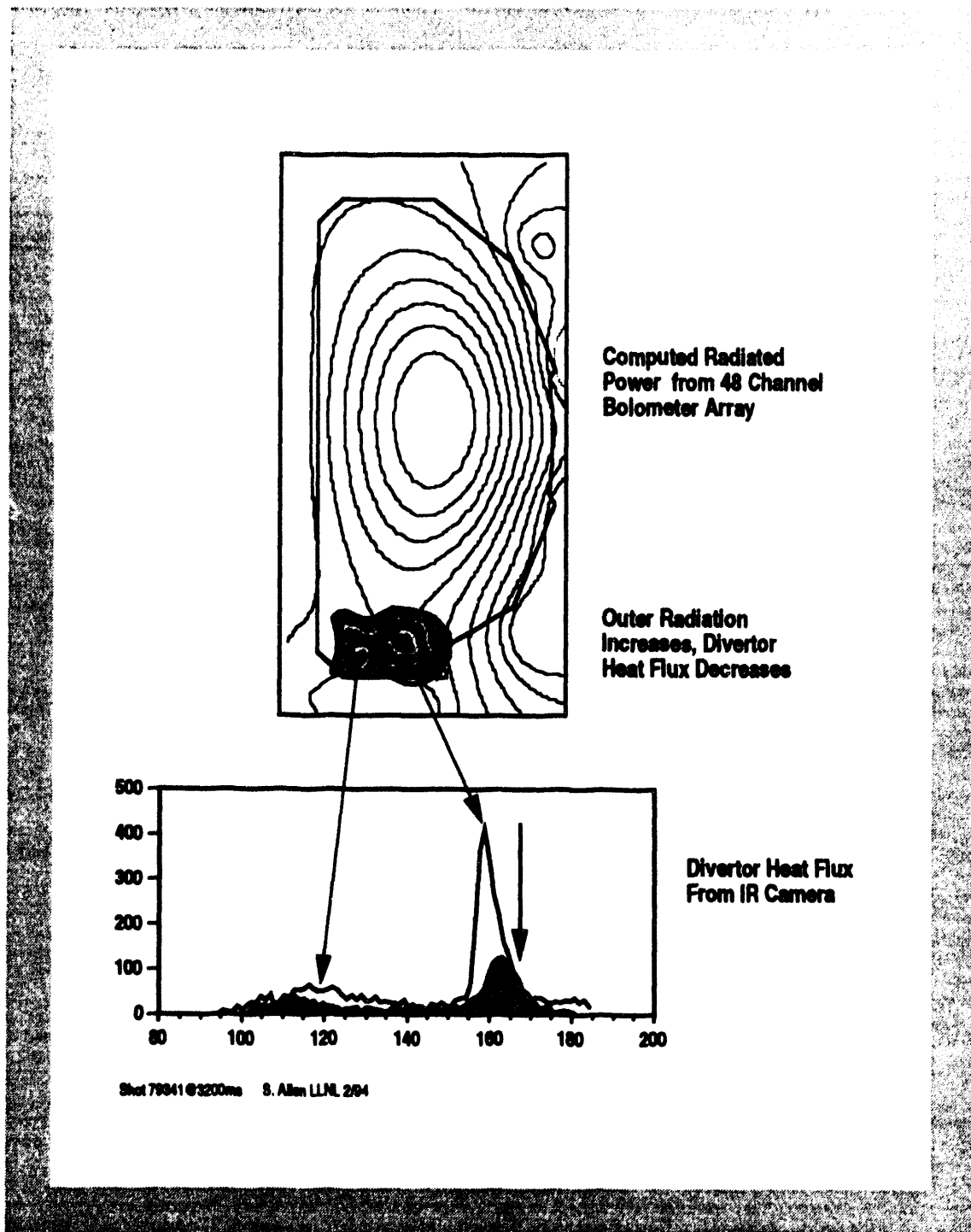


Fig. 2.2-1. A "natural" radiative divertor reduces inner strikepoint heat flux in DIII-D



**Fig. 2.2-2. Divertor heat flux is reduced with deuterium gas puffing**

outboard divertor leg. The inboard side is already in a radiative divertor state. The parameters that most control this transition are the input power and the neutral gas pressure just outside the divertor plasma. Another observation of the radiative divertor is the loss of power balance along field lines near the separatrix in the divertor. This indicates

that charge-exchange losses are an important mechanism in the transition. This also helps to understand the process of the radiative divertor so better divertors can be designed in the future. This past year the principle of feedback control of the radiative divertor was also demonstrated. With feedback control the neutral pressure can be regulated just outside the divertor plasma to maintain the radiative state, but limit the perturbation to the core plasma to keep good confinement.

Another technique to radiate more power is to inject a modest amount of impurities. Injection of neon achieved significant reduction in divertor heat flux. The neon produced a radiating layer just inside the separatrix, dissipating half of the input power. Most of the rest of the power radiated in the divertor region. Though neon injection radiates inside the separatrix only a small effect on confinement was observed.

### **2.3. BOUNDARY PHYSICS MODELING**

Considerable edge physics code development was made during FY93. Significant upgrades to the UEDGE code were made. This 2-D plasma fluid code is used to model the behavior of the DIII-D SOL, and to assist in the design of the radiative divertor. Detailed power balance routines were written to determine where the power was flowing in the SOL. This work was instrumental in identifying some errors and weak physics in the code. Correcting these difficulties produced much better agreement between code simulations and measurements on DIII-D. The number of options were expanded which can be used for the boundary conditions at the outer wall in the UEDGE simulation. In the past, a fixed temperature, and zero particle flux boundary condition was used. The capability was added to have fixed density, fixed particle and/or thermal flux, and the "extrapolation" boundary condition used by some modelers using the B2 code. This latter boundary condition forces a zero radial second derivative in either the density or temperature at the outer wall, so the temperature at the wall is not arbitrarily fixed. This work has permitted examination of the sensitivity of simulations to boundary conditions. A post processor was written which calculates the local emissivity for Lyman alpha emission, in addition, to the line integral of emission which corresponds to the views obtained in the photodiodes used on DIII-D. This post processor allows direct comparison of the emission measured on the experiment with that calculated in the code, and hence to better understand the physics of recycling neutrals at the divertor plate. Any portion of the outer wall, or the private flux wall, can be made a source of gas of arbitrary intensity. If the wall is not a gas source, one can specify the neutral particle albedo of that portion of the wall. In this way, portions of the wall simulate a pumping orifice. These modifications permit simulation of gas puffing and pumping experiments on DIII-D. The capability of the grid generation routines for UEDGE and DEGAS was expanded to permit generation of grids with divertor plates which are not orthogonal to flux surfaces. This will permit simulation of more realistic divertor geometry when the numerics of UEDGE is expanded to utilize this capability.

### **2.4. IMPURITY TRANSPORT AND CONTROL IN DIII-D**

The ability to measure and control impurities in the DIII-D plasma improved steadily during the course of FY93. Spectroscopic measurement and interpretation capabilities in the core plasma were influenced by the improvement of spectral analysis codes and the development of input and output processors for application the MIST code to DIII-D. The application of the multichord divertor spectrometer to the monitoring of divertor impurities was implemented and development of interpretation capabilities using a Monte Carlo impurity transport model continued. The installation of an all carbon wall, coupled with thorough conditioning, dramatically reduced the influx of metallic impurities, and with boronization the influx of carbon and oxygen were also significantly reduced.

The study of the transport and exhaust of He ash made major progress on DIII-D during the last year. Preliminary scaling studies and divertor measurements both showed favorable trends for a tokamak reactor. The installation of the DiMES (Divertor Materials Erosion Studies) sample exchange system marked the beginning of the capability to use the DIII-D divertor plasma to make direct measurement of material erosion rates, and will provide impurity transport study capability in the future.

### 2.4.1. SPECTROSCOPY AND MODELING

Spectroscopy is key to both the operation of DIII-D and to the interpretation of almost all of the experiments. The SPRED instrument, a low resolution VUV spectrometer, is the work horse for spectroscopy on DIII-D, routinely providing information of the core impurity content. Several improvements in the analysis of the SPRED data were implemented during the past year: 1) The SPRED spectrometer sensitivity was absolutely calibrated, 2) input and output processors for the MIST impurity transport model were developed, and 3) improvement of inter-shot spectral analysis routines was initiated.

The interpretation of the divertor spectra is not straightforward, since the transport of impurities in the divertor is not well understood. To assist in the interpretation of the spectroscopic data, and to help develop an understanding of the transport of impurities in the divertor, a Monte Carlo edge impurity transport model is being developed. The code is modeled after codes developed previously by Stangeby at the University of Toronto and Jeff Brooks at ANL.

### 2.4.2. HELIUM TRANSPORT/EXHAUST

Considerable progress has been made in the study of helium transport and exhaust on DIII-D during FY93. This includes improvements in diagnostic capabilities and calibration, planning and execution of experiments to study helium transport, and the analysis of the obtained data. In the diagnostic area, a modified Penning gauge was installed in the divertor baffle region of DIII-D and has been used extensively to monitor the helium partial pressure in this region during dedicated helium transport experiments. Also, improvements have been made in the techniques to calibrate the CER system, allowing more accurate reconstruction of the helium density profiles.

The most significant experiment conducted during FY93 in this area was devoted to characterizing helium transport properties of ELMing H-mode plasmas as the plasma current and injected power were systematically varied. Simulation of this data via the MIST code was used to determine the helium diffusivity  $D_{\text{He}}$  and pinch velocity in the various plasma conditions. Energy transport analysis of data from the same discharges using the energy transport code ONETWO has also been done to determine the local thermal conductivity  $\chi_{\text{eff}}$ . The obtained  $D_{\text{He}}/\chi_{\text{eff}}$  can then be used as a measure of helium particle confinement relative to energy confinement in these discharges. Results of this analysis suggests that  $D_{\text{He}}/\chi_{\text{eff}}$  is insensitive to changes in plasma current but increases strongly with increasing injected power or ELM frequency.

### 2.4.3. DIMES

The DiMES (Divertor Materials Erosion Studies) program focused on the development of a sample exchange system, allowing well characterized divertor material samples to be inserted and removed into/from the divertor floor of DIII-D on a routine basis. The system was installed and after a shakedown period, experiments began. See Fig. 2.4-1. Most notably, a graphite sample implanted with  $^{29}\text{Si}$ , provided by R. Bastasz of SNLL, was exposed to the outer strike point plasma. The depth of the implanted Si was measured using Rutherford backscattering by



**Fig. 2.4-1. A DIMES sample is shown inserted into the DIII-D divertor floor. This sample has a silicon wafer attached and is designed to help characterize the boronization films used to condition the DIII-D walls.**

W. Wampler at SNLA both before and after exposure, and thus the amount of erosion was determined. These data, along with heat and particle flux data and magnetic data, were given to J. Brooks and T. Hua at ANL who will use this data to begin benchmarking their modeling codes of the erosion/redeposition process.

#### **2.4.4. WALL CONDITIONING**

The installation of an all carbon wall, coupled with thorough conditioning, dramatically reduced the influx of metallic impurities and allowed the first observations of VH-mode without boronization and a record triple product,  $nDT_iT_E$ , after subsequent boronizations. Several improvements were made in FY93 to achieve these results: careful preparation of graphite tiles before installation, wall conditioning with helium fill gas only, and an improved boronization system.

Before tokamak operations commenced with the all-graphite wall there was considerable concern that plasma performance would be degraded due to excessive particle fueling from the additional graphite. To address these concerns, tile preparation was carefully monitored. Tiles previously exposed to DIII-D discharges were sandblasted using B<sub>4</sub>C pellets to remove surface layers which analysis had shown to have considerable metal deposits, primarily nickel. These tiles, and all new tiles, were baked in vacuum ovens to 800°–1000°C. All vacuum ovens were carefully qualified before use. After baking, tiles were cooled and placed in an inert argon atmosphere until installation. To further minimize metal impurity influxes, the interface between the graphite tiles and the Inconel walls was changed from copper foam to GRAFOIL, a spongy graphite material.

During the vent recovery phase, wall conditioning procedures were also changed. The reason for this is that Taylor discharge cleaning (TDC) or glow discharge cleaning with hydrogen or deuterium can create a layer of loosely bound carbon, i.e. "soot", on plasma facing surfaces. This soot has a large surface area and can desorb large amounts of deuterium during a discharge. In addition, chemical sputtering in the form of C<sub>x</sub>H<sub>y</sub> hydrocarbons, is enhanced in the presence of a sooty surface layer. To avoid this potential problem, conditioning consisted of baking to 350°C and helium glow discharges. No hydrogen or deuterium was introduced into the machine until the first plasma attempt.

With the improvements described above the 1993 campaign was very successful. As shown in Fig. 2.4-2, impurities were dramatically reduced when compared to 1992 VH-mode discharges with similar parameters. H-mode was achieved on the 14th plasma attempt (the 5th discharge with beam heating) which is rather remarkable after a six-month machine opening. A further indication of the rapid vent recovery was that VH-mode, which requires an extremely well conditioned wall, was readily reestablished even without boronization. This was the first time that VH-mode had been observed in DIII-D with unboronized walls. Furthermore, the first ohmic H-mode discharges at full toroidal field, 2.1 T, were obtained.

After a series of experiments to characterize the new graphite wall, boronization was again implemented. In order to improve film uniformity, the previous 2 injector system was upgraded to allow a more distributed gas injection using 16 injection points. After boronization, high performance VH-mode discharges produced a new record ion temperature of 21 keV and the highest triple product yet observed in DIII-D,  $n_D(0)T_{Ei} = 5 \times 10^{20} \text{ m}^{-3}\text{-s-keV}$ .

## 2.5. DIVERTOR CRYOPUMPING AND DENSITY CONTROL

During the past year, intensive efforts for developing an effective particle control technique came to fruition and for the first time since the discovery of the H-mode density controlled H-mode plasmas were produced. The advanced divertor cryopump project was successfully completed early in the CY94 and with its operation several important physics and technological "firsts" were achieved. These include: application of divertor cryopumping in a tokamak, attainment of density controlled H-mode plasmas, observation of helium exhaust in H-mode plasmas, and a systematic measurement of the dependence of confinement on H-mode plasma density.

The construction and installation of the DIII-D Advanced Divertor cryopump was completed in February. The cryopump was designed and constructed in collaboration with ORNL. Since the commissioning of the system in February of 1994, it has been functioning flawlessly, under some of the most severe conditions of thermal and disruption induced electromechanical stresses. The pumping speed was measured to be ~3500 l/s for deuterium. Thermal loads of up to 300 W did not affect the pumping speed. During the course of plasma operations last year, the pump withstood many high current disruptions. The successful operation of such a delicate system in the hostile environment of DIII-D is a significant engineering achievement.

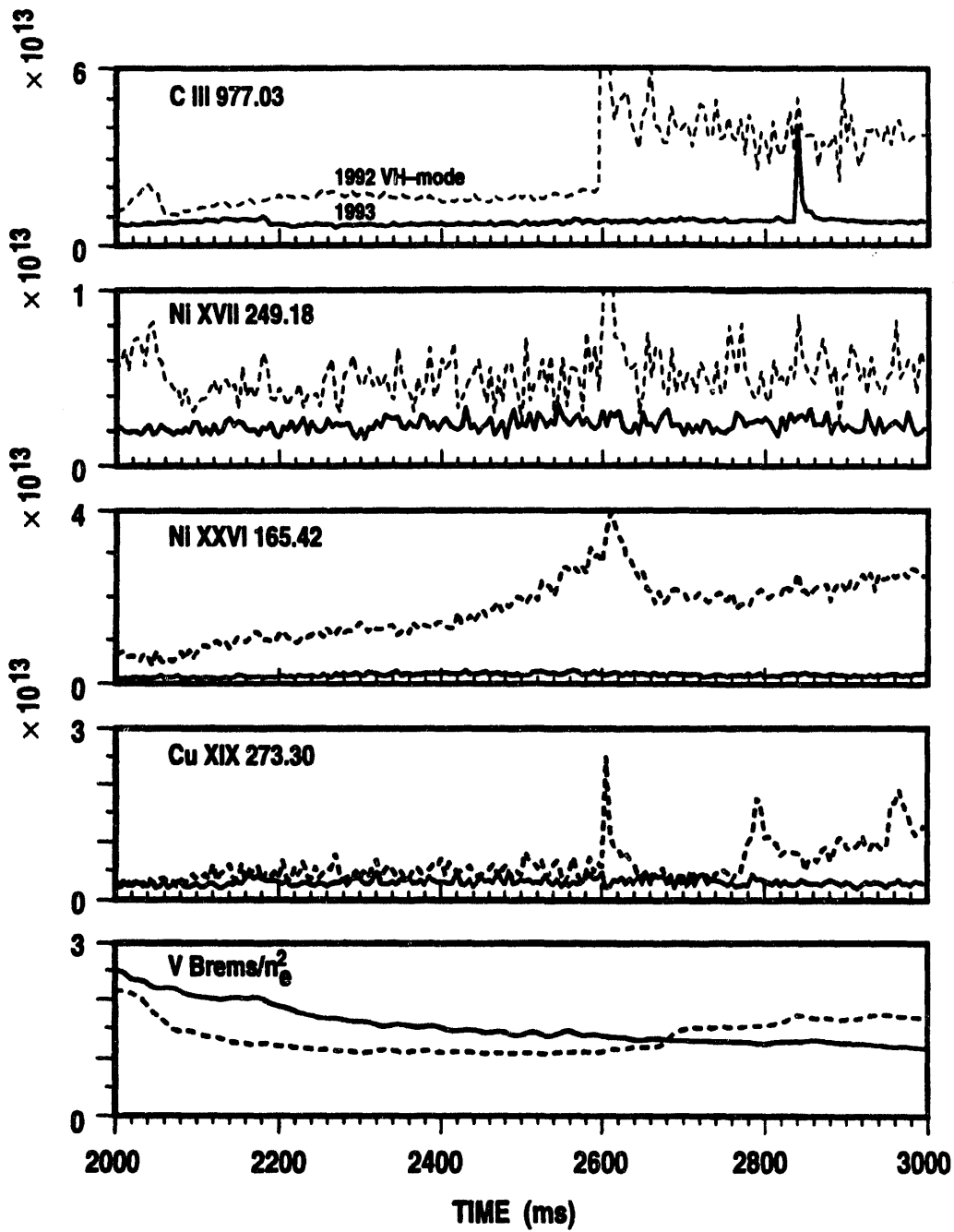


Fig. 2.4-2. UV impurity line radiation is reduced with the all-graphite wall

The primary objective of the advanced divertor program was to develop a technique for controlling the density of H-mode plasmas for transport studies and for increasing current drive efficiency. With the operation of the cryopump this goal was achieved. Plasma density of the H-mode plasma was controlled up to a range of factor of two, providing H-mode target plasmas for current drive and a sufficient range to measure the dependence of plasma confinement on density (Fig. 1.2-3).

Using the divertor cryopump, a systematic density scan of H-mode plasmas was carried out and energy confinement measured as a function of density at constant plasma current. For this purpose density controlled quasi steady-state H-mode plasmas were developed with plasma currents in the 0.75-1.5 MA range and densities in the  $3.5$  to  $9 \times 10^{13} \text{ cm}^{-3}$  range. Detailed energy and particle transport measurements were made on these plasmas. The data showed that heat transport in H-mode is very similar to the L-mode, i.e., confinement is roughly proportional to  $I_p$  and is insensitive to the plasma density. In contrast, particle transport was found to be a strong function of density, increasing rapidly with plasma density.

The ADP cryopump was also used to study helium exhaust in H-mode plasmas. To afford helium pumping, a thin layer of argon frost was deposited on the liquid helium-cooled cryopanel. With an argon frost layer of  $\sim 100$  monolayer thick, pumping speed for helium was measured to be 12,000  $\ell/\text{s}$ . Preliminary results show that helium can be exhausted efficiently from ELMing H-mode plasmas. The ratio  $\tau_{\text{He}}^*/\tau_E$  is in the range 10-15 which is within the acceptable range for a tokamak reactor.

## 3. ADVANCED TOKAMAK STUDIES

### 3.1. OVERVIEW

The goals of the DIII-D Advanced Tokamak Program are: to experimentally validate the simultaneous achievement of high confinement ( $H = \tau_E/\tau_{ITER-89P} \approx 4$ ) and high beta [ $\beta_N = \beta_T(\%) a(m) B(T)/I_p(MA) \approx 6$ ] in a noninductively driven, near steady-state discharge; and to develop the physics understanding in confinement, stability, and current drive needed to confidently build a compact DEMO reactor.

The feasibility of an advanced physics approach to tokamak reactors is clearly demonstrated by DIII-D experimental results. Several operational regimes have been explored which have shown improved confinement beyond that predicted by H-mode scaling relations. These high confinement regimes include VH-mode; high  $\ell_i$  H-mode, high  $\epsilon\beta_P$  ( $\epsilon$  is the inverse aspect ratio  $a/R_0$ ), and also possibly second stable core discharges. Several features of these discharges which have been shown to be important in obtaining the high confinement are sheared  $E \times B$  rotation, strong plasma shaping, and details of the current density profile.

This fiscal year, a considerable experimental effort was devoted to determine the role of plasma shape on energy confinement. It was found that energy confinement enhancement over L-mode (the factor H) increased with increasing triangularity  $\delta$  and varied at most weakly with elongation  $\kappa$ . From these experiments, it was concluded that the best configuration for the advanced tokamak would be the present full sized DIII-D double null divertor discharge,  $\kappa = 2.1$ ,  $\delta = 0.9$ . A compromise equilibria with  $\kappa = 1.75$ ,  $\delta = 0.8$ , compatible with both the radiative divertor and the advanced tokamak programs was chosen for future development. The cryopumps included in the radiative divertor with this configuration will provide particle control for a high triangularity discharge, needed for the advanced tokamak program.

With new experimental data, considerable progress was made in the understanding of the role of sheared toroidal rotation ( $E \times B$  flow) in reduced transport. The magnetic braking of the plasma with the  $n=1$  coil was used as an independent means of controlling core toroidal rotation and evaluating the effect of sheared rotation on two improved confinement regimes, VH-mode and high  $\ell_i$  H-mode. ( $\ell_i$  is the plasma internal inductance.) The thermal transport is shown to be reduced in the same location as the flow shear is reduced and in the correct relative magnitude as predicted by simple models which include the reduction in transport by the shear in the Doppler shifting of the turbulence. This verification of the importance of sheared rotation on the reduction of core transport puts renewed emphasis on the inclusion of a means of momentum input (co-injected neutral beams, applied rotating helical fields, etc.) on advanced tokamak scenarios.

The strategy chosen for simultaneously obtaining high confinement and high beta is to maintain the features necessary for the high confinement, and modify the current density profile with modest amounts of localized current drive to improve the stability at high beta. Modeling efforts are underway to verify that current profiles, consistent with simple transport models and rf current drive, can be obtained that are stable at high beta. In these modeling efforts, it is important to obtain the pressure profile and the current density profile (including the bootstrap current) consistent with reasonable transport models that give high confinement. In particular, the experimental high

confinement equilibria always exhibit a substantial pressure gradient near the boundary, with the associated bootstrap current that leads to higher edge current and lower internal inductance. The higher edge current density and the lower  $\ell_i$  are both features of the current density profile that contribute to lower beta limits.

Modeling efforts are focused on two operational scenarios. These scenarios the extended high  $\ell_i$  scenario and the second stable core VH-mode scenario. In the high  $\ell_i$  scenario, the discharge conditions begin with high  $\ell_i$ ,  $\kappa$ -ramped, ELMing H-mode; in these discharges both the improved confinement and the high beta limit are associated with the peaked current density profile, or high  $\ell_i$ , obtained transiently but the discharge relaxes to a near stationary lower  $\ell_i$  state. The challenge is to evaluate the maximum  $\ell_i$  that can be maintained with central current drive, consistent with the bootstrap current. Preliminary calculations indicate that  $\ell_i \approx 1.3$  and  $\beta_N \approx 3.5$  can be obtained self-consistently with 6 MW of FWCD and 11 MW of NBI. The relatively lower value of  $\ell_i$  is a result of the substantial bootstrap current that is obtained at high  $\beta_N$  and  $\beta_P$  ( $I_p = 1$  MA in this simulation), and the fact that the bootstrap current is highest near the plasma boundary. The details depend critically on the absorption of fast waves on the beam ions and the exact bootstrap current distribution which in turn depends on details of the transport and density profile. These details will be determined by experiment. In this high  $\ell_i$  model, it is assumed that  $q(0)$  is limited to approximately 1.0 by sawteeth. Stabilization of the sawteeth by fast particles, either from beams or ICRF could result in higher  $\ell_i$  discharges.

In the second stable core VH-mode scenario, conditions are obtained in a VH-mode discharge, and the profiles are maintained in the outer region of the discharge ( $\rho > 0.7$ ) needed for the high confinement. The VH-mode discharges already have very high confinement, but the stability limit at high beta is reduced as a consequence of the high edge pressure gradient and the high edge bootstrap current, both of which may be required for the improved confinement. The challenge is then to change the current density in the interior region of the plasma to improve the beta limit.

To increase the beta limit of the VH-mode against low  $n$  kink modes,  $q(0)$  on axis is increased to just below a rational value, 3.9, 2.9, 2.4, 1.9, etc. The  $q$  profile is made hollow with the minimum value just above a rational value, 3.1, 2.5, 2.1, 1.6, etc. Initial simulations were completed with  $q(0) = 2.4$ , and  $q_{\min} = 2.1$ . Difficulties in accurately controlling the detailed  $q$  profile were anticipated with such a small difference in the value of  $q(0)$  and  $q_{\min}$  and led to a choice of a larger value of  $q(0)$ . High beta equilibria were obtained stable to  $n=1$  kink with  $q(0) = 2.9$ , and  $q_{\min} = 2.1$ . It was shown that only modest amounts of FWCD and ECCD were needed to maintain the hollow  $q$  profile, with a plasma current of 1.6 MA.

More recently  $q(0)$  was further increased to 3.9 in the modeling of the second stable core VH-mode. This increase in  $q(0)$  leads to a better alignment of the total current and the bootstrap current, requiring less total current drive, and less current drive on axis. In addition, the larger negative shear near the axis and the larger difference in  $q(0)$  and  $q_{\min}$  is expected to be easier to control with localized rf current drive. With  $q_{\min} = 2.1$  or 2.5, high beta equilibria, stable to  $n=1$  kink are obtained. In particular, taking account of wall stabilization by the DIII-D vacuum vessel, equilibria with beta up to  $\beta_N = 6.4$  are obtained with  $q(0) = 3.9$ , and  $q_{\min} = 2.5$ ; stable to  $n=1$  kink. About 70% of the total current (1.6 MA) is bootstrap current, and 0.35 MA is driven locally by ECCD to maintain the hollow  $q$  profile, while the remaining 0.25 MA is driven by NBI. The stabilizing influence of the DIII-D wall is critical; with no wall stabilization, the maximum beta with  $q(0) = 3.9$ , and  $q_{\min} = 2.5$  is  $\beta_N = 2.4$ .  $n=1$  ideal stability is maintained in these second stable core VH-mode equilibria, although  $q$  passes through the 3/1 surface twice. Initial transport and stability simulations have been carried out for reactor size second stable core VH-mode scenarios. The equilibria are obtained by scaling DIII-D by a factor of 3.5, maintaining the same elongation, triangularity, and aspect ratio. The toroidal field of the reactor case is 5 T. Maintaining the same  $q_{95}$  as the DIII-D cases gives  $I_p =$

13.5 MA. Transport simulations readily give ignition with a fusion power of 1.5 GW using either the simple transport models consistent with DIII-D experiment or using RLW transport model. In the RLW model, the transport becomes neoclassical in the region where  $\nabla q < 0$ , and remains very high in the exterior region. Stability calculations have not yet been completed.

### 3.2. BETA-LIMITING INSTABILITIES IN DIII-D VERY HIGH PERFORMANCE DISCHARGES

Many high-performance discharges in DIII-D, such as VH-mode or high  $\beta_N$  H-mode discharges, have an ELM-free phase with good energy confinement that ends with a rapidly growing low- $n$  MHD instability. This event most often occurs at moderately large values of normalized beta,  $\beta/(I/aB) \sim 2.8$  to 3.5. The instability causes the loss of a significant fraction of the stored energy and, in the case of VH-mode, a transition to the lower level confinement of H-mode. Examination of fluctuation measurements and stability analysis of these discharges has shown that this instability may be a low- $n$  ideal kink mode destabilized by the combination of a large current density and a large pressure gradient near the discharge edge. A large edge pressure gradient is characteristic of the edge transport barrier associated with H-mode and VH-mode and, in low collisionality discharges, a large bootstrap current can result from this pressure gradient.

Figure 3.2-1 shows an example of a VH-mode termination. In the figure, the stored energy in a double-null divertor discharge increases steadily during ELM-free VH-mode, until a sudden MHD event causes the loss of about 20% of the plasma energy. In contrast to subsequent ELMs which primarily affect the edge of the plasma, soft x-ray emission indicates a sudden loss of energy beginning at the edge and extending across the entire profile within 100 to 300  $\mu$ s. The event is typically initiated by an MHD mode with toroidal mode number  $n \sim 3$  to 5. In the time-expanded plot of Fig. 3.2-1(b), about two cycles of an  $n = 5$  oscillation can be seen where the signals from two magnetic probes separated by  $36^\circ$  in toroidal angle are about  $180^\circ$  out of phase. This magnetic precursor suddenly grows within 20 to 50  $\mu$ s, consistent with ideal MHD time scales. An internal mode with  $m=1$ ,  $n=1$  is also present before the rapid instability, and probably contributes to the rapid loss of energy from the discharge core. In many cases the mode which initiates the instability has very little toroidal rotation or rotates in the electron diamagnetic direction, opposite to the direction of beam injection, which indicates that the mode is located near the edge of the plasma.

These observations are consistent with ideal kink mode stability calculations were made with the GATO code for another VH-mode discharge at the time of a similar MHD event. The equilibrium incorporated measured temperature and density profiles, leading to a large pressure gradient near the edge. The equilibrium reconstruction, including motional Stark effect (MSE) polarimetry measurements of the field line pitch near the center of the discharge, was most consistent with the presence of a large current density near the edge, as predicted by transport calculations of the bootstrap current. Edge-localized kink modes with  $n = 2$  to 4 were found to become unstable at the maximum beta reached experimentally, while the  $n=1$  mode was marginally unstable, in good agreement with experimental observations.

Both the pressure gradient and the current density at the edge appear to be important for destabilizing these modes. Results were obtained from model calculations with equilibria and profiles similar to the experimental VH-mode cases. With similar edge current density profiles (fixed current density at  $r/a=1$  and at  $r/a=0.95$ ) and fixed volume-averaged beta, increasing the edge pressure gradient causes  $n=2$  and 3 modes to become unstable. With fixed edge pressure gradient, increasing the edge current density again results in unstable modes with  $n=2$  and 3.

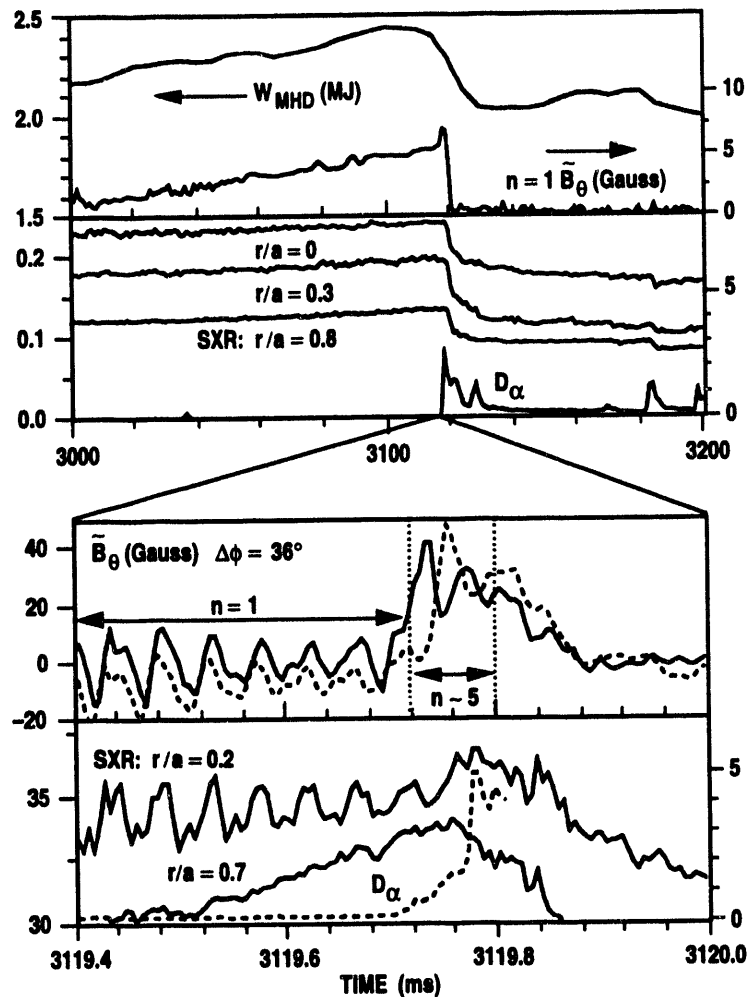


Fig. 3.2-1. Time evolution of the MHD event ending the ELM-free VH-mode phase of discharge 73203 ( $B_t = 2.1$  T,  $I_p = 1.6$  MA,  $\beta = 4.0\% = 3.2$  I/aB,  $\ell_i = 1.0$ ). Note the suppressed zero for several traces.

These results suggest that the combination of the edge pressure gradient and its associated bootstrap current destabilizes an edge-localized ideal kink mode or low- $n$  ballooning mode. Then if an internal mode ( $m/n=1/1$  for example) is already present and marginally stable, the profile changes caused by the edge mode can lead to rapid growth of the internal mode and sudden loss of energy from the core of the discharge.

Values of normalized beta [ $\beta/(I/aB)$ ] as large as 5 to 7 with optimized pressure and current density profiles have been predicted theoretically and confirmed experimentally. However, in reactor-relevant plasmas with low collisionality, high beta, and long pulse duration, the pressure and current density profiles cannot be chosen independently, but must be self-consistent through Ohm's law including the bootstrap current contribution. The resulting higher edge current and lower  $\ell_i$  lead to lower calculated beta limits.

The use of non-inductive current drive near the edge may break the constraint between current and pressure profiles, allowing the promise of high normalized beta to be realized in low-collisionality reactor-relevant plasmas. However, experimental evidence from DIII-D suggests that if the reduction of the edge current density is too large there can be a simultaneous reduction in confinement in H-mode or VH-mode discharges. For instance, in an ELMing H-mode discharge, a very rapid negative current ramp (2 MA/s), which reduces the edge current density, was used to increase  $\ell_i$ . The stored energy was observed to decrease simultaneously with the decrease in plasma current so the confinement normalized to  $I_p$  was approximately constant. This is opposite to the effect in L-mode discharges where normalized confinement increases with  $\ell_i$ . In this H-mode discharge, however, the large edge pressure gradient associated with the H-mode thermal barrier disappeared during the negative current ramp, resulting in a loss of about 50% of the stored energy. In other discharges, a rapid negative current ramp has been shown to prevent the transition from H-mode to VH-mode.

### 3.3. NONINDUCTIVE CURRENT DRIVE

Experimental programs are underway on DIII-D on fast wave current drive (FWCD) and electron cyclotron current drive (ECCD) to develop means of controlling the current profile. The FWCD tends to be deposited where the electron temperature is highest, which is near the center of the discharge. FWCD is therefore particularly useful for generating discharges with high  $\ell_i$ , in which the current is highly peaked on axis. ECCD has highest efficiency when it is localized near the axis, but it can also be conveniently placed well off axis by aiming the antennas toward the desired location or by changing the frequency or magnetic field to move the resonance to the proper place. This is important for generating discharges in which the core is in the second stable regime. The combination of FWCD and ECCD will provide a unique degree of control over the current profile in DIII-D.

The fast wave current drive antenna is located on the outer midplane of the vessel. It has four current straps spaced 22 cm between centers. Each strap has a vacuum feedthrough to provide for independent phasing. The straps are 45 cm high and 11 cm wide. The antenna was powered by a 2 MW source operating at 60 MHz. The maximum power delivered to the plasma was 1.6 MW. The Faraday screen used in these experiments is a single layer of Inconel rods which are tilted to be parallel with the total magnetic field. Tuning of the antenna is facilitated by use of feedback control of the plasma position to keep the loading resistance of the antenna fixed, which is implemented through the digital control system that controls the parameters of the plasma equilibrium.

A newly installed array of rf pickup loops was placed at several locations to study the propagation and absorption of fast waves. Measurements of the phase, amplitude, and polarization of the wave magnetic field at the location of each loop tend to support the expected wave physics. For example, with the antenna straps all at the same phase ( $0^\circ$ ), the wave travels directly across the plasma to the centerpost, but for phasings like  $(0, \pi, \pi, 0)$  or  $(0, 0, \pi, \pi)$  the wave does not travel directly across the plasma but it is seen as the wave travels toroidally. Most importantly, when the antenna is phased for current drive,  $(0, \pi/2, \pi, 3\pi/2)$ , the wave is in the direction launched. This indicates that the spectrum of parallel wavenumber  $k_{\parallel}$  excited in the plasma by the antenna is in fact directional.

Three types of fast wave current drive experiments were performed. In the first, the plasma was held in L-mode with fixed plasma current. On different discharges, the current was changed in order to determine the conditions under which the maximum fraction of the plasma current could be maintained noninductively. In the second type of FWCD experiment, the plasma current was ramped rapidly down just before or during the FWCD. In the third, the plasma was put into the H-mode through high power neutral beam injection before the FWCD was applied. The first two types of experiments used low toroidal field, about 1 T, along with second harmonic 60 GHz ECH. The high electron beta and high electron temperature generated in this manner improve the single pass damping, but the

density is limited to below  $1.5 \times 10^{19} \text{ m}^{-3}$  by the ECH cutoff. The experiments with NBI were performed at 1.9 T, which was chosen to minimize the second harmonic hydrogen minority damping which can be a moderately strong absorber in NBI discharges with higher ion temperature.

Experiments with fixed plasma current showed that the largest fraction of the plasma current was supported noninductively when the total plasma current was 0.3 MA. For currents significantly smaller than 0.3 MA, the electron temperature was too low for effective absorption of the fast wave, while at higher currents the relative fraction of the noninductive current fell. At 0.3 MA, up to 0.18 MA of the current was driven noninductively using 1.5 MW of fast wave power plus about 1 MW of ECH power. The divertor cryopump was used to help control the density rise which normally accompanies fast wave power. These FWCD results represent a moderate improvement over results presented previously, due primarily to increased rf power.

The current drive efficiency of FWCD in this regime is about  $\eta = 0.02$  to  $0.03 \times 10^{20} \text{ A/m}^2\text{W}$ . The new data points are shown in Fig. 3.3-1 along with the data points previously published. It appears from this figure that the measured efficiency is improving linearly with electron temperature.

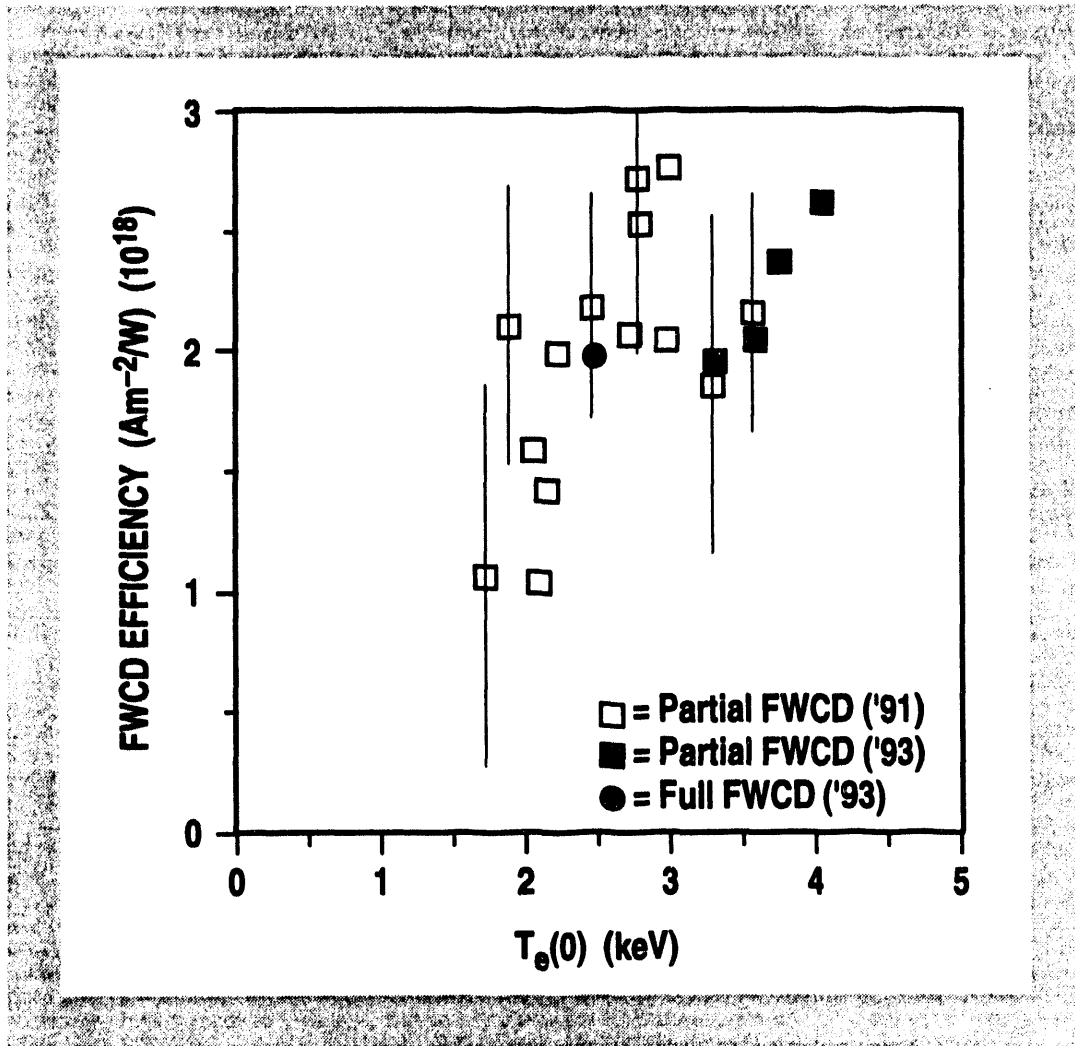


Fig. 3.3-1. The current drive efficiency as a function of central electron temperature.

In the second set of experiments, in which FWCD was combined with a ramp-down of the plasma current, full current drive was demonstrated. For these experiments, the plasma current was ramped down from 0.4 MA to around 0.2 MA during combined FWCD and ECH injection. The purpose of the current ramp was to generate a discharge with high confinement relative to that of a steady discharge of the same current, due to the improved current profile (high  $\ell_i$ ) which is generated when current is removed preferentially from the outer part of the discharge. In this manner, a discharge with improved characteristics (higher temperature and lower current to support) is generated. The resultant high  $\ell_i$  profile is also expected to more closely match the profile of driven current characteristic of FWCD.

Discharges with co-FWCD and with symmetric phasing were compared. During and just after the current ramp, the loop voltage was negative in order to decrease the current in accordance with the preprogrammed decrease in the reference current. In the co-FWCD case, the surface loop voltage was observed to remain negative while the high power FWCD and ECH were applied. Changing the FWCD antenna phasing from co-current to a nondirectional phasing (0,  $\pi$ ,  $\pi$ , 0) resulted in a more positive loop voltage, the analysis of which found no measurable current drive. These results indicate that complete current drive was achieved, albeit for a short period, and the amount of current drive depends upon the phasing of the FWCD antenna. The measured FWCD efficiency for full current drive cases is in reasonable agreement with the values determined experimentally for discharges with fixed current, as shown by the data point for a ramp-down case in Fig. 3.3-1.

In the third set of experiments, FWCD power was applied to H-mode discharges with several MW of neutral beam heating. The principal difficulty was coupling high power through the edge of the plasma in the presence of ELMs. For low frequency "giant" ELMs, the large changes in the plasma density near and just outside the separatrix caused very large excursions in the loading. Typically, the loading increases during a giant ELM by a factor 5, from 1-2  $\Omega$  to nearly 10  $\Omega$ . These large increases in loading have the same effect on the VSWR as an arc would have, and therefore they invariably trip the reflected power monitor and cause the transmitter to roll back. This severely limits the power which may be applied to the plasma in the presence of giant ELMs. For small frequent "grassy" ELMs, however, the effect is much smaller. The ELMs are changed from giant to grassy by increasing the neutral beam power. Under this condition, it appears that the loading is able to average over the ELMs and produce loading which is independent of the phase of the ELM. The average loading stays at an acceptable level in the neighborhood of 2  $\Omega$ . The peak fast wave power which has been coupled in such discharges is 1 MW. These discharges were at higher density than normally used for current drive experiments, and due to the relatively low power and high density, current drive effects were not measurable.

Modeling of transport and current drive in DIII-D shows that 4.6 MW of fast wave power plus 2.5 MW of neutral beam power or ECH power can support a fully noninductive high  $\ell_i$  discharge with average beta of 2% and total current of 1 MA. In order to achieve a second stable core configuration, it is necessary to drive current well off axis, and ECH is suitable for this purpose. With 8.5 MW of ECCD, 0.4 MA of current can be driven near  $r/a \approx 0.5$ , which supports the current profile expected to be stable to a beta above 5.7%.

### 3.4. HIGH $\beta_p$ IMPROVED CONFINEMENT

Experiments to explore the long-time evolution of noninductive, high  $\beta_p$  plasmas in the DIII-D tokamak have identified a new, quiescent, high performance regime. The experiments were carried out at low current (400-800 kA) with the medium power neutral beam injection (3-10 MW). This regime is characterized by high  $q_0$  ( $>2$ ) and moderate  $\ell_i$  ( $\sim 1.3$ ). It is reached by slow relaxation of the current profile, on the resistive time scale (Fig. 3.4-1). As the profiles relax,  $q_0$  rises and  $\ell_i$  falls. When  $q_0$  goes above 2 (approximately), MHD activity

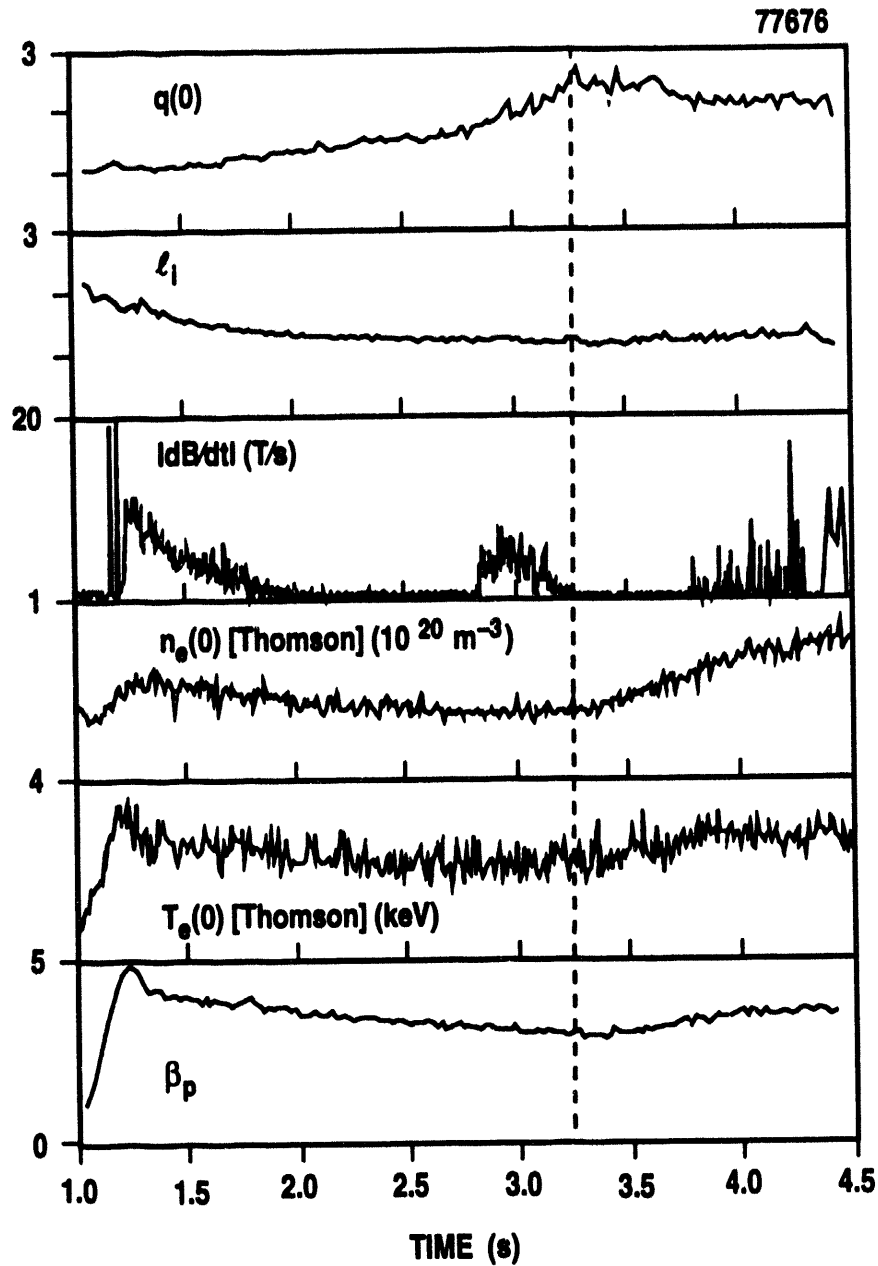


**Fig. 3.4-1.** Time history for discharge 77676. NBI starts at 1 s. Note that before 3.3 s,  $q_0$  is rising and  $l_1$  is falling, indicating relaxation from the initial peaked Ohmic current profile to a broader, noninductive (~50% bootstrap and 50% NBCD) profile. At about 3.3 s,  $q_0$  is above 2, Mirnov activity vanishes, and the central density, central temperature, and total energy begins to rise.

disappears, and the stored energy rises. Most dramatic is the strong peaking of the central density, which increases by as much as a factor of two (Fig. 3.4-2). The improved central confinement appears similar to the PEP/reversed central shear/second stable core modes seen in other tokamak experiments, but in this case without external intervention or transient excitation. At the time of transition to the improved core confinement regime, when the density begins to peak up, the entire plasma profile is calculated to either be in or have access to the second ballooning stability regime.

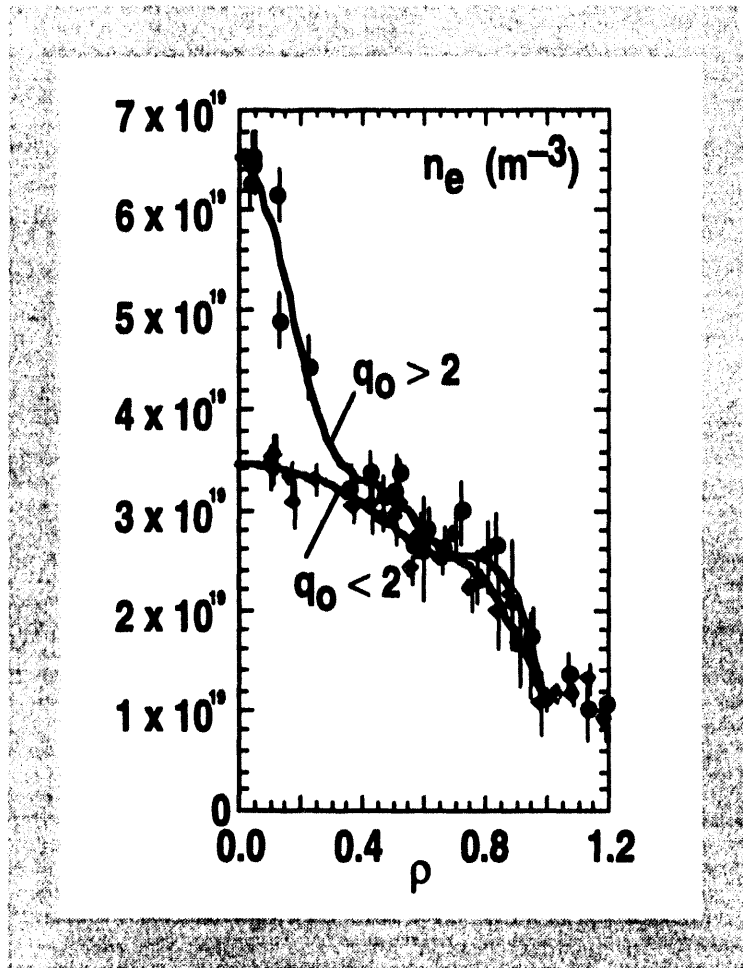


Fig. 3.4-2. Comparison of density profiles at 3.36 s (◆; just after beginning of improved core confinement regime) and at 4.36 s (●; just before end of discharge), showing doubling of central density and strong peaking.

At higher current, a similar but slower relaxation is seen. Also notable in connection with these discharges is the behavior of the edge and SOL. The ELMs, as seen previously, are small and very rapid (up to 1 kHz). The SOL exhibits high density ( $\geq 1 \times 10^{19} \text{ m}^{-3}$ ), which shows little or no fall-off with radius. Also the power deposition at the divertor surface is very broad, up to four times the width usually seen in ELMing H-mode. This regime is of particular interest for the development of steady-state tokamak operating scenarios, for the TPX experiment and for following reactors.

## 4. TOKAMAK PHYSICS

### 4.1. OVERVIEW

During the past year the DIII-D experimental program made significant progress toward a better understanding of confinement in enhanced confinement modes such as H-mode and VH-mode as well as determining the role of plasma shape in confinement. A plasma shape study resulted in the identification of a high triangularity, moderate elongation double-null divertor configuration that is compatible with both the enhanced confinement and high beta needs of an advanced tokamak and the enhanced radiation and impurity entrainment needs of a radiative divertor configuration. It is anticipated that this plasma shape will allow us to meet our long range program goals.

H-mode studies were focused in the areas of L-H transition studies including further studies on the role of fluctuation suppression by sheared  $E \times B$  flows, threshold power studies, and decorrelation of density and current. H-mode power threshold studies were revisited with the vessel walls covered with graphite tiles and boronized and with deuterium NBI into deuterium plasmas. The power threshold was reduced by 60%--70% compared to previous results with hydrogen beams and unboronized, predominantly inconel vessel walls. Although the general scaling of the threshold power remained similar to the previous study in 1988, differences in scaling between single-null and double-null divertor configurations were identified. Utilizing the divertor cryopump to hold density constant while varying plasma current it was verified that energy confinement is linearly related to current with little or no dependence on density.

With the combination of boronized, graphite covered vessel walls a new record triple product was obtained in VH-mode of  $n_D(0) \tau_E T_i(0) = 5 \times 10^{20} \text{ m}^{-3} \text{ s keV}$ . Further studies of transport in the VH-mode utilizing the  $n=1$  coil to vary the plasma rotation ("magnetic braking") supported the hypothesis that the enhanced confinement is a result of increased shear in plasma rotation near the plasma edge that extends further in toward the plasma core when compared to H-mode discharges. Similar magnetic braking experiments performed in elongation ramped high  $\ell_i$  H-mode discharges showed a similar correlation between reduced core flow shear and reduced confinement.

Confinement scaling experiments with rf heated dimensionally similar discharges brought a more unified understanding to this area. Electron transport was found to be gyro-Bohm like while ion transport was found to be worse than Bohm. Single fluid transport analysis yields a result which is dependent on which species is the dominant loss channel. When the losses are comparable in each species, as was typically the case in previous experiments with NBI heating, the single fluid transport appeared to be Bohm-like, the average of electron and ion behavior.

### 4.2. H-MODE CONFINEMENT

A standard characteristic of the L-mode to H-mode transition is the rapid density ( $n_e$ ) increase following the transition. In most tokamaks, and especially DIII-D, the steady-state H-mode density and plasma current ( $I_p$ ) are closely coupled. This colinearity has prevented an independent determination of the scaling of the thermal plasma confinement  $\tau_{th}$  with  $n_e$  and  $I_p$ . Previous single machine empirical H-modes scalings have for the most

part assumed that the density scaling of confinement was weak and may therefore be ignored. Even some of the multi-machine collaborative efforts that have produced confinement scalings have not been able to separate the  $I_p$  and  $n_e$  dependencies.

The DIII-D advanced divertor system was designed and built with the primary goal of particle control in H-mode plasmas. For the first time in the DIII-D H-mode confinement regime, orthogonal scans in  $I_p$  and  $n_e$  have been obtained by utilizing the in-vessel divertor cryopump. The plasma density was controlled by a combination of gas puffing and divertor pumping. The pumping rate was controlled by magnetically adjusting the position of the divertor strike point relative to the pumping aperture. For operational stability simultaneous pumping and gas puffing was not allowed. The deuterium single-null target plasmas were operated at  $B_T = 2.0$  T,  $\kappa = 1.8$ , with the  $\nabla B_T$  drift towards the X-point, and at 0.75 MA and 1.5 MA (Fig. 4.2-1). The H-mode was obtained by the application of 6 MW of deuterium neutral beam heating at an average energy of 65 keV.

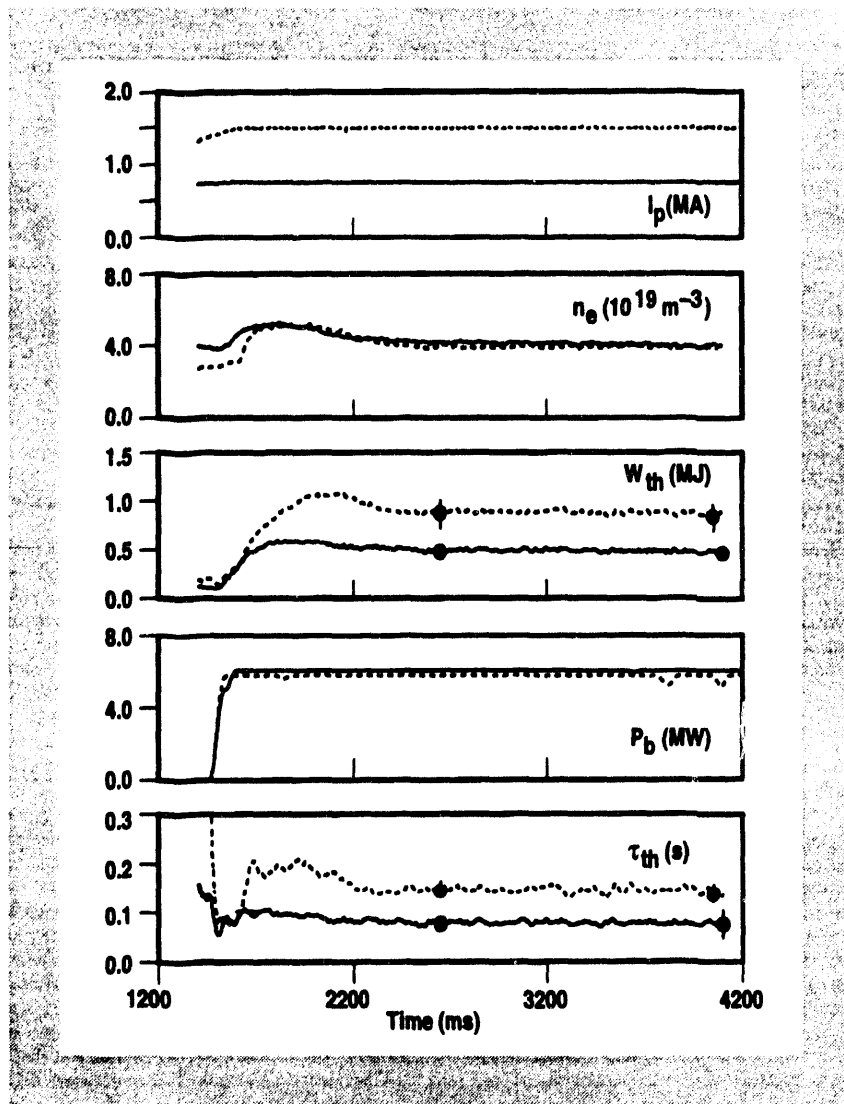


Fig. 4.2-1. Use of cryopumping to keep  $n_e$  fixed at two different values of  $I_p$ . (Beam power is same.)

With the colinearity broken it was possible to examine the independent effect that  $n_e$  and  $I_p$  had on the thermal energy confinement time. It was found that a power law representation of  $\tau_{th}$  implies that  $\tau_{th} = 0.13 I_p^{0.94 \pm 0.06} n_e^{0.13 \pm 0.06}$ . In a one-fluid power balance analysis the effective thermal diffusivity ( $\chi$ ) was reduced with increasing  $I_p$  and was basically independent of  $n_e$  (Fig. 4.2-2). Our results therefore validate the previous assumptions that have been made regarding the independence of the global confinement on density. Additionally, it was observed that the core particle confinement increases with plasma density. This result suggests that for future machines low density operation may be more favorable since it would reduce the ratio of particle confinement to energy confinement ( $\tau_p/\tau_E$ ).

### 4.3. VH-MODE EXPERIMENTS

The VH-mode experiments in 1993 had three main goals. First, reproducing last year's results with the new, all-carbon vessel walls to be sure that these walls were compatible with VH-mode operation. Second, further

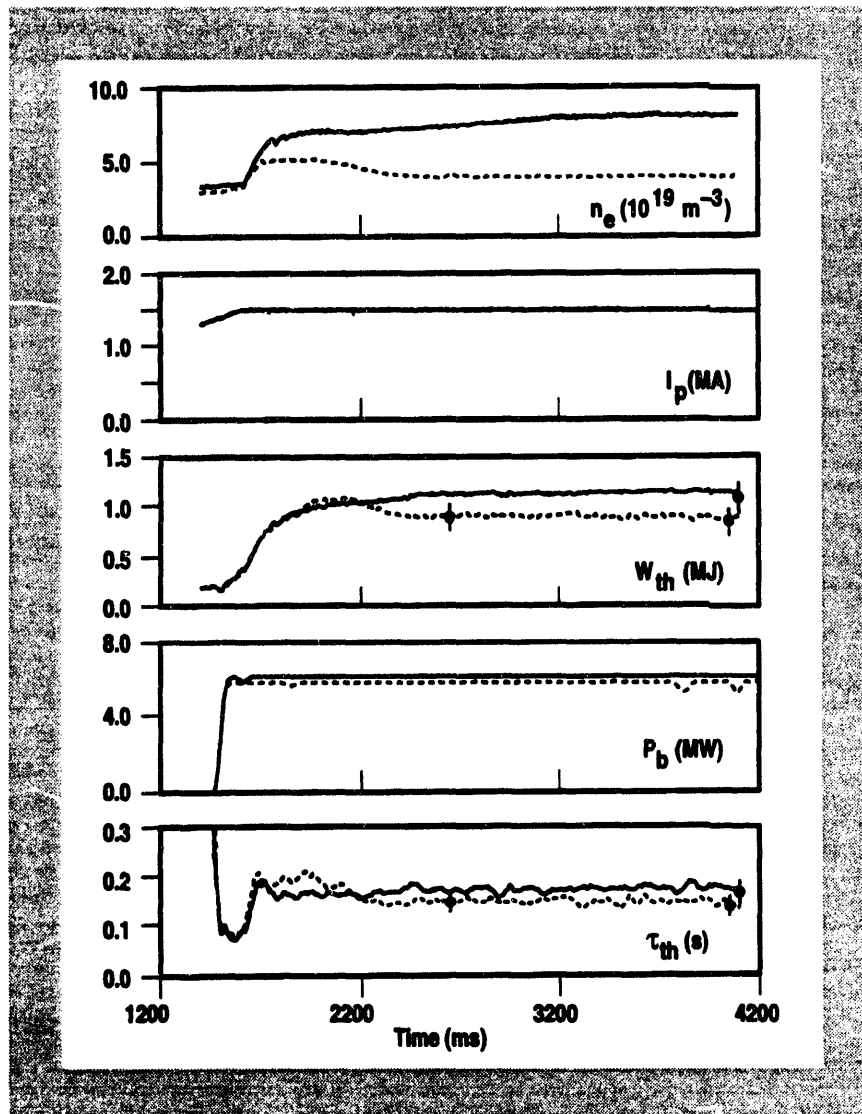


Fig. 4.2-2. Use of cryopumping to vary  $n_e$  at fixed  $I_p$  and beam power.

experiments to investigate the role of sheared  $E \times B$  flow in the confinement improvement in VH-mode. Third, high triangularity VH-mode plasmas were the focus of the plasma shape experiments that are discussed in Section 4.4.

At the beginning of the run period in 1993, the new, all-carbon vessel walls presented a new challenge for the DIII-D experimentalists. Although several other groups had run tokamak plasmas in all-carbon vessels, no one had achieved VH-mode in an all-carbon vacuum vessel. Machines like JET had required vessel conditioning with beryllium to get VH-mode. A complete set of plans was developed for cleaning the new walls with a number of options, depending on how difficult the cleaning was found to be. Possibly because of the extensive pre-installation cleaning of the tiles, the vessel cleanup actually went significantly faster than expected and high performance, VH-mode plasmas were achieved in an all-carbon vacuum vessel without need for the boronization that was used in 1991 and 1992. The lesson from this result is that VH-mode requires clean wall conditions, but there are a variety of ways of reaching those conditions.

The core confinement improvement seen when the double-null plasmas go from H- to VH-mode has been clearly related to the change in the  $E \times B$  flow shear. Both spatial and temporal correlations have been established between the change in local  $E \times B$  shear and the change in thermal transport. Local transport and density fluctuations change significantly in the same region where the sheared  $E \times B$  flow changes most. In addition, the  $E \times B$  shear begins to change 20 to 40 ms prior to the first detectable change in the ion thermal transport.

In the plasma core,  $E_r$  is associated primarily with the ion toroidal rotation. Previous work with magnetic braking using a non-axisymmetric vertical field had shown that the toroidal rotation could be significantly altered without changing the neutral beam input power by means of this technique. Accordingly, we devised an experiment to test the  $E \times B$  shear stabilization hypothesis in which the toroidal rotation was altered and then investigated the effect on the local thermal transport.

In Fig. 1.2-5(a) and (b), the magnetic braking technique is shown to alter the electric field and the shear in the  $E \times B$  flow quite significantly. More importantly, as is seen in Fig. 1.2-5(c), there is a clear change in the local single-fluid thermal diffusivity in the same region where the shear in the  $E \times B$  flow has changed. There is also a corresponding change in the density fluctuations, with the level increasing when the  $E \times B$  shear is reduced. Accordingly, the results of this experiment are consistent with the predictions of the  $E \times B$  shear stabilization hypothesis.

Figure 1.2-5(b) also shows that the shear in the  $E \times B$  flow is significantly larger than that required theoretically to stabilize turbulence. At the right hand edge of the figure, the level predicted by the theory of Biglari et al. is indicated. (This has been evaluated using edge measurements of radial correlation length, wavenumber and decorrelation frequency.) The measured  $E \times B$  shear at the plasma edge is well above this level. Another theoretical estimate of the shear level needed to stabilize turbulence is given by  $C_s/R$ , where  $C_s$  is the sound speed and  $R$  is the major radius of the magnetic axis. Since  $C_s$  is the largest at the magnetic axis where the electron temperature is maximum, we have evaluated this quantity at that point. Clearly, in the region of the plasma where significant shear stabilization appears to be taking place, the measured shear in the  $E \times B$  speed is above this upper limit.

In utilizing magnetic braking in a transport study, one must be sure that the effects of the non-axisymmetric magnetic perturbation itself are not affecting the transport by creating magnetic islands. There are several reasons to believe these islands have little if any effect. First, in L-mode and ELMing H-mode discharges, the effect of magnetic braking on local transport was studied and found to be negligible. These experiments were done with error field levels comparable to those used in the present experiment. Second, theoretical predictions of the effect of islands on confinement indicate that even the vacuum field islands caused by our non-axisymmetric coil would only affect the total calculations which, when applied to our case, indicate that the island width including the

plasma response should be about a factor of 30 less than that of the vacuum islands. Since these calculations are the same ones which allow us to understand the locked MHD mode threshold there is some independent confirmation of their accuracy.

Loss of fast ions due to  $n=1$  ripple from the magnetic perturbation coil is another direct effect which can be ruled out. If the loss of fast ions were large enough to significantly affect the transport analysis shown in Fig. 1.2-5, there would have to be a loss of about half of the fast ions before they could deliver their heat to the plasma. This would result in at least a factor of two decrease in the neutron rate from the plasma, since most of the fusion neutron emission comes from fast ions from the neutral beams interacting with the background plasma. One would actually expect more than a factor of two change in the neutron emission, since the shot with the magnetic braking is colder, resulting in a reduced fusion yield due to more rapid slowing down of the fast ions. The transport analysis calculates that the neutron rate should differ by a factor of 1.5 between the two shots due to this effect. The measured ratio of the neutron rates is 1.4. Since the transport analysis ignores effects of ripple loss, the agreement between calculation and measurement indicates that the ripple loss is unimportant.

Improved confinement has also been seen in discharges in which the elongation has been suddenly increased, thus increasing the plasma internal inductance. Although a portion of this confinement improvement is probably associated with the change in inductance, a portion is apparently also due to the change in  $E \times B$  velocity shear. This has been investigated by using the magnetic braking technique to slow the toroidal rotation in some of these shots after the elongation ramp is over. Changes in local thermal transport were seen, with the biggest changes occurring when the change in the  $E \times B$  velocity shear was the greatest.

#### 4.4. PLASMA SHAPE EXPERIMENTS

An experiment was carried out this year to explore the effect of plasma shape on confinement. The basis of the experiment lies in a previous observation that there is a systematic difference single-null and double-null diverted plasmas in plasma performance, as measured by the product  $\beta \cdot \tau$ .

The goals of the experiment were to further explore the underlying cause of this difference and to explore the performance characteristics of particular plasma shapes of interest for the DIII-D radiative divertor. Of major importance is finding a configuration which is consistent with the goals of the DIII-D Advanced Tokamak and Radiative Divertor Programs. The results are also of considerable interest for the designs of TPX, JT-60SU, and possible improvements to JET.

The principal result of the experiment is that plasma triangularity,  $\delta$ , is critical to plasma performance, while plasma elongation,  $\kappa$ , plays a lesser role. Whether the plasma is single- or double-null is not of importance, aside from the attendant limitation on  $\delta$ . The difference in energy content of the low and high triangularity lies principally in the temperature profiles for normalized radius less than 0.8. The high triangularity plasmas exhibit a temperature gradient all the way to the magnetic axis, whereas the low triangularity plasmas have a large central region where the temperature profile is flat. This results in about a factor of two difference in axial values of ion and electron temperature. It is observed that  $q_0$  rises above unity when the triangularity is high, but this is not the case when the triangularity is low.

The product  $\beta \cdot \tau$  is used as the principal figure-of-merit, although we also shall refer to the normalized product  $\beta_N H$ , where  $H \equiv \tau_E / \tau_E^{\text{ITER-89P}}$  is the confinement enhancement over L-mode, and  $\beta_N \equiv \beta / (I_p / a B_T)$ . Furthermore, our focus remains the transient, high performance phase of the discharge (VH-mode) since the overall goal of the

DIII-D program is to provide the necessary profile control to sustain such performance. Of particular interest is central electron temperature because of its importance to current drive efficiency.

In the experiment four double-null shapes were investigated, including the standard DIII-D double-null, a)  $\kappa \approx 1.8$ ,  $\delta \approx 0.9$ , b)  $\kappa \approx 2.1$ ,  $\delta \approx 0.3$ , c)  $\kappa \approx 1.8$ ,  $\delta \approx 0.3$ , and d)  $\kappa \approx 1.8$ ,  $\delta \approx 0.8$ , (Fig. 4.4-1). The particular choices are determined partly from physics motivation, and partly from preliminary design work done on the Radiative Divertor. It was felt to be necessary to return to the standard configuration because the addition of carbon armor tiles to the outer wall of the DIII-D vacuum vessel introduced uncertainty as to the performance capability. A descriptor of plasma shape is  $S \equiv (I_p/aB_T)q\psi$ . If combined with JET/DIII-D confinement scaling, then

$$\beta \cdot \tau = \text{const.} \left( \frac{S^2 R^2}{\kappa} \right) \left( \frac{F}{q} \right)^2,$$

where  $F \equiv \tau_E/\tau_{E,JET/DIII-D}$ .

In Fig. 4.4-1 is plotted  $\beta \cdot \tau$  versus the geometric factor ( $S^2 R^2/\kappa$ ). The large symbols are results from this experiment, and the small plus signs are previous data, much of which is in single-null plasmas. Each point represents a separate discharge. As can be seen, the results are consistent with previous work. Also shown is the plasma shape for each category of discharge in this experiment.

In Table 4.4-1 the results of these experiments are summarized. For shape D  $\beta \tau_E^{th} = 1300$  (% ms) is achieved as opposed to a best value of 1700 in shape A. Similar values of  $\beta$ ,  $\beta_N$ ,  $T_i(0)$ ,  $T_e(0)$ , and  $n_D(0)T_i(0) \tau_E^{th}$  were achieved in both. One notable difference was in the duration of the ELM-free period. For shape A, the ELM-free period was usually a large fraction of a second and has reached 1.3 s. For shape D the ELM-free period was typically about 200 ms. While this does make the  $\dot{W}$  correction to  $\tau_E^{th}$  somewhat larger, as noted above similar values in absolute quantities were achieved as the rate of rise of stored energy was much faster. This shows that the plasma parameters achieved do not depend directly on the length of the ELM-free period. In both cases the optimum  $\beta \cdot \tau$  occurs for  $q_{95} \geq 4$  while the optimum  $\beta_N H$  occurs at  $q_{95} \geq 4$   $H$  drops so rapidly that  $\beta \cdot \tau$  actually decreases.

Plasmas with low triangularity ( $\delta < 0.4$ ) did not perform well. They exhibit longer L-mode durations prior to the L-H transition, still shorter ELM-free periods of order 100 ms, no "spin-up" of the toroidal velocity, and considerably lower plasma parameters compared to the plasmas discussed above. While the high performance plasmas are greatly affected by the vessel wall conditions, these low triangularity plasmas are insensitive to such changes.  $\beta \cdot \tau$  values reached 700 and 500 (% ms) at  $\kappa$  values of 2.1 and 1.8 respectively. For shape C recycling was reduced by use of the ADP cryopump, however there was no lengthened ELM-free period as is seen with reduced recycle for high triangularity plasmas. It is noteworthy that the difference in performance is very much reflected in reduced central  $T_e$ .

## 4.5. WALL STABILIZATION OF IDEAL KINK MODES

During FY93, stronger, more convincing evidence of wall stabilization was obtained on DIII-D. The most promising Advanced Tokamak scenarios envisaged in DIII-D and TPX (notably, the Second Stable Core and High Poloidal Beta scenarios), require complete wall stabilization on a steady state time scale in order to reach even

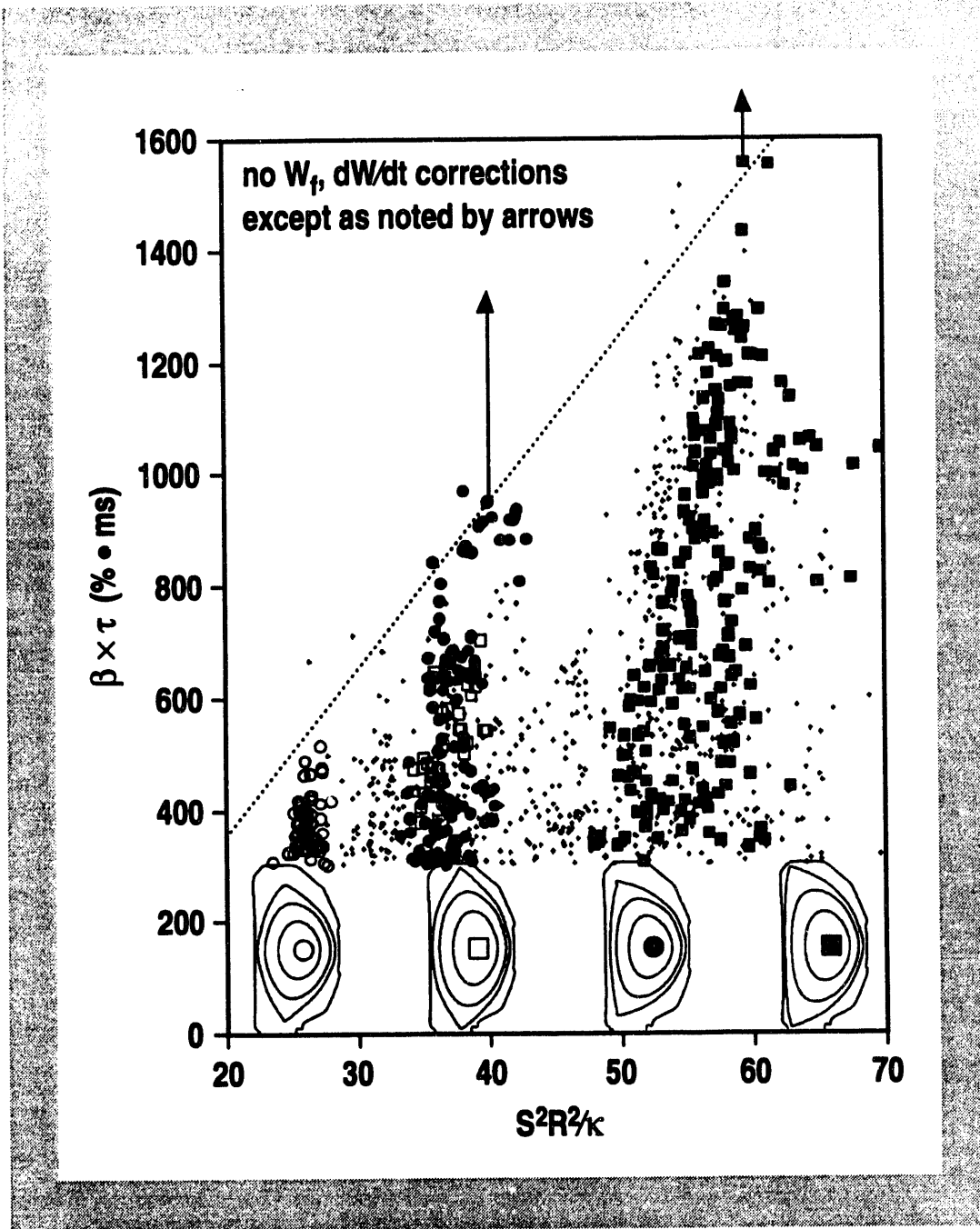


Fig. 4.4-1. Performance figure-of-merit  $\beta\tau$  versus shape parameter  $S^2 R^2 / \kappa$

moderate beta values. With wall stabilization from the vacuum vessel (in DIII-D) or nearby conducting plates (in TPX), the gain in the beta limit is large — up to a factor 2. However, simple theoretical models predict an instability which grows on a characteristic time scale for a resistive wall  $\tau_{res}$  when the plasma is ideally stable with a perfectly conducting wall but unstable for no wall. With no plasma rotation, this mode is simply the external kink "soaking through" the resistive wall. With plasma rotation, the situation is a little more complicated, but the theory

**Table 4.1**  
**BEST PERFORMANCE IN DIFFERENT CONFIGURATIONS**

	$\kappa \approx 2.1$	$\kappa \approx 1.7$
$\delta \approx 0.9$	$\beta \gtrsim 5\%$ , $\beta_N \gtrsim 4$ $T_e(0) \approx 7.5$ keV, $T_i(0) \gtrsim 20$ keV $\tau_E^{th} \gtrsim 0.4$ s, $H \gtrsim 3.3$ $n_D(0)T_i(0)\tau_E^{th} \approx 4 \times 10^{20}$ keV $\cdot$ s $\cdot$ m $^{-3}$ $\beta\tau^{th} \approx 1.7\% \cdot$ s Typical ELM-free period 0.65 s	$\beta \gtrsim 5\%$ , $\beta_N \gtrsim 4$ $T_e(0) \approx 7.5$ keV, $T_i(0) \gtrsim 15$ keV $\tau_E^{th} \gtrsim 0.4$ s, $H \gtrsim 3$ $n_D(0)T_i(0)\tau_E^{th} \approx 3 \times 10^{20}$ keV $\cdot$ s $\cdot$ m $^{-3}$ $\beta\tau^{th} \approx 1.3\% \cdot$ s Typical ELM-free period 0.22 s
$\delta \approx 0.3$	$\beta \lesssim 3.7\%$ , $\beta_n \lesssim 3.2$ $T_e(0) \lesssim 5$ keV $\tau_E^{th} \lesssim 0.3$ s, $H \lesssim 2.2$ $\beta\tau^{th} \lesssim 0.7\% \cdot$ s* Typical ELM-free period 0.10 s	$\beta \lesssim 2.8\%$ , $\beta_n \lesssim 3.5$ $T_e(0) \lesssim 5$ keV $\tau_E^{th} \lesssim 0.3$ s, $H \lesssim 2.5$ $\beta\tau^{th} \lesssim 0.5\% \cdot$ s* Typical ELM-free period 0.15 s

\*Maximum occurs after ELMs begin.

predicts that even though the ideal kink is stabilized by AC stabilization when  $\omega$  is greater than the wall  $\tau_{res}^{-1}$  growth rate (essentially, the image currents in the wall are continually regenerated by the rotating mode so they don't decay), a new "resistive wall mode" that is locked to the resistive wall appears with a growth time of the order of the wall resistive time.

On the other hand, stability analysis of DIII-D discharges over the past several years has provided strong hints that the DIII-D vacuum vessel is playing a role in stabilizing the ideal kink for times much longer than the wall resistive time. The evidence comes from several sources. First, when displayed in the parameter space of normalized beta ( $\beta_N$ ) and internal inductance ( $\ell_i$ ), many discharges fall between the theoretically predicted stability boundaries computed with and without wall stabilization but none fall very far outside the boundary computed with wall stabilization. Second, the beta limit in DIII-D is at  $\beta_N \approx 3.5$  (in the absence of current and elongation ramps), whereas in ASDEX, as well as in ASDEX-like discharges in DIII-D, where the wall is much further from the plasma, the beta limit is  $\beta_N \approx 2.8$ . Although other explanations are possible, the most obvious and likely one is that wall stabilization in the full-sized DIII-D discharges stabilizes the external kink and allows a higher beta limit, up to the point where the ideal kink mode is unstable even with a perfectly conducting wall. Third, in DIII-D discharge 69608, a detailed equilibrium and stability analysis revealed that with no wall, the discharge would be unstable to an ideal predominantly  $m/n = 1/1$  kink mode but with a large mode displacement at the plasma edge coupled to the  $1/1$  mode. Such a global instability is not consistent with the observed saturated rotating internal  $1/1$  mode. However, the calculations with a perfectly conducting wall found a  $1/1$  mode with much reduced edge displacement that is consistent with the observed saturated mode.

The experimental evidence appears to contradict the simple theory but none of the evidence is entirely convincing, since, except in the single case of discharge 69608, no detailed analysis was done for individual discharges — the improved stability of the full-sized DIII-D discharges over the ASDEX discharges, and over the theoretically predicted limits which assumed straightforward monotonic Ohmic-like profiles, could arguably be attributed to the well known profile dependence of the beta limit. The detailed analysis done for discharge 69608 is also open to some interpretation since the plasma was predicted to be linearly unstable with or without the wall.

Stability calculations were done for several alternative equilibrium reconstructions of DIII-D discharge 75824 with varying wall position. The results are shown in Fig. 4.5-1, where we plot the square of the unstable ideal growth rate against wall distance normalized to the plasma minor radius. This was a slow elongation ramp discharge which reached  $\beta_N = 5.1$  at the analysis time (2700 ms). The several curves in Fig. 4.5-1 correspond to equilibrium reconstructions with varying  $q_0$  and central pressure; there was some uncertainty in these as a result of the significant fishbone and TAE (toroidal Alfvén eigenmode) mode activity present in the discharge. However, all the curves with  $q_0$  above 1.0 show the discharge to be near marginal stability if the DIII-D wall is assumed to provide stabilization but gross ideal instability if there were no wall. At the analysis time, the discharge was in a sawtooth-free phase with  $q_0$  about 1.0 plus or minus 0.05. The reconstruction with  $q_0 = 0.95$  also showed a definite transition in the growth rate at the DIII-D wall location. Here, though, the calculations indicate an internal kink instability with either the DIII-D wall or with a wall on the plasma boundary, but there is a transition to an instability with much larger edge amplitude as the wall is moved out from the real DIII-D wall location. This discharge showed no evidence of an unstable external kink. The results strongly suggest, therefore, that the resistive wall in DIII-D has stabilized the external kink mode. The only uncertainty in this conclusion arises in interpreting the results from the case when  $q_0$  is below 1.0 — one cannot unambiguously determine from the ideal linear growth rate whether the predicted unstable mode at any wall location would be manifested as an external kink. Even here, however, the clear transition in growth rate is strongly suggestive and the edge amplitude is a factor 5 larger with no wall. The mode with no wall has most of the features of an external or global kink mode.

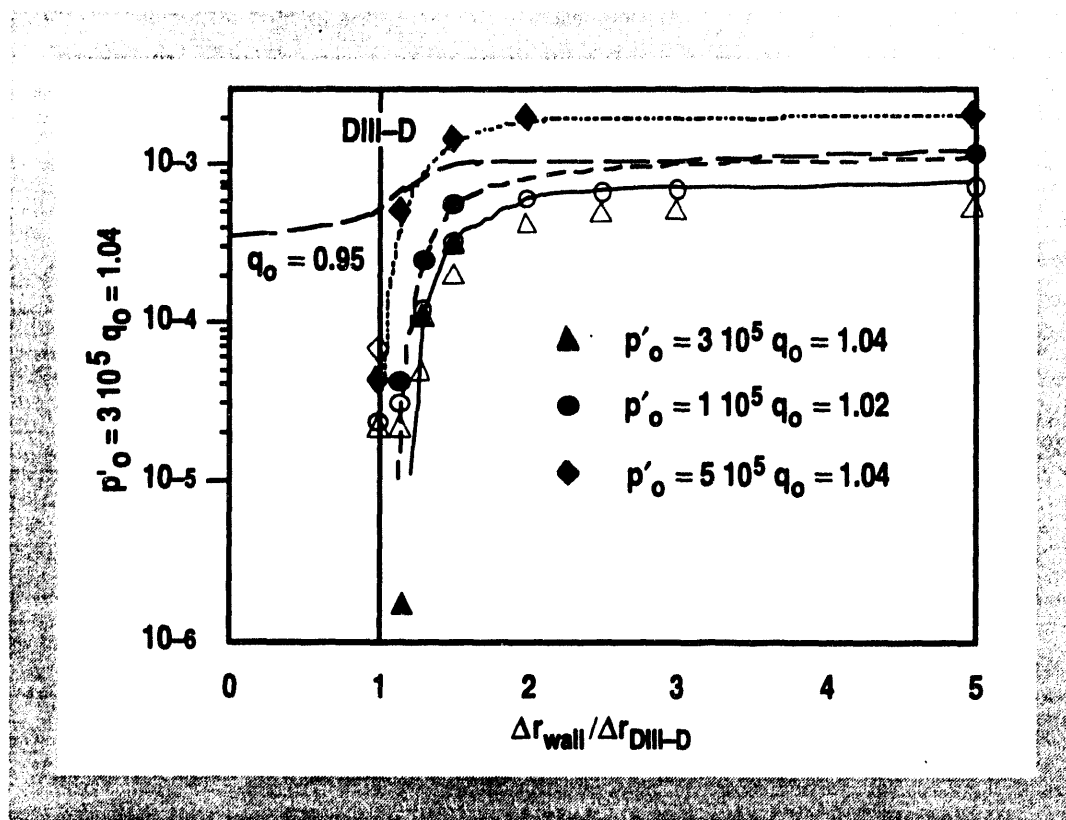


Fig. 4.5-1. Growth rate (squared) versus wall distance normalized to the DIII-D wall position for DIII-D discharge 75828 at 2700 ms. The growth rate is normalized to a poloidal Alfvén time. The several curves correspond to different possible equilibrium reconstructions from the discharge data.

A second example is shown in Fig. 4.5-2 for a high poloidal beta discharge 67700 analyzed 15 ms. before a  $\beta_p$  collapse occurred. The collapse coincided with a large ELM-like MHD instability observed on the Mirnov coils. Again, the several curves correspond to different equilibrium reconstructions consistent with the available data. The variation here results specifically from a large uncertainty in the central pressure profile, due to an anomalous loss of neutral beam ions and a large uncertainty in  $q_0$  since there was no Motional Stark Effect (MSE) measurement. All the reconstructions in this case indicate marginal stability with the wall, consistent with the  $\beta_p$  collapse and MHD instability 15 ms later. All of the reconstructions show a clearly unstable external mode with no wall. However, the sensitivity studies for the fits with  $q_0$  near unity are not yet complete and it remains to be verified that instability with no wall will necessarily result for all possible variations in the other parameters.

More recent theoretical analyses have now suggested that the simplest MHD theory, which was for a straight cylinder with periodic end boundary conditions, is inadequate for a finite aspect ratio, finite beta torus and that complete wall stabilization is possible under some circumstances if the plasma is rotating at a small but significant fraction of the sound speed. The discharges 75824 and 67700 were strongly neutral beam heated and were consequently rotating, consistent with the more recent theories. Recently, several high beta, low  $\ell_i$  discharges were also obtained in DIII-D in which beta reached much higher beta values than the beta limit expected from the scaling of  $\beta_N$  with  $\ell_i$ . Wall stabilization, however, is expected to be most effective at low  $\ell_i$  so the high beta observed in these discharges seems to be likely due to stabilization by the DIII-D vacuum vessel.

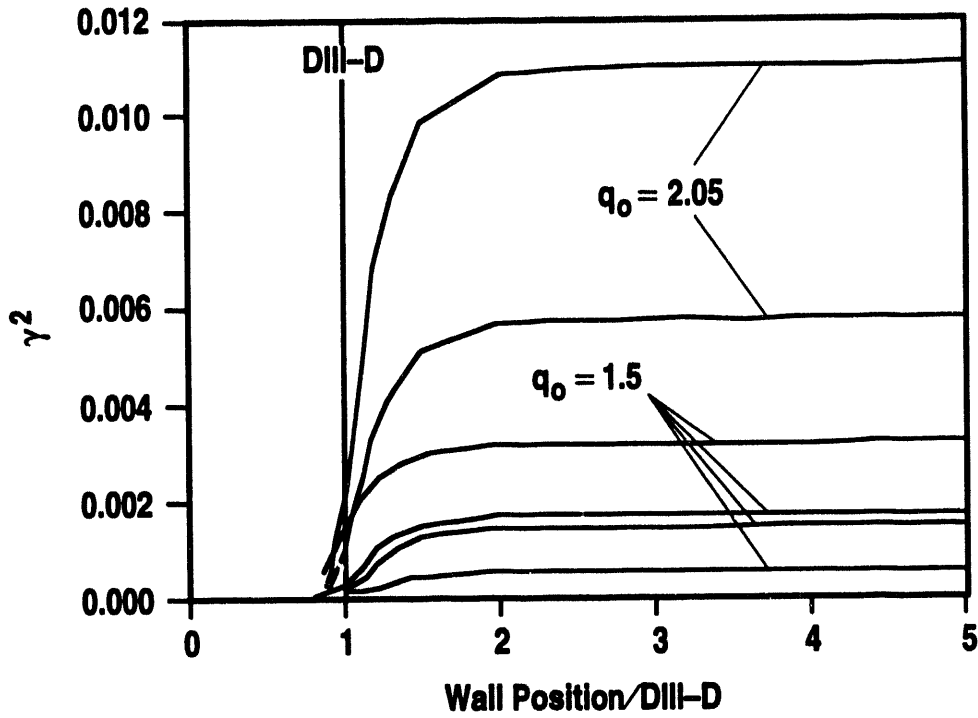


Fig. 4.5-2. Growth rate (squared) versus wall distance normalized to the DIII-D wall position for DIII-D discharge 67700 at 1750 ms. The growth rate is normalized to a poloidal Alfvén time. The several curves correspond to different possible equilibrium reconstructions from the discharge data.

## 5. OPERATIONS

### 5.1. TOKAMAK OPERATIONS

#### 5.1.1. INTRODUCTION

Major highlights of 1993 included the successful and rapid resumption of tokamak operations after a six month vent, achievement of VH-mode operation in a fully graphite covered, unboronized wall, and the successful commissioning and subsequent routine operation of a number of new tokamak systems, including the divertor cryopump for density control. During the past year, the emphasis has been on making extensive use of the new hardware added during the 1992/93 vent and also identifying and upgrading existing equipment in the DIII-D facility in order to maintain and possibly improve the reliability of the DIII-D device. Significant progress has been made and continues to be made in that direction despite the age and increasing complexity of the facility.

#### 5.1.2. VENT RECOVERY

A major accomplishment of the 1992/93 vent was the addition of graphite armor tiles on the outer wall of the vessel. This increased the graphite tile coverage of the Inconel wall from 45% to nearly 100%. Previous experience with the addition of significant numbers of new graphite tiles had resulted in high wall recycling and difficulty in achieving good H-mode confinement. Because of this concern, significant effort was expended on improving both the pre-installation conditioning of the new tiles and the vessel conditioning techniques used after installation. The result was a rapid and unprecedented recovery of high performance plasma discharges. H-mode transitions were observed on the 14th plasma attempt, and VH-mode discharges with an unboronized wall were readily obtained during the first experimental day after changing the configuration to a high triangularity double null divertor. Previously, VH-mode had only been obtained with a boronized wall. In addition, the first full field ohmic H-mode was obtained. This requires both clean vacuum conditions and very low recycling. Metal impurity radiation was virtually eliminated, oxygen was reduced approximately a factor of 3 to 5, and despite the addition of all the graphite, recycling levels were low and carbon impurities were not a problem. A major change in the vessel conditioning technique during the cleanup period was the exclusive use of He glow discharge cleaning rather than the use of H<sub>2</sub> or D<sub>2</sub> glow or Taylor discharge cleaning. This was done in order to avoid the buildup of a "sooty" carbon layer on the tiles that is believed to result from the use of H<sub>2</sub> and D<sub>2</sub>. The sole use of HeGDC has now been adopted as the standard conditioning technique following a vent and this, in conjunction with simultaneous high temperature baking has resulted in rapid recovery from all subsequent vents.

#### 5.1.3. TOKAMAK OPERATION

Following the startup period in February and March, the tokamak was operated for 19 weeks with an availability of 73.4%. The last week of operations was at the end of October. The majority of the downtime in the power systems, computer, and other categories was associated with increased demands on aging equipment. Examination of the failures has identified key systems that would benefit the most from replacement or upgrading and much of

that work is now in progress. Examples of the systems that had frequent failures during the past year and are now being replaced included the tokamak gas system, EPSSIC (E Power Supply System Integrated Control), the MODCOMP computers, circuit breakers for the ohmic (E) and toroidal field (B) supplies, power supply-control system interface stations, and E and B gate driver circuitry. Some of these systems are also being upgraded in order to keep pace with the increasing demands of the experimental program. The gas system and the new computer system are two examples of this. It is only through this continuing process of identifying the recurring sources of downtime and replacing those systems that we will be able to maintain the machine availability as the complexity of the facility increases.

The most serious issue faced during the year and the single largest source of downtime was the repair of the toroidal field coil prestress system. During a daily inspection of the vessel prior to the start of plasma operation, it was discovered that a G-10 wedge was missing from the toroidal field support structure. Operations were suspended and following further inspection of the toroidal field structure, additional wedges and epoxy shim bags were discovered to be either loose or out of position. The repairs were completed and the coil was tested to confirm that there was no excessive motion of any of the individual coil bundles and that the overall rotation of the toroidal coil system was acceptable. Following the repair of the TF coil, a review of the instrumentation of the coil was held. As a result of the review, the twist measurement is being upgraded and new automated measurements will be taken on the vertical preloads and outer plane motion of the individual coil bundles. Previously, the only automated monitoring system for the coil was for the radial preload. These actions should help to maintain the integrity of the TF coil.

Throughout the year there were a larger than usual number of vents of the vessel, some of which required in-vessel entry to perform the required repairs. A total of eight separate vents were performed. The first of these was for completion of the tasks from the long vent, in particular the installation of the cryopump and the completion of the graphite tile installation. Following the start of plasma conditioning after this vent, a significant copper contamination was observed spectroscopically in the discharges. This coupled with a severe stray light problem observed with the Thomson scattering system, required the reopening of the vessel in early March. The source of the copper was identified as oxidized copper wire on the new bolometer array. The array was removed, and after being rebuilt was reinstalled in a subsequent vent. A baffle plate was modified to eliminate the stray light in the Thomson system. During this vent, a number of other problems were also remedied, including recessing the Fast Wave Current Drive (FWCD) antenna by 0.5 cm to reduce plasma interaction, an insulation failure of the ADP ring, a leaky valve in the DIMES system, a jammed shutter, and leaky braze joints on one of the new diagnostic feedthroughs.

One additional in-vessel entry was required this year in August. During plasma operation in July, flying debris was observed by the divertor IR camera and high levels of aluminum radiation were observed from single null divertor discharges with the outer strikepoint near the advanced divertor ring. Concurrent with the TF coil repair work, the vessel was vented for 3 days to investigate the source of aluminum. Inspection inside revealed that approximately 50% of the alumina heat shields on the bottom of the ring had failures ranging from small cracks to major broken pieces. Three-dimensional stress analysis showed that the alumina was unable to handle the thermal loads and the design has now been modified to replace the alumina with a thicker piece of boron nitride which can handle higher stress due to thermal loading. This modification will be implemented early in 1994.

To make the use of the new cryopump part of routine operation, a number of new operational systems and procedures were implemented. A new control system is being used to ramp up the ohmic heating coil more slowly in order to reduce the ohmic input power to the toroidally continuous cryopump. The new system which has performed well, uses loop voltage feedback during the startup of the ohmic coil and required modification to the EPSSIC system and the timing of the vertical field coil supplies.

In addition to the pump, a number of new systems and procedures have been added to the operation of the tokamak. In the area of vacuum conditioning, a new, higher current power supply has been added to the glow system to increase the removal of  $D_2$  from the graphite tiles between shots and thus maintain the low recycling level necessary for VH-mode operation. In addition, the boronization procedure has been modified to cycle the glow gas between pure He and a 10% diborane/90% He glow; this technique noticeably decreases the deuterated compounds resulting in lower  $D_2$  recycling from the walls. To improve personnel safety, a new pit-closed permit system was installed that provides improved control of personnel access in the machine area during testing or operation of hardware or diagnostic systems. To improve our ability to rapidly identify locations of ground faults, ground current monitoring systems have been added to the DIII-D vessel and to the metal boxes housing the outer field shaping coils. These new systems complement those already monitoring the ground currents on the E and B coils.

## **5.2. NEUTRAL BEAM OPERATIONS**

### **5.2.1. OPERATIONS SUMMARY**

Fifteen weeks of plasma heating experiments were supported by neutral beams in FY93. The first quarter of FY93 was spent on system inspection, maintenance, and repair. Neutral beam system check-out and conditioning of all eight ion sources started in the second quarter to ready the system for plasma heating experiments. Eight beam systems were available to support plasma experiments during the DIII-D FY93 experimental period from March to September.

Extensive efforts were required in conditioning two ion sources, one was damaged by a water leak internal to the source in 1992 and the other has new accelerator grids installed by Burle Industries. The ion source, which had a water leak was reconditioned after several hundred shots. However, it had persistent beam "blocking" during beam pulse, which was caused by the arcing (due to water spots) between the end plates of the plasma and gradient grids. The end plates were polished to a mirror finish to eliminate pits left by arcing and original machine tool marks and scratches. This ion source will be conditioned during the second quarter of FY94. The ion source with new accelerator grids was conditioned very quickly without a problem to 75 keV beam operation in five days (compared to about three months to condition the first new ion source seven years ago). This success is attributed to our experience and understanding of the ion source.

### **5.2.2. SYSTEM IMPROVEMENT, MAINTENANCE AND TESTING**

The ion source preventive maintenance and inspection program was completed during the vent period in the first quarter. This work required removing several ion source arc chambers to the neutral beam lab to replace insulating gaskets between plates of the arc chamber, to clean up the arc marks, and to tighten some loosened filaments.

Efforts to modify the beam system to extend the beam pulse length to 6 seconds to support the long pulse VH-mode experiment were very successful. Four ion sources have injected 6 second deuterium beams at 65 keV beam energy (1.9 MW injected beam power per source) into the plasma. All eight beam systems are now capable of 6 seconds beam pulse operations at a reduced beam energy/beam power. Beam power at long pulse operations is limited by the capabilities of the power supply and the beamline internal component heat handling.

Preventive maintenance was performed on various subsystems during the vent period and the maintenance weeks between operation periods during the fiscal year. These included the pyrometer system used to protect the target tiles of the shinethrough beams, the drift duct photodiode system used to protect the drift duct from damage by the

excessive reionized neutrals, the fast interlock system used to terminate beam pulse to prevent damage to the beam system, and the alarm system used for warning of failure in water cooling and vacuum systems.

### 5.2.3. SYSTEM AVAILABILITY

Overall average availability for the year is very good at 92.3% compared to 91.5% for FY92. Availability of the neutral beam system by month is shown in Fig. 5.2-1. The "Available" category is based on the beam system requirement requested by the physics experiments. The difference between the "Available" and "Injecting" categories represents beam systems which were available but were not used for injection during particular physics experiments.

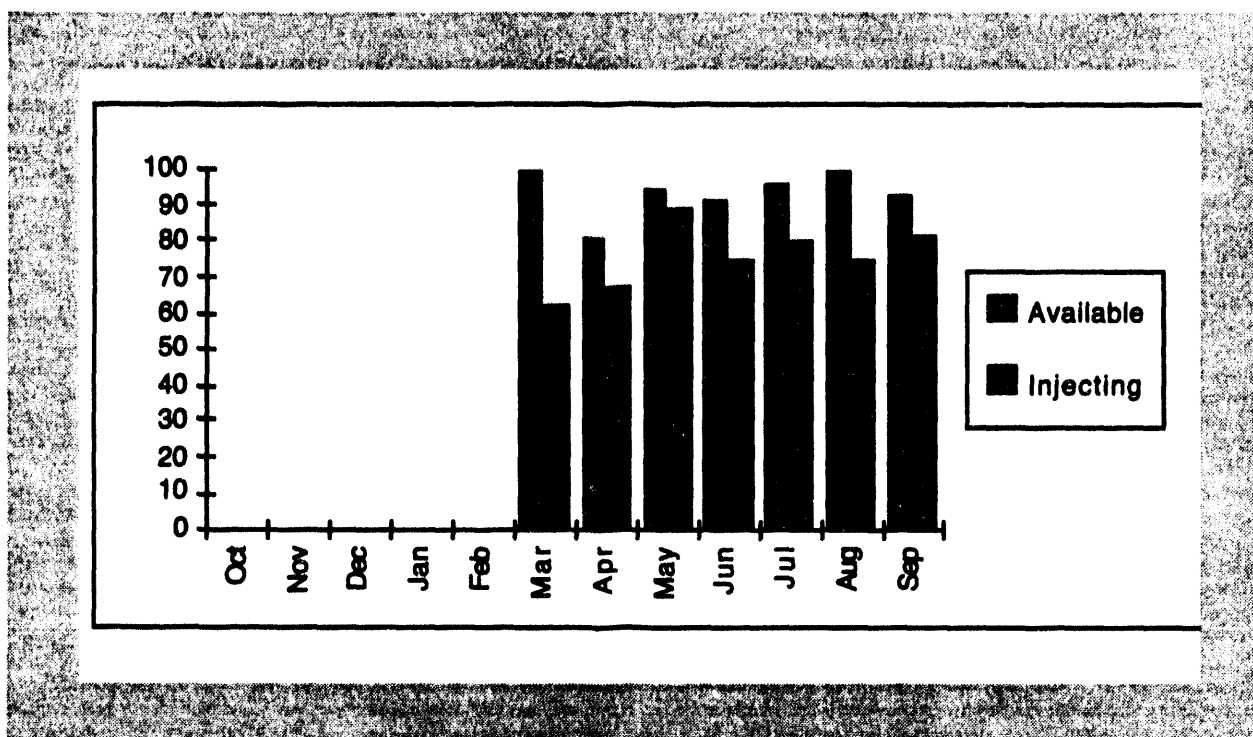


Fig. 5.2-1. Neutral beam availability by month.

## 5.3. ELECTRON CYCLOTRON AND ION CYCLOTRON HEATING OPERATIONS

### 5.3.1. ECH 60 GHz

There were no operations of the 60 GHz ECH rf system during the first quarter due to DIII-D vent related activities. The through-port extensions and mode converter, which were reported damaged in 4th quarter FY93, have been repaired. The nitrogen (gas) cooling lines for the machine windows had been rerun and the support structure near the 45° area has been removed. This allows for greater crane access in the area. A visual inspection of the in-vessel components was made to verify that the installation was correct. There were six gyrotron systems available for operations the most of the year. The systems were used to support experiments with pulse lengths in excess of 750 ms in a modulated output or 500 ms in the non-modulated mode.

### 5.3.2. ICH OPERATIONS

There were no operational days for the ICH system the first quarter of FY93. Dummy load testing of the system continued. It was determined that the triode in the first tube stage was not producing power at its rated capacity. After conversations with the tube manufacturer it was decided that the tube had gone through its life time and should be replaced with the spare. After replacement the output from this stage was back up to specifications.

A new, in pit, transmission line configuration was proposed in order to investigate a means of minimizing the effect the mutual coupling between antennas has on tuning and to limit the impact this coupling has on the VSWR protection. ORNL and JET had been looking into this problem for some time and it is hoped that some early information from DIII-D may confirm their theories.

Final design and layout of the de-coupler configuration was completed with the actual installation also be completed in time for plasma operations (Fig. 5.3-1).

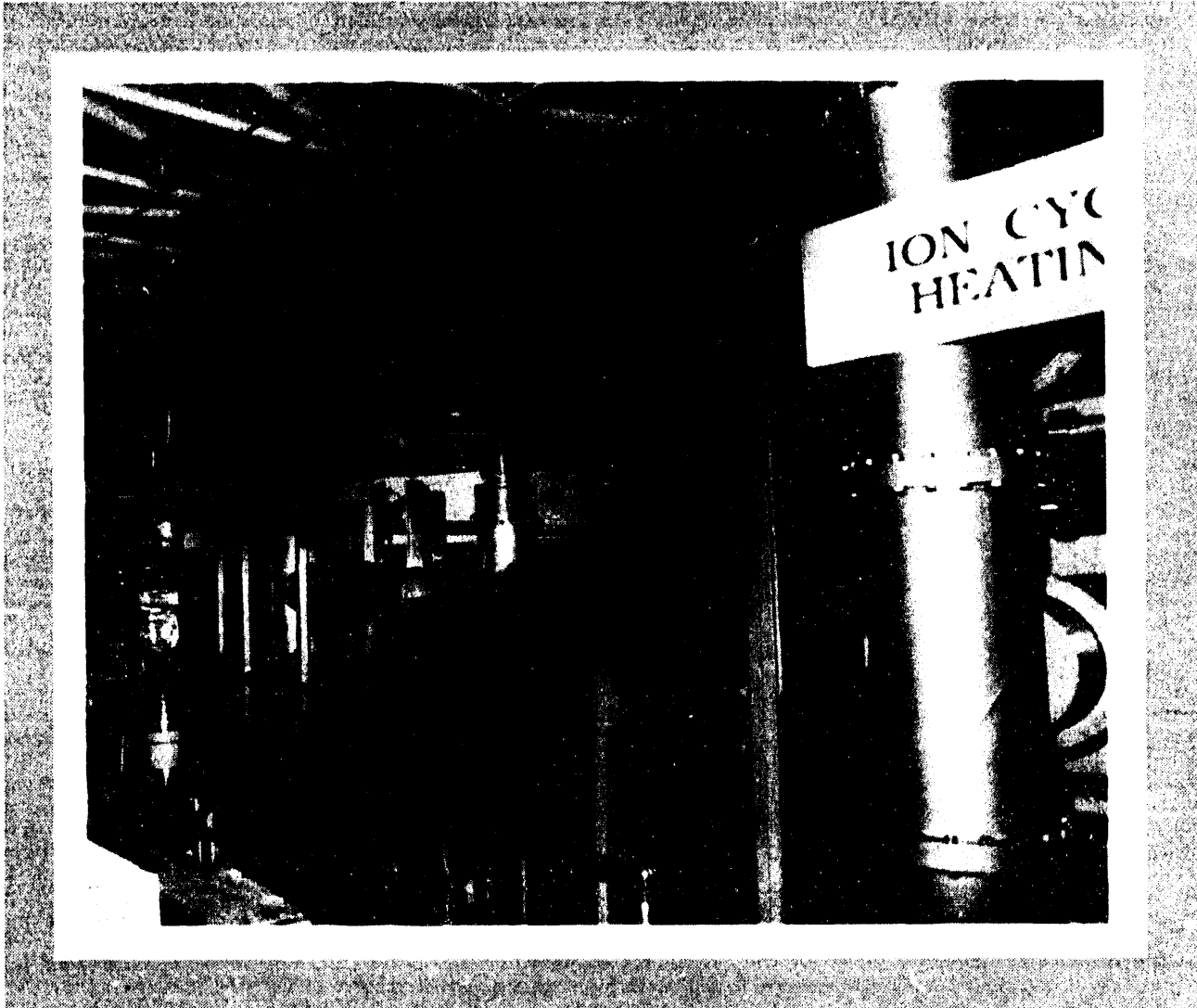


Fig. 5.3-1. ICRF de-coupler

First low power (<200 watts) testing and tuning was conducted in vacuum and plasma conditions and later several experimental days were spent at higher power levels (~100 kW). Full power (>1.5 MW) experiments were run with the decoupler installed with very good results. The de coupler will become a permanent part of the tuning system with only minor changes to upgrade its power capability.

Low power decoupler tests were completed and the resonant loops were reconfigured for heating experiments. Dummy load testing continued with the help of G. Barber from ORNL. The system was run in dummy load with power levels of up to 2.03 MW and pulse lengths of 2 seconds. Extensive antenna conditioning paid off with a new high, in net power to the plasma, of 1.60 MW.

## **5.4. DISRUPTION STUDIES AND PLASMA CONTROL**

### **5.4.1. INTRODUCTION**

Progress in the areas of disruption studies and DIII-D plasma control has been significant in FY93. Both areas have moved well beyond development and testing of basic tools and into routine application. Disruption simulation and analysis tools were applied to both the International Thermonuclear Experimental Reactor (ITER) design and DIII-D experimental cases. Significant disruption analysis accomplishments have included completion of a scoping study of ITER vertical disruption event (VDE) scenarios with varying halo parameters and application of an analytic model of disruption and halo phenomena to DIII-D and ITER disruption simulations. Extensive improvements were made to increase the capability and flexibility's of the DIII-D digital control system. Major DIII-D plasma control accomplishments have included application of the digital control system to real-time regulation of cryopumping and thus plasma density, ICRF power, antenna loading, loop voltage, and plasma beta.

### **5.4.2. DISRUPTION STUDIES**

The strong disruption simulation and analysis capabilities developed during FY92 were applied to both ITER disruption scenarios and DIII-D experimental cases in FY93. Continued collaborative efforts with the TRINITI Laboratory resulted in the further development and extensive application of the DINA disruption simulation code to these cases. Analytic models were also developed and used to further the understanding of disruption processes and complement DINA code simulations.

A study of ITER VDE scenarios was performed using the DINA code in which the halo temperature and width was varied in order to determine the maximum forces experienced by various conducting structures. The results of the study demonstrated that for a post-thermal quench bulk plasma electron temperature of 50 eV, the maximum pressure experienced by the vessel and shield structure is approximately 0.2 MPa. The maximum net vertical load on the conducting structure was found to be approximately 70 MN. The scoping study is being extended to include variation in the bulk plasma temperature.

An analytic model of halo current and plasma evolution during disruption was developed and applied to both DIII-D experimental results and DINA simulations of DIII-D and ITER. Applications of the analytic model to DIII-D disruptions served to check the accuracy of the physical assumptions of the model, and comparisons with DINA simulations revealed important differences between DIII-D disruptions and those expected in ITER.

### 5.4.3. PLASMA CONTROL

Significant improvements were made in the digital plasma control system hardware and software to improve the flexibility and capability of the system. The implementation of the custom data acquisition circuit as a printed circuit board was completed giving the capability of increased real time computing power through operation with multiple computers executing in parallel (presently three computers are available). A second generation version of the software was designed and implemented using experience gained during the first year of operation of the digital control system on DIII-D. The new software design allows rapid implementation of new control schemes to meet the rapidly evolving needs of the DIII-D experimental program and provides increased flexibility for variation of controlled parameters during a discharge. All standard DIII-D discharge parameters are now under the control of the digital system with the exception of vertical position (implementation of vertical position control is planned in the future). Only the plasma shape was controlled with the digital system during the system's initial operation in FY92. In FY93, control of plasma current, density, and gas puff rate was added.

In addition, entirely new control elements were added. The plasma density can now be controlled with a combination of gas puff rate and cryopumping by using feedback control of the radial position of the single null divertor X-point. Also implemented were control of ICRF power (in addition to control of antenna load resistance), control of the gas puff rate through feedback control of the neutral pressure (rather than the density), control of the loop voltage or surface voltage, and feedback control of poloidal beta, toroidal beta or normalized beta through feedback control of the neutral beam power (in addition to the control of the diamagnetism implemented previously).

## 5.5. DIAGNOSTICS

### 5.5.1. OVERVIEW

The DIII-D diagnostic effort in FY93 concentrated the limited available resources on improvements and additions to the divertor diagnostic set, both to exploit the pumped divertor and in anticipation of the planned radiative divertor. While the divertor diagnostic set has been greatly strengthened during the last two years there are still large gaps in our ability to measure important divertor quantities, particularly density and temperatures. Plans for filling in these gaps have been in place since 1992 but primarily due to budget constraints these plans have been pushed further into the future. Still, major progress was made during FY93, two new imaging bolometer arrays were installed and have been important in locating the radiated power from the divertor region, and new diagnostics aimed at measuring toroidal asymmetries associated with divertor operation have been added with promising results. There are 46 major diagnostic systems now operating on DIII-D with eight diagnostic systems in some stage of development. Table 5.5-1 lists the major diagnostic systems along with the quantities measured. Many of the diagnostic systems on DIII-D have been operating for many years (some where initially built for Doublet III) and are in need of major refurbishment. During FY93 we started a major effort to systematically refurbish diagnostics that are known to be operating critical components that are near or beyond their expected life expectancy. We expect this effort to continue at some level throughout the life of DIII-D.

### 5.5.2. NEW OR UPGRADED DIAGNOSTICS

In FY93 the DIII-D diagnostic resources were concentrated on the divertor diagnostic set. Two new imaging arrays of bolometers were installed and operated in collaboration with LLNL. As shown in Fig. 5.5-1 the arrays have

**TABLE 5.5-1**  
**PLASMA DIAGNOSTICS**

Diagnostic	Quantity Measured	Comments
<b>Operations-Related Diagnostics</b>		
Magnetics	$\dot{B}$ , Magnetic flux, $I_p$	2 poloidal (58), 1 toroidal (8) mag. probe arrays with 50 kHz response; 41 flux loops, 9 diamagnetic loops, 30 saddle loops, 3 $I_p$ Rogowskis
Hard X-rays		2 toroidal locations, 4 detectors, 1 kHz response
Plasma TV	Visible TV	Radial view, divertor, rf antennas
IR cameras	Heat load to armored surfaces	Upper divertor; inside wall, 2 toroidal locations, lower divertor
$H_\alpha$ monitors	$H_\alpha$ radiation, recycling	$H_\alpha$ filtered, 16 locations, 10 kHz response
Neutron detectors	Fusion and photo-neutrons	3 toroidal locations, 200 Hz response
Soft X-ray arrays	Internal fluctuations	1 vertical, 1 horizontal, 32 ch. ea. $\sim 4$ cm resolution, 4 toroidal locations, 12 ch. ea. $> 250$ kHz response.
<b>Electron Profiles</b>		
ECE grating radiometer	$T_e(r, t)$	Radial profile, 10 ch., 0.1 ms
Multipulse Thomson profile	$T_e(r, t)$ , $n_e(r)$	8 lasers, 6 ms, vertical profile, 40 pts., $< 1$ cm in edge resolution, $20 \text{ keV} > T_e > 10 \text{ eV}$
$\text{CO}_2$ interferometers	$\bar{n}_e$	Vertical, 3 chords; radial, 1 chord
ECE Michelson	$T_e(r, t)$	Radial profile, each 25 ms
<b>Fluctuations</b>		
Microwave reflectometer	$n_e(r, t)$ , $\bar{n}_e(r, t)$	UCLA collaboration - broadband; system gives profile in 5 ms, narrowband system, 400 kHz bandwidth
Correlation reflectometer	Radial correlation lengths in $\bar{n}_e$	UCLA

**TABLE 5.5-1  
PLASMA DIAGNOSTICS (CONT)**

Diagnostic	Quantity Measured	Comments
<b>Fluctuations (Cont.)</b>		
FIR scattering	$\tilde{n}_e(r, t)$	UCLA collaboration - 4 MHz bandwidth
CO <sub>2</sub> scattering	$\tilde{n}_e(r, t)$	MIT collaboration - phase contrast 1kHz, 100 MHz bandwidth
Fast magnetic probes	$\tilde{B}_\theta$	1 MHz resolution, 2 arrays totaling 7 probes
Li beam	Edge $\tilde{n}_e(r, t)$	Turbulence measurement near the edge
<b>Ion Temperature and Rotation</b>		
Charge exchange recombination	$T_i(r, t), v_\phi(r, t), v_\theta(r, t)$	16 channels bulk plasma; 16 channels edge plasma; 3 mm T <sub>i</sub> edge resolution; 6 mm v <sub>φ</sub> , v <sub>θ</sub> , edge resolution
<b>Impurities and Boundary Parameters</b>		
Visible bremsstrahlung	$Z_{\text{eff}}(r, t)$	Radial profile, 16 chords, 1 kHz
Bolometer arrays	Radiated power	Tomographic reconstructions, 3 arrays, 69 ch., 1 kHz
Graphite foil bolometers	Heat load to the wall	7 on the outer wall, 2 inside wall, 2 lower divertor, 1 upper divertor
SPRED (dual range)	Impurity concentrations	280-1200Å; 100-290Å, spectrum every 1 ms; edge profiles with scanning capability
H <sub>α</sub> TV	Divertor H <sub>α</sub>	LLNL
Divertor IR cameras	Heat load to divertors	LLNL, GA, 125 ms for a profile, upper, 2 lower
Langmuir probes	Edge T <sub>e</sub> (t), n <sub>e</sub> (t)	On divertor tiles
Laser blowoff system	Impurity injection	Impurity transport
Fast stroke langmuir probe	Edge T <sub>e</sub> (t), n <sub>e</sub> (t)	SNL, UCLA
DIMES	Surface erosion	Divertor Material Exposure System
Penning gauges	He pressure	ORNL - He pressure under the divertor baffle

**TABLE 5.5-1  
PLASMA DIAGNOSTICS (CONT)**

Diagnostic	Quantity Measured	Comments
<u>Impurities and Boundary Parameters (Cont.)</u>		
Fast pressure gauges	Neutral pressure	Near divertor region (ASDEX, LLNL), toroidal array, 2-3 ms response
Tile current monitors	Poloidal tile currents	Includes tile currents in the ADP, toroidal array
Multichannel divertor visible spectrometer (MDS)	Divertor impurity concentrations	ORNL - 7 channels
Divertor Baratron gauge	Neutral pressure	ORNL - verified ASDEX gauge measurements
<u>Fast Ion Diagnostics</u>		
Scintillator	Neutron fluctuations	50 kHz response time
E  B charge exchange	Beam-ion density profile	Conventional charge exchange analyzer coupled with H $\alpha$ detectors used to measure beam neutral density profile, scannable, spectrum in 1 ms
Fusion products	Fast neutrons, tritons He <sup>3</sup> , other fast ions	UCI collaboration; movable probe assembly
<u>Current Drive Diagnostics</u>		
Motional stark effect (MSE)	B <sub>p</sub> ( $r$ )	8 radial channels; 2 cm resolution, 5 ms response
ECE Michelson	Microwave emission	Detects tail population in the electron distribution function, profile in 25 ms (LLNL and Maryland)
SXR pulse height	High energy X-ray spectrum	Russian collaboration; detects tail population in electron distribution; spectrum every 100 ms
RF probes	RF radiation	Phase and amplitude of ICH rf on inside wall

**TABLE 5.5-1  
PLASMA DIAGNOSTICS (CONT)**

Diagnostic	Quantity Measured	Comments
<b>In Development</b>		
Edge MSE	$B_p(\tau)$	Additional 8 ch. concentration at the edge
Divertor microwave interferometer	$\bar{n}_e$ in divertor legs	2 chords (LLNL)
Divertor reflectometer	Peak $n_e$ in divertor	12 ch. in lower divertor (LLNL)
Bias ring IRTV	Heat load to bias ring	Heat flux measurement on the inside bias ring surface
DIMES interferometer	Surface erosion	In situ measurement (Júlich)
Microwave radiometer	$\tilde{T}_e(\tau)$	16 ch. (UCLA)
Divertor Thomson scattering	$n_e(\tau), T_e(\tau)$ in divertor	Design work only in FY94 (LLNL, GA)
Beam emission spectroscopy	$\bar{n}_e(\tau)$ in the core	Design work only in FY94

crossed poloidal views in the plasma that allow tomographic inversions, an example of such an inversion is shown on the report cover and in Fig. 5.5-2 from a radiative divertor experiment. Each of the new bolometer arrays (the old 21 channel bolometer array is still operated and the data from the old array will be used in the inversions) has 24 channels with a resolution of about 10 cm in the divertor. The new capabilities of this diagnostic, principally the ability to reconstruct the radiation contours in the divertor and edge region, have already contributed to the divertor program. Some of the observations during the past year include: during ELMing H-mode discharges in single-null configuration, the inboard divertor leg radiates much more strongly than the outboard leg; during radiative divertor experiments, the increase in divertor radiation occurs just outside the X-point; Neon injection produces a radiating layer just inside the separatrix 5-10 cm wide at the outside midplane.

Three diagnostic systems were expanded with the aim of addressing toroidal asymmetries in the divertor region. ORNL has installed a fast pressure gauge under the divertor baffle toroidally displaced from the gauges that have been operating in DIII-D. A second toroidally displaced IR TV camera viewing the divertor floor has been added by LLNL and the tile current monitor arrays have been substantially upgraded to include a comprehensive toroidal array of tile current monitors in the lower divertor. Toroidal asymmetries have been observed by these systems in FY93 however a comprehensive study of this issue must wait until at least the FY94 experimental campaign.

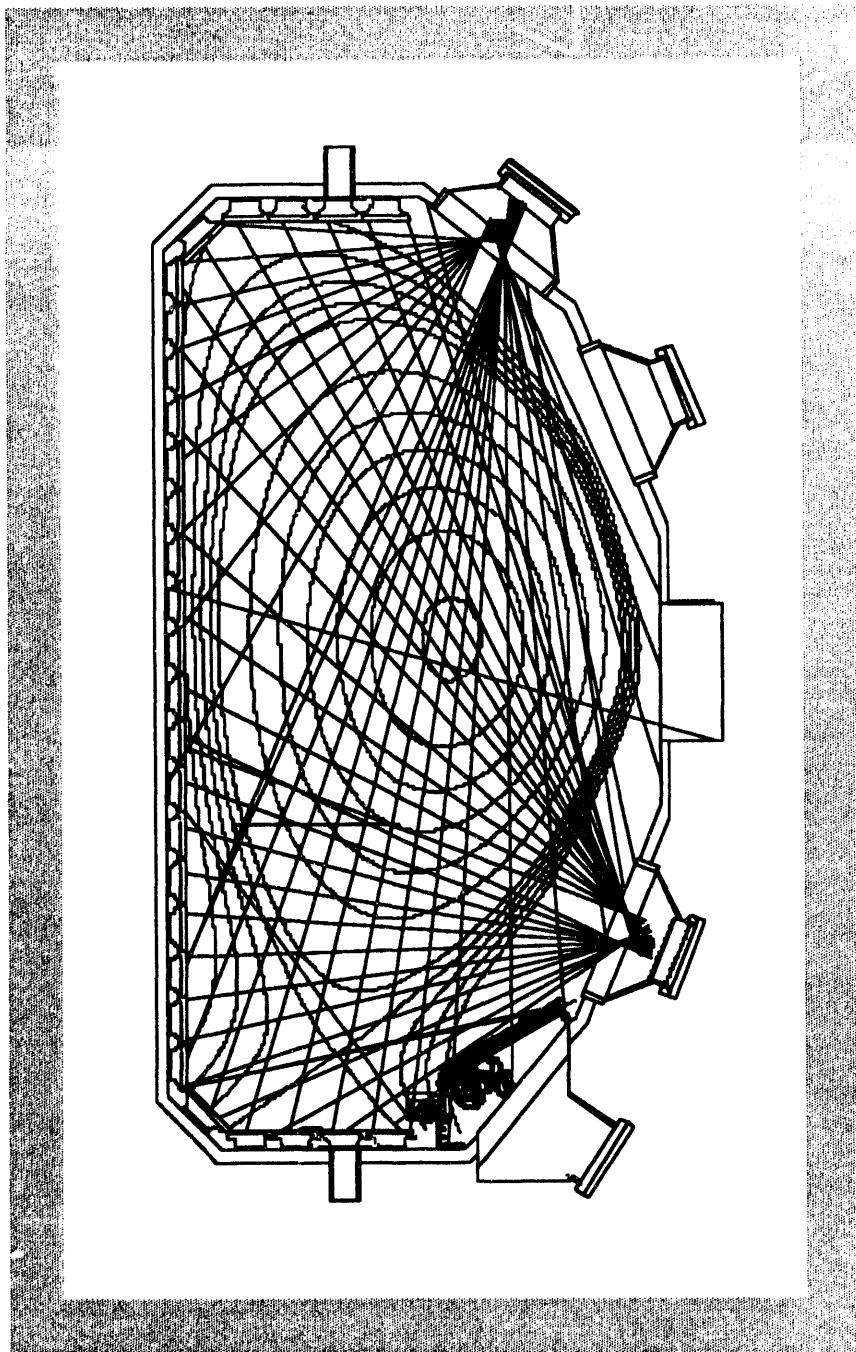


**Fig. 5.5-1. Views of new imaging arrays of bolometers**

Graphite foil bolometers were installed in the divertor baffle and divertor floor in FY93 in order to improve the heat flux measurements in those areas. ORNL completed the installation of a modified Penning gauge in the baffle region. The Penning gauge has been used extensively to monitor the helium partial pressure in the baffle region during dedicated helium transport experiments.

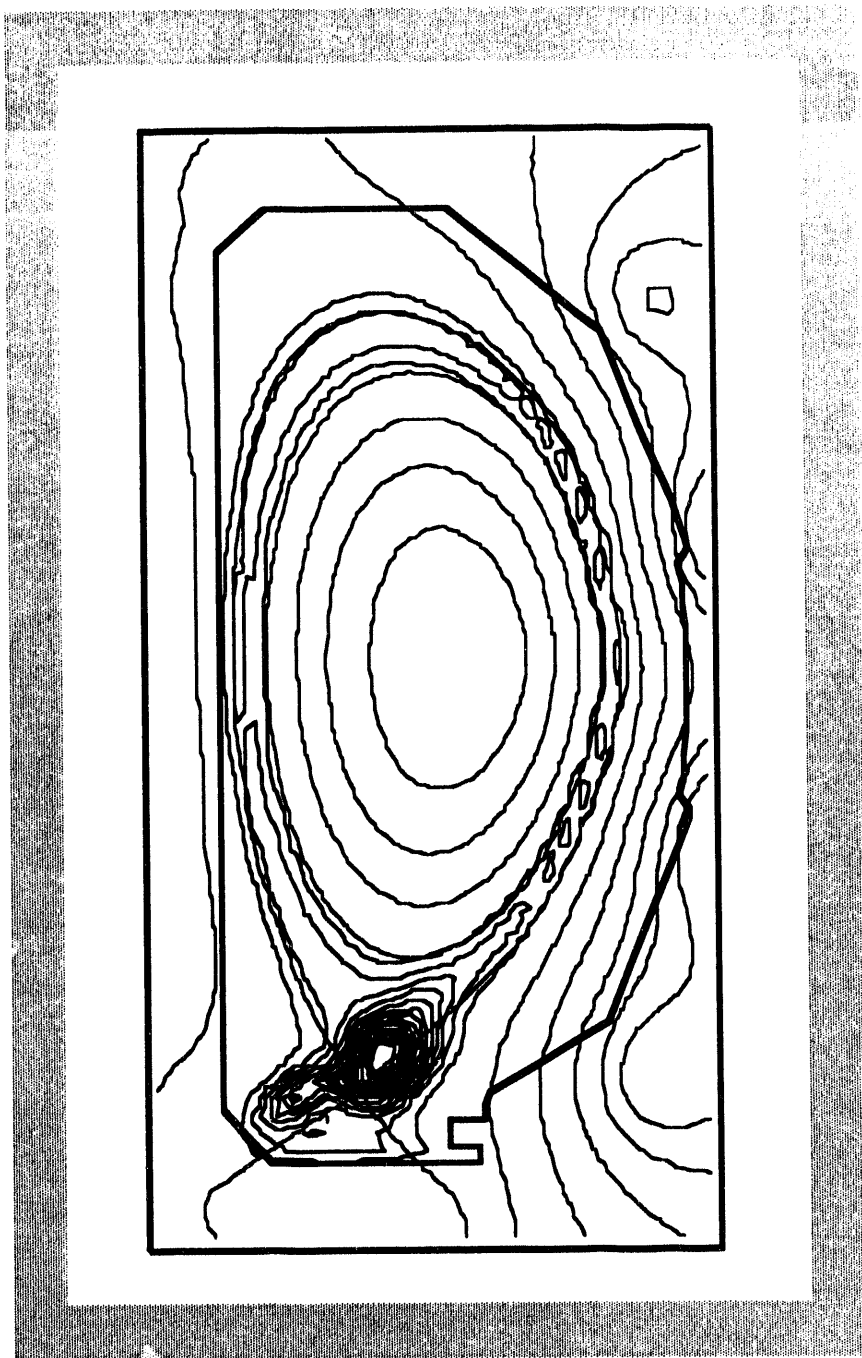


**Fig. 5.5-2. Contour plot of radiation during N<sub>2</sub> injection from divertor region**

The high frequency magnetic probe diagnostic was upgraded with the addition of a second, toroidally displaced array. The two arrays have seven magnetic probes with 2 MHz digital sampling. Among other new observations from this diagnostic are what appear to be high  $n$  ballooning modes from 308 to 385 kHz with toroidal mode number  $n=5$  to 9, separated by  $\Delta f = 10$  kHz and  $\Delta n = 1$ . The modes occur in repetitive bursts during high beta, low  $B_T$  discharges.

### **5.5.3. DIAGNOSTICS UNDER DEVELOPMENT**

Our FY94 plans again emphasize expanding the divertor diagnostics both for the existing pumped divertor and in anticipation of the radiative divertor now in the design stages. Measurement of the electron density contours in the divertor is very desirable in order to validate divertor models and to develop methods for heat flux control. But, because of the complicated plasma geometry in the divertor and access restrictions, it is extremely difficult to make complete density measurements in the divertor. There are several approaches toward this problem. In FY94 LLNL intends to install a microwave interferometer in the divertor with two chords, one through each leg. A microwave reflectometer will be installed by UCLA in the divertor. Meanwhile the design for a divertor Thomson scattering system will be developed. The interferometer will provide two line integrals of the density in the divertor legs and the reflectometer should provide some information about the peak density. A more complete picture of both the density and electron temperature will become available when the divertor Thomson scattering system is completed some time in FY95.

At present it is not possible to monitor the heat flux to the inside portion of the bias ring, a region that during pumping experiments is exposed to large amounts of power. In FY94 a tangentially viewing IR camera with a view of the inside surface of the bias ring will be installed.

The DIMES diagnostic will be upgraded in collaboration with IPP Julich with a backlit, thin film, visible interferometer. This system uses a visible interferometer to measure the thickness in situ of a thin substrate exposed to the plasma. This will allow accurate measurements of erosion of the divertor tiles under a wide variety of conditions.

The MSE diagnostic will be expanded by LLNL with the addition of an additional eight spatial channels, with the goal of significantly improving the resolution at the edge of current profile reconstructions. This will double the number of MSE spatial channels and will give DIII-D unique capabilities in the edge region.

A conceptual design of a BES (Beam Emission Spectroscopy) diagnostic will be undertaken in FY94 in collaboration with the University of Wisconsin. The BES diagnostic will measure density fluctuations in the core region and is based on the successful BES system on TFTR. The diagnostic will not be completed until late FY95 or early FY96.

Three aging diagnostics will undergo major refurbishment during FY94. The CER system will have a new detector system designed and built for the edge chords of the diagnostic. The new detector system is based on a fast readout CCD and will replace aging and obsolete image intensifiers. The CO<sub>2</sub> interferometer system will have the CO<sub>2</sub> laser systems reworked and new laser heads installed along with the replacement of a number of other optical components. The failure rate of the old laser systems was approaching an unacceptable level for this essential diagnostic. The 112 soft x-ray detectors are over 10 years old and have degraded significantly. New, modern detectors and front end electronics will be installed in early FY94.

## **5.6. RELIABILITY & AVAILABILITY**

### **5.6.1. INTEGRATED PREVENTIVE MAINTENANCE PROGRAM (IPMP)**

During October 1993 the IPMP changed its data base management software from Bender Engineering's MAINTSTAR Program to the PACMAIN Program. PACMAIN was developed by General Atomic's Fusion Group

and offers several advantages over the previous program. Fusion personnel can quickly access up-to-date preventive maintenance data and reports via computer terminals.

All cyclic hardware such as valves, shutters, bellows, etc., had been entered into the IPMP by the end of December. This meant work orders could be issued for the procurement and/or fabrication of cyclic equipment prior to their end-of-life estimates. It also allowed for the planned replacement of this equipment without any major disruption to DIII-D operations. Additionally, a more accurate log of critical end-of-life cycle data can now be maintained for future use.

Trouble Reports have been brought into the IPMP and cross-referenced with Corrective Maintenance Reports. This ensures the implementation of long term or permanent solutions to equipment failures. It also provides a more complete history for equipment in the IPMP. Additionally, the corrective action to failures of components, systems, and procedures, which do not require maintenance and thus are not in the IPMP, can now be documented and tracked.

There were 2923 maintenance tasks identified for all of FY93. Of this number; 2220 preventive maintenance (PM) and 285 corrective maintenance (CM) tasks were completed, and 754 tasks were not completed due primarily to equipment not being in use during vent periods. At the end of FY93 there were 23 PM and 10 CM outstanding tasks. Of the outstanding tasks; there were 4 priority 1's (affect machine operation) and 19 priority 2's (may affect machine operation). The remaining 10 outstanding tasks are priority 3's which have no affect on machine operation. At the end of FY93 there were 1202 pieces of equipment in the IPMP. This is an 11% increase over FY92.

### 5.8.2. SIGNIFICANT EVENT REVIEWS (SER)

In March of 1991 DIII-D Management initiated a Significant Event Review (SER). The purpose of these reviews is to learn from past events with the objective of determining the root cause of problems and thus eliminate the re-occurrence of those events which result in unanticipated costs or expended effort which could have been avoided with better design, procedures, etc. The SER brings together key personnel involved in the event with key people from related parts of the organization to discuss the event and propose courses of action.

There have been 3 SER's held during FY93 on the following issues;

1. **B-Coil Prestress Ring.** A dislodged wedge made of G-10 material was discovered during a routine inspection of the vessel upper prestress ring tensioning system. Further inspection revealed that other wedges were either dislodged or out of their nominal positions. Several shim bags were also found to be loose or fallen. These conditions allow greater deflections in the B-coils causing more strain in the finger joints at the center post of the vessel. All of the wedges were re-installed or re-aligned per specification. Also, some shim bags were removed and new shim bags installed in their place. The upper prestress ring vertical studs were then retensioned. It was decided to instrument the prestress ring with B-coil deflection monitors and load cells to monitor the force in the vertical studs.
2. **Halon Discharge in the Pit Area.** In late August 1993 smoke detectors in the lower access pit tunnel's 1, 4, and 5 went into alarm. The thump of the Halon fire suppressant system's tanks being discharged, and the whooshing sound connected with the discharge was heard. No reason for the discharge could be determined, and no equipment failure was identified. The system is manually operated by pulling a ring outside the pit area which closes the contacts on a micro-switch, providing 24 Vdc to the solenoid in the Halon System. The solenoid plunger depresses a Schrader valve which causes the Halon to discharge. It was definitely

established that the ring had not been pulled. Also, a printout of the Notifier Alarm System indicated that the Halon System was never alarmed and that the solenoid had not been activated. It was decided to separate the Halon System from the Notifier Alarm System.

3. **Copper Impurities in Vessel from Bolometer.** Copper braided Nextel wiring in the new bolometer arrays was prebaked in an air atmosphere rather than in vacuum causing copper oxide to form on the wiring. Copper impurities were then discovered in the DIII-D vessel after installation of the bolometers. It was determined that the copper impurities were flaking off of the Nextel wiring, and dropping into the vessel through a small aperture opening in the bolometer housing. It was decided to replace the copper oxide braid with Kapton. It was also decided that a visual review of the hardware be conducted as part of the normal design review process.

The course of action followed for these SERs resulted in changes to documentation such as procedures, drawings, check lists, etc.

## 5.7. RADIATION MANAGEMENT

Radiation management tasks include monitoring the site boundary radiation, monitoring the dose exposures of individuals from pit runs and vessel entries, ensuring compliance with legal limits, DOE guidelines and DIII-D procedures, monitoring material for activation, maintenance and operation of the radiation monitoring detectors (neutron and gamma), and maintaining a database of radiation measurements and of personnel dose exposures.

The total neutron radiation at the site boundary for FY93 was 4.6 millirem, the total gamma radiation was 2.2 millirem, giving a total site dose for the year of 6.8 millirem. (This is below the SAN DOE annual guideline limit of 20 millirem and the California annual limit of 500 millirem.)

The total dose exposure personnel received was kept below the DIII-D procedural limits of 25 millirem per day, 100 millirem per week, and 300 millirem per quarter (1200 millirem per year). The highest dose accumulated by an individual from pit runs and vessel entries (but not operations) for FY93 was 246 millirem. A total of 132 individuals received such doses as follows which were logged in the database of personnel radiation doses:

Dose Range (millirem)	Number of People	Dose Range (millirem)	Number of People
0-25	114	101-150	1
25-50	9	151-200	2
51-100	4	201-250	2

The yearly radiological safety audit of DIII-D was conducted by GA Health Physics, six minor action items were identified and completed. The yearly radiation audit by the GA criticality radiation safety committee was completed; no action items were generated. The DIII-D work authorization (WA) with updated DIII-D emergency procedures was renewed and approved by Health Physics. A radiation class was held for 24 new individuals. The vessel was vented four times: for 99 days in the first quarter continuing the vent of August 92, for 21 days starting January 13, for 12 days starting March 4, and for three days starting August 18. Radiation monitoring was performed for all vessel entries.

As part of the carbon tile cleaning procedure, tests were made to arrive at an estimate of the amount of tritium in the tiles in order to determine the precautions required for the tile baking WA. Initial estimates for all the tritium in the tiles were used to write the first work authorization for baking tiles at GA. Based on the results of a test bake the required amendment to the tile baking WA to permit sending tiles to an outside vendor for baking was written and approved. Only tiles with a surface contamination below the DOE release limit of 1000 DPM/100 cm<sup>2</sup> were sent to the vendor for baking; the remaining tiles were baked at GA. The concentration of tritium in the exhaust of the grit blaster used for the carbon tile cleaning was measured and found to be not distinguishable from background.

An ALARA plan for DIII-D operations was written along with a DIII-D Radiation Plan Summary document to separate the specific details of the DIII-D radiation limits from the procedures described in the ALARA plan. As part of the ALARA plan an ALARA subcommittee to the DIII-D safety committee was formed and the first meeting of the subcommittee was held to review the ALARA document.

Disposal of sample fluids was pursued through discussions with Health Physics and radiochemistry. The total sample fluid (4.4 l of ultima gold, 0.4 microcuries) from over 500 tritium wipe samples was disposed of by radiochemistry. Some water samples (0.9 l, 13 microcuries) was also disposed by radiochemistry. The more than 500 empty sample bottles were sent to the waste yard for disposal.

Disposal of mixed waste (oil and alcohol contaminated with tritium) continued to be pursued with the waste yard; they are contacting mixed waste haulers to move the drums to the waste yard. Dated labels were placed on the drums; once the labels are attached the rules permit the drums to remain up to 1 year as they are filled but require the drums to be removed within 90 days once they are filled. Instructions were received from the waste yard to keep separate the synthetic oil and the non-synthetic oil in future disposals as one can be solidified by absorbent and disposed as low level solid waste.

A conservative calculation of the increased radiation from planned penetrations of the pit wall for a set of RF lines were made. Due to the predicted increase (16%) it was decided to reduce the radiation by eliminating the straight through holes with a right angle jog in each line. A radiation survey in the nearby walkway prior to the penetrations was performed for later comparisons.

The continuing survey of the site boundary proceeded; within the error bars there were no changes from past measurements.

Due to requests to dispose of the original Doublet III vessel, a preliminary survey was done and no radioactivity above background was seen. Using the results of a gamma survey after the end of operations in 1984 with the known half lives a calculation of the present expected activity also predicts a level below background. Release of the vessel awaits a final survey and approval by Health Physics.

## **5.8. ELECTRICAL ENGINEERING**

### **5.8.1. OVERVIEW**

The extended shutdown period which ended in February was used to upgrade the control system for the toroidal field (B) power system, to make room for the new C-coil power supplies from LLNL, and to perform preventive maintenance on the electrical systems. Significant progress was also made in implementing the new digital plasma control system (PCS) for the DIII-D tokamak. Electrical engineering support of the DIII-D experimental program continued routinely throughout the operating period.

The Electrical Engineering branch also provided support to Thomson Profile System, Li-Beam System, Cryogenic Systems, and Computer Systems.

### **5.8.2. OPERATION SUPPORT**

The electrical systems were used in both forward and reverse toroidal and poloidal field configurations during the operational period. All the electrical systems were available with only relatively few incidents of downtime. Work to improve power system availability is under way and is described in the following sections.

The start logic for motor generator two (MG2) was modified to insure that startup will fall within the optimal window for power rate charges. Additional cost savings to the project was realized by rebuilding modulator/regulator power tetrodes used in the neutral beam power systems instead of purchasing new tubes. Rebuilt tubes have performed satisfactorily in the system throughout the operations.

Tests to validate and characterize models of the DIII-D coil/vessel and electrical power systems were also conducted during maintenance periods. The models which will be used in the development of new control schemes for the tokamak will be described in a report when the tests are completed early in FY94.

### **5.8.3. COIL AND NEUTRAL BEAM POWER SYSTEMS**

Failure reports and associated downtime records were used in planning upgrades to the electrical systems. These records showed that problems with the B and E power supply circuit breakers and the programmable controller (PLC) for the E power supply were main contributors to the downtime of the electrical systems. A gate driver card which is used in both the B and E power supplies also continued to log excessive failures. The CAMAC interface to the F power system also failed on several occasions during operations. Additionally, a number of power outages during the year contributed to several problems with the control computers for the tokamak this year.

Of these problem areas, upgrade of the 15 kV vacuum circuit breakers was given high priority, and the purchase of new circuit breakers was initiated. A new uninterruptible power supply (UPS) was also selected to replace the old motor generator set. This UPS has sufficient energy storage capacity to power the computer through power outages, and will provide flexibility for maintenance of the AC systems involving transfer of power. Upgrade of the F system CAMAC station has also been given high priority. The C-coil power supplies were received and installed during the year, but still need to be integrated into the DIII-D control system. A new gate driver card has been designed to replace the cards used in the B and E power supplies. Implementation of these upgrades were planned to start in the first quarter of FY94 to be ready in time for startup of operation early in FY94.

The B power supply which had been upgraded with a new programmable controller during the first quarter of the year performed reliably throughout the operations. A water leak in the upper guide bearing for the motor generator MG2 was identified and fixed during the year. The fuel tank for the standby diesel motor generator was replaced with an above ground tank to meet environmental regulations. Oil processing of several transformers was also performed to remove sludge buildup.

New coax termination networks were installed in the capacitor banks for the neutral beam systems. These terminations replace old terminations which have exhibited undesirable failure modes.

#### **5.8.4. INSTRUMENTATION AND CONTROL SYSTEMS**

Engineering of the printed circuit cards for the plasma control system (PCS) was completed in the first quarter of the fiscal year. Production version printed circuit cards were installed and have been used in operation since January 1993. The digital PCS platform has provided enhanced flexibility for exploring new control regimes for the DIII-D tokamak. Reports on the performance and results achieved for this system is reported in a different section of this report. It is becoming widely recognized in the control community that classical orthogonal control approaches are not ideally suited for highly coupled systems such as tokamaks. Integrated control of the plasma parameters for Advanced Tokamak Scenarios must exploit the coupled behavior of the system in order to achieve the target plasma parameter specifications. General Atomics is developing advanced plasma control algorithms based on a multiple-input multiple-output (MIMO) control scheme on an internally funded (IR&D) project to be implemented in the new PCS.

The laser timing and patch panel circuit boards were completed and the Thomson system was used in operation. A new fast encoding and readout A/D (FERA) system diagnostic module was designed which will read out to the data acquisition system time stamp, identification number and other information.

### **5.9. MECHANICAL ENGINEERING**

#### **5.9.1. TOKAMAK SYSTEMS**

The 300° FWCD antenna enclosures were refurbished by Oak Ridge National Laboratory and installed in the tokamak in November 1992. The Faraday shields were sent out by ORNL for application of a new coating of boron carbide. This was completed successfully after which the shields were returned to GA for installation.

A new support structure was designed and installed on the north side B-Coil feed point buswork. The structure was required to decrease the deflections of the buswork which were the result of Lorentz forces induced during the high current operation of the B-Coil. Deflections of the unrestrained busbars in the past had resulted in bent and twisted busbars which caused bad connections, arcing, and difficulty of installation.

All solenoid valves for the pneumatically operated vacuum valves and shutters were replaced with new valves. The old system consisted of several valve boxes scattered throughout the pit. The new system employs computer operated modular solenoid valves which are located in a common area in the lower pit to thereby saving space, reducing clutter and simplifying trouble-shooting and maintenance. The solenoid system has performed reliably throughout the year. Newly installed pneumatic tubing has resulted in greater reliability by reducing tubing failures due to rupture.

Options to the originally proposed design of the error field correction coil (C-coil) were reviewed along with alternate locations for the installation of correction coils away from the machine. The coils will be oriented in a vertical plane and will each cover a 60 degree sector toroidally around the vessel. A project status/kick-off meeting was held to review the previously developed design concepts and to plan a course of action to complete the project.

A redesign of the two glow discharge cleaning electrodes, located at 135° R-1 and 315° R+1, was undertaken to permit variable repositioning of these elements at a greater distance into the plasma. This redesign was required since placement of the new outer wall tile array has altered the geometric relationship between the electrode and the plasma.

A preventive maintenance operation was undertaken to verify the correct torque on the DIII-D vessel seismic support structure and anti-torque structure fasteners. A number (hundreds) of water cooling lines and electrical conduits required rerouting to gain access to many of the fasteners. The tensioning and torquing operations were completed with the exception of seven studs on the seismic support structure which were not accessible. An analysis of the potential consequences due to the potentially under torqued fasteners was completed and the worst case loads were found to be well below the failure strength of the studs.

A new series of procedures are being developed by the Fusion Group in response to recent requirements initiated by DOE. A new Fusion Engineering Procedures Manual has been defined, and work continues to develop the contents and outlines of the various procedures. This work must be responsive to the ten criteria for quality considerations set forth by DOE in their most recent QA document, 5700.6C. The procedure will cover Engineering activities such as design, design reviews, documentation, and other activities related to the engineering process as applied to fusion projects.

A dislodged G-10 wedge was discovered during a routine inspection of the vessel upper prestress ring tensioning system. Upon further inspection numerous wedges were found to be dislodged or out of their desired location. Numerous shim bags were also found to be loose or fallen. These conditions allowed greater deflections in the B-coils causing more strain in the finger joints at the center post of the vessel. All of the dislodged or misaligned wedges were reinstalled per specification and five loose shim bags were removed and new shim bags were installed in their place. The upper prestress ring vertical studs were then retensioned.

The DIII-D gas system supplies time varying gas pulses to the tokamak. The system is being upgraded to increase flexibility, giving the experimentalist a greater variety of gases to work with and the ability to puff these gases at different locations on the tokamak.

A new work floor to facilitate in-vessel work has been designed and fabricated for use during vent periods. The new floor will be suspended from brackets attached to the wall studs, and is expected to be positioned about 20 in. above the existing tile floor. The floor panels are a honeycomb sandwich design, for which the material has been ordered.

## **5.9.2. DIAGNOSTIC SUPPORT ACTIVITIES**

Mechanical engineering continues to provide design and analytical support for a number of diagnostics. Some of these activities involve extensive projects while others are simple modifications intended to improve existing equipment.

Fabrication of both bolometer arrays was completed and the bolometers were installed in the vessel. During a machine vent it was determined that the wiring in the array was causing copper contamination in the plasma. Both

bolometer arrays were reworked to eliminate the source of copper as a machine contaminant. The arrays were rewired using Kapton™ insulated conductors and nickel plated copper braid shielding and were then reinstalled on the vessel. The arrays were then baked in vacuum and the residual gases were analyzed to ensure that the problem has been resolved. The arrays were reinstalled in the vessel during a clean vent and functioned satisfactorily. An alternate bolometer housing material was selected (Vespel™ and Alumina) to provide better electrical isolation than the existing anodized aluminum housings.

Design, fabrication, and installation was completed on the shield plate and integral shutter assemblies for the ports at 285°, R+1 and R-1 inside the vessel. Carbon-carbon tiles which face the plasma were then installed.

Existing inconel port cover plates at six R-2 locations in the vessel were replaced with new inconel plates covered with a carbon-carbon composite tile material on the plasma facing surfaces. These plates serve to protect sensitive thermocouples and other instrumentation and diagnostics. Installation of new shield plates at six in-vessel locations has been completed.

A reflectometer diagnostic was installed on the vessel mid-plane in the 300° R-0 port immediately adjacent to the Fast Wave Current Drive antenna. The reflectometer is a four channel arrangement incorporating a small graphite horn assembly situated just behind the plane of protective wall tiles. The design and fabrication of the reflectometer was completed by ORNL and was installed in the vessel by GA.

Analysis of failure modes for the Thomson scattering actuator system led to a new design of the supports for the shutter actuating cylinders. The original design mounted the air cylinders directly on the port flange, making them subject to cyclic heating as the vessel was baked from time to time. As a result, the air cylinder o-rings were prone to failure thus making the actuator inoperative. New mounts have been designed to position the cylinders at a distance from the flange to eliminate recurrence of the overheating problem.

Additional supports were designed for one of the large 8-in. interferometer mirrors to eliminate suspected vibrations in the external mirror system. Supports included a larger more robust mount for the mirror itself, plus rigid horizontal legs affixed to adjacent massive structures. Results indicate a substantial improvement in the interferometer data acquired.

### **5.9.3. FLUID SYSTEMS**

The decision was made to replace two of the four, fifteen year old, leaking, shell and copper tube heat exchangers in the DIII-D deionized water system with one plate and frame exchanger.

A 3600 gallons per day reverse osmosis unit was purchased and installed. Performance tests indicate that the unit is operating at an excellent impurities rejection rate of almost 97%. The design of an automatic control system utilizing the new, 3600 gallons per day R/O unit was completed and the controls procured, assembled and installed. This system which controls DIII-D deionized cooling water make-up and conductivity was successfully checked-out and placed into operation.

Fabrication and erection of the fiberglass piping portion of the water cooling system for the ABB transmitters was completed. Also completed were the connections to the MFTF power supply and existing ICH transmitter. These systems, all connected to the new, Low Pressure Cooling Water System were successfully started-up, checked-out and placed into operation. A water chiller to provide cooling solely for the Thomson lasers was received and installed.

#### 5.9.4. ADP CRYOGENIC OPERATION

The ADP cryopump was used during plasma operations for the first time. Operation of the pump went very smoothly during the active density control experiments. The cryosystem was supporting all presently connected loads: four beamlines, seven ECH magnets, and the ADP cryopump. Cryosystem operation was stable under these conditions with both Sullair compressors running and a positive liquid helium make rate. ADP cryopump liquid helium flow was stable during the deuterium plasma discharges with no noticeable warming of the pump. The LHe massflow was about 5 g/s. The pump was regenerated during every glow discharge cleaning session. LHe flow was stopped after each shot. The pump remained cold and then regenerated the adsorbed deuterium immediately when helium glow was initiated. Recooling of the pump was completed 1 to 2 minutes after the end of glow. The in-vessel liquid nitrogen cooled shield was kept cold both day and night. Cooldown of the complete ADP cryopump system from completely warm conditions takes about 2.5 hours. Cooldown takes about 1 hour on the second day of operations if the LN2 shield was kept cold overnight. Operation of the ADP cryopump during plasma operations has been without incident.

#### 5.10 . COMPUTER DATA SYSTEMS

During the startup and operations period of DIII-D, 2660 shots were taken, containing over 126 Gigabytes of data, with the largest shot being 93.4 Megabytes. This is the largest amount of data taken during any year for DIII-D. Seven Gbytes of additional disk storage was added at DIII-D. Faster units replaced old units with small capacity. This allows approximately 60 to 80 additional shots to be kept on line. Several new printers were added at DIII-D. These are all located on the network so that they can be reached by any of our computers (VAXes and UNIX workstations located at DIII-D or Bldg. 13).

A study of an appropriate replacement for the old 16-bit MODCOMP real-time control systems was completed. A RISC system, running UNIX, using the Motorola 88100 chip was selected. This system is sold by MODCOMP and has many real-time features not available on other UNIX systems. The computer arrived in January, 1993. The CAMAC driver and hardware arrived in May and some needed database software arrived in July. Programming was done to test the CAMAC hardware and in September, a mini-system ran automatically and collected 2 MB of soft x-ray array data each shot. The CAMAC performance exceeded expectations, so that possibly only one computer system will be needed for the data acquisition function. Subroutines were developed to control screen interfaces and to access shot data stored on other machines. Skeleton programs were written to handle database entry and access, task scheduling, CAMAC interface, setup and collection of data from CAMAC modules, and generation of data files for the user.

The DIII-D shot data access system continues evolving into a client/server relationship, with shot data residing on the VAX cluster and accessed by multiple workstations that perform most of the data analysis, PTDATA, the interface program between all DIII-D data and the application codes, was rewritten to allow the users to access and translate the VAX -based data from any of the different types of workstations. LLNL personnel assisted in this effort by converting the PDATA data compression algorithm into the C language, allowing it to be run on all of the user workstations. The data, compressed because of its volume, can now be decompressed on the requestor's workstation rather than on the slower VAX. At the same time, the capability of breaking down the monolithic single shot file into multiple files representing meaningful subsystems was added. The reworking of the data access system was a significant accomplishment which will increase data acquisition speed and enable efficient data flow across nine different computer operating systems. The redistribution of the computational load should prevent the computer

slowdowns of the past and contribute to increased efficiency in the analysis of experimental data. The User Service Center DIII-D shot restore procedures are also being rewritten to handle the multiple file per shot concept.

A program to provide shaping control for the plasma control system was completed. This program allows the user to push and pull (graphically with a cursor) on the desired plasma shape and calculated the various parameters which result from the displayed changes. To do this, an energy fit is run which computes about 50 parameters and which displays the results to the user immediately. Work was completed on the coding for the Thomson Laser diagnostic which monitors all of the interrupts from the various pieces of hardware. This was a large change necessary due to the reconfiguration of the hardware. Several new applications have been developed to keep a record of all maintenance technicians, their skills and training, and to track of all the materials used in installations inside the vessel.

High performance workstations have been installed in several areas in the fusion office building (Bldg 13). Notable among these is a DEC 4000-300 AXP running OpenVMS installed for the charge exchange recombination diagnostic. It out performs all other processors in fusion and is surpassed only by the Crays. Two Hewlett-Packard (HP) workstations were installed, one for the USC and the other for the rf group. SAS, the statistical analysis software from SAS Institute, Inc., was procured. SAS is used by JET to analyze their data, and having the same package locally will enhance GA's participation in that collaboration.

## 6. PROGRAM DEVELOPMENT

### 6.1. FAST WAVE CURRENT DRIVE UPGRADE

In FY92 the decision was made to upgrade the DIII-D Fast Wave Current Drive (FWCD) system by an additional 4 Megawatts of generator power capability, beyond the existing 2 Megawatts of FWCD power which has been used to establish the physics basis of current drive in the fast wave domain. Long range DIII-D advanced tokamak scenarios typically call for a total of 8 MW of fast wave power to be combined with the ECH gyrotron capability. This 4 MW upgrade makes a significant step toward the final goal.

FWCD on DIII-D is a collaborative program between GA and ORNL. For the upgrade, ORNL will provide two new modular four strap fast wave antennas which will be installed in FY94 on midplane ports at 0° and 180° toroidally in DIII-D. GA is responsible for the necessary preparation of the DIII-D vacuum vessel for the antennas, the high power rf generators, the transmission system, the control system, and all aspects of interface with DIII-D operations. Subsequent physics experiments will also be a collaborative effort.

To define the collaboration in relation to this upgrade project, a Memorandum of Understanding (MOU) was established between GA and ORNL, with representatives from DOE also cosigning. The MOU defines a Work Breakdown Schedule (WBS) for the project. The following description of FY93 activities is presented by WBS element. The MOU defines the technical scope of the project, the responsibilities of each party, the project management organization for each party, and establishes the schedule, budgets, milestones and reporting requirements. A separate monthly report of project activities was submitted to DOE in FY93.

In mid-FY93 it became apparent that the DOE funding profile for ORNL to manufacture, assemble and test the two new antennas was not sufficient to allow the antennas to be installed on DIII-D prior to late FY94. Because of the importance of the FWCD experiments to the DIII-D five year plan, it was decided that GA would accelerate the antenna delivery schedule by assuming financial responsibility for the manufacturing of the antenna components in outside machine shops. GA also performed engineering liaison with the shops as necessary. Additional capital funding was transferred from GA to ORNL for the antenna project. The GA support of ORNL to meet the DIII-D programmatic needs was defined by a written agreement between GA, ORNL, and DOE. The present schedule calls for completion of antenna installation by April, 1994.

An overall schematic of the new FWCD system is shown in Fig. 6.1-1. There will be two identical 2 MW systems. The primary elements of each system are the antenna, the transmitter, the transmission system, and the control system. The transmission system must perform an impedance match of the transmitter to the antenna under varying plasma conditions and allow flexibility in the intratrap phase shift for various experiments.

A lengthy competitive bid and technical evaluation cycle held in FY92 resulted in the selection of transmitters from Asea Brown Boveri (ABB). These units are of the type used on the ASDEX-Upgrade tokamak in Germany, and

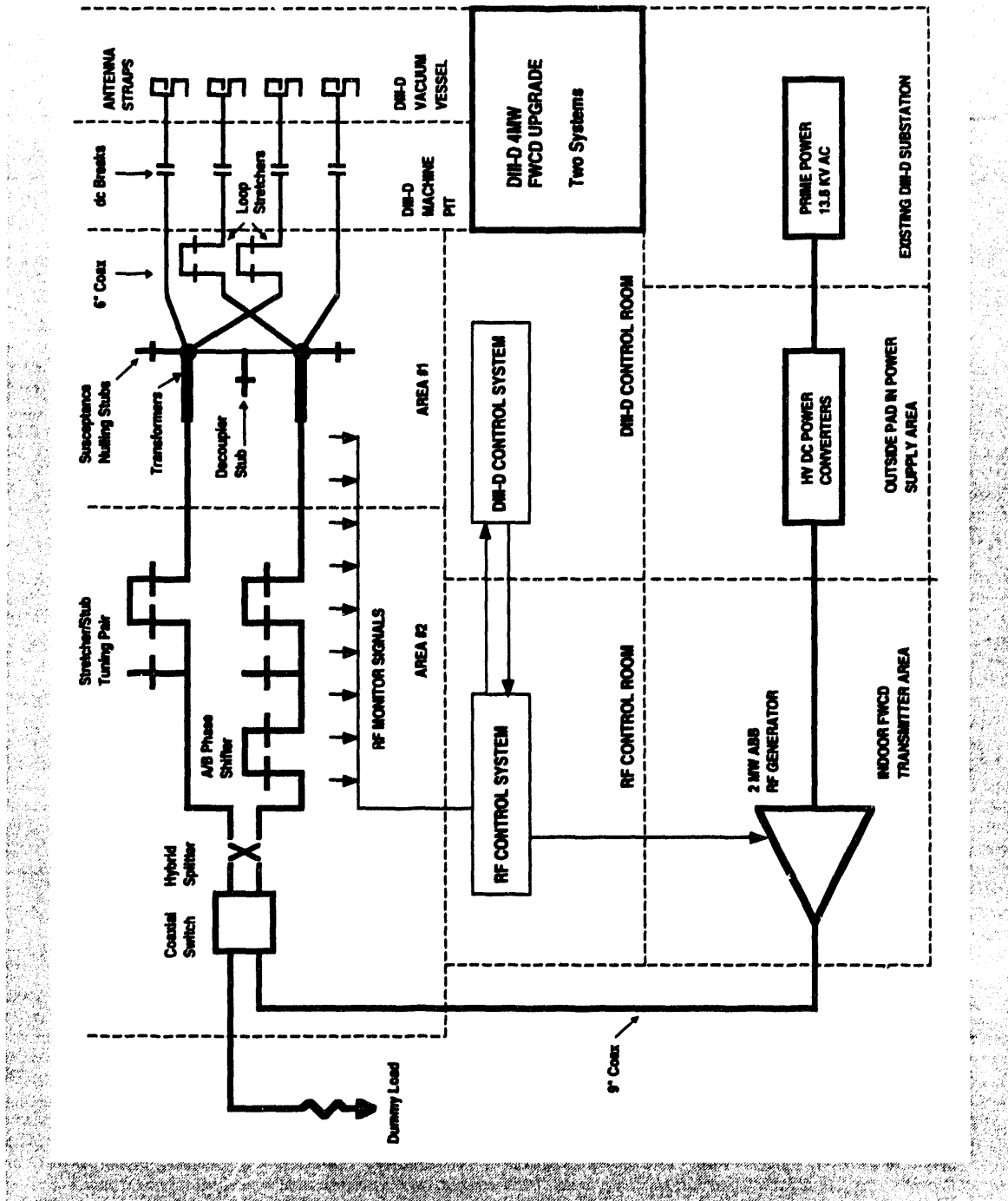


Fig. 6.1-1. Overall schematic of new FWCD system

have proven very reliable in operation there. The transmitter contract included the necessary high voltage power supplies and switchgear.

Both transmitters were delivered to DIII-D in late FY93, together with one of the two power supplies. The second power supply will be shipped in October, 1993. A photograph of the transmitter units in the FWCD generator area is shown in Fig. 6.1-2. Modifications of this area were required for the siting of the transmitters. The power supplies are placed on a new dedicated concrete pad in the yard area behind DIII-D. Extensive electrical contractor work was required to connect power between the units, and to the prime power coming into the DIII-D site. Transmitter checkout is scheduled for FY94. The transmitters are capable of operation over the 30-120 MHz frequency range. The higher frequency capability meets the physics requirement from extensive modeling studies which showed enhanced wave absorption with higher frequency. The output power of a unit is nominally 2 MW. It is actually higher, 2.5 MW, below 80 MHz and then falls off linearly with frequency to 1.5 MW at 120 MHz. The operating frequency can be changed in roughly 10 minutes, or between shots on DIII-D. The design of the transmission system has also kept the 10 minute frequency changeover capability so that the effect of frequency on FWCD efficiency can be readily determined on a shot-to-shot basis. With the existing 2 MW system, a frequency change requires several days.

The two ports which will house the two new antennas require extensive modification. A pumped limiter was installed on the 180° port and a moveable limiter blade is installed on the 0° port. Removal of the pumped limiter and preparation of the 180° port was completed in early 1993, during the last major vent before the 1993 experimental campaign. The other location will be prepared in the vent in the fall 1993.

The dummy loads, exciters and test equipment were specified in FY93 and ordered to arrive in early FY94. A microcomputer was acquired to begin the programming necessary for control of the two new systems. A conceptual design of the instrumentation system was developed.

The transmission system topology is based upon the successful one developed for the existing DIII-D system, with some significant upgrades. The coaxial transmission lines will use ceramic insulators, rather than Teflon, to avoid irrecoverable arc damage tracking. The lines will be capable of pressurization to three atmospheres with a variety of insulating gases. A simplified decoupler network (see Fig. 6.1-1), developed and tested at GA, will be incorporated near the tokamak in order to negate the deleterious effects of mutual inductance between the current straps of the antenna. Additional prematching stubs will be located near the decoupler together with a transmission line transformer which will lower the standing wave ratio in the main tuning elements. The line stretchers in the resonant loops are necessary for frequency changeover on the 10 minute timescale. All large transmission line tuning elements will be sited outside of the DIII-D torus hall in order to conserve valuable space near the machine. The first designs had much of this hardware in the torus hall, but the project reworked the design more than once at the request of the DIII-D operations group. A competitive bid process resulted in the selection of two U.S. vendors to supply the majority of the transmission system components. The procurement is a major one, with approximately 150 line items. Delivery is scheduled for early 1994 with installation commencing immediately upon receipt.

The facility modifications which were completed in FY93 were the new outdoor concrete pads required for the transmitter power supplies, the indoor site preparation for the transmitters which included a rearrangement of the FWCD control room, and the tie in of an additional water cooling system to the overall DIII-D system. Major rework of the area just outside of the torus hall is required for the construction of two new mezzanines for the large transmission system tuning elements, and the preparation of the area just outside of the hall at 0° which



**Fig. 6.1-2. Photograph of FWCD transmitter units**

was formerly occupied by the 60 GHz gyrotron system, which will be removed at the beginning of FY94. The mezzanines were designed in FY93 and will be installed in early FY94 to be ready for the transmission system delivery.

The design, manufacture, assembly and initial check-out of the two new antennas is the responsibility of ORNL, with close interaction with the DIII-D RF Physics and Operations groups. The final design review was held in Oak Ridge in January, 1993. Title II engineering was completed at the end of March with the approval and issuance of drawings. Figure 6.1-3 shows a sketch of one of the two identical antennas. Each of the strap assemblies is based upon a modular design for efficiency in the manufacturing process. GA became immersed in the manufacturing process when GA DOE FY93 funds were required for the outside machine shop work in order to expedite the schedule. GA handled the fabrication of eight major drawing packages; Port Cover Assemblies, Faraday Shield Rod Assembly, Inside Assembly Fixturing, Outside Assembly Fixturing, Mounting Hardware, Current Straps, Cavity Box Assemblies, and the Inner Conductor Transition Details and Sealing Flanges. Essentially all of the parts were completed by the end of the fiscal year and shipped to ORNL.

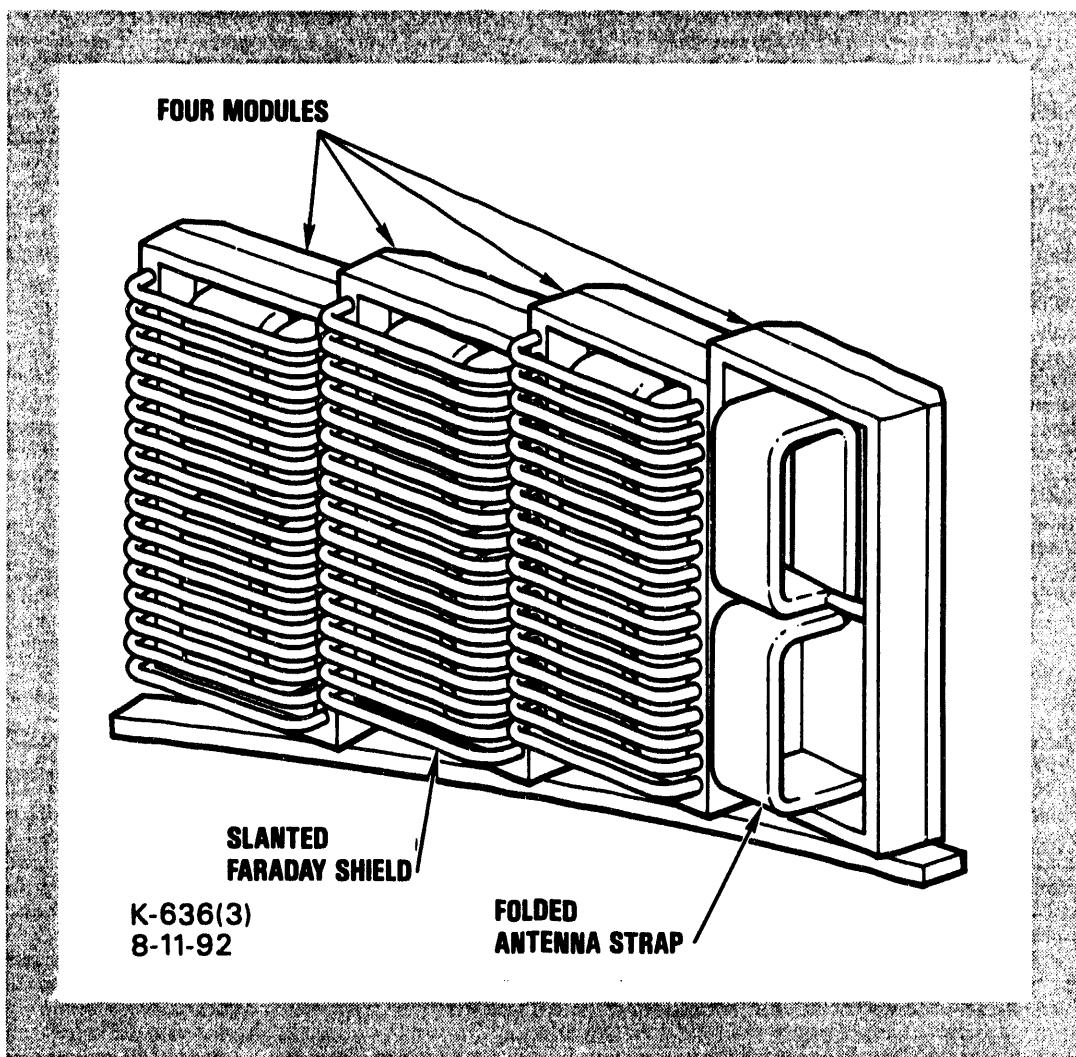


Fig. 6.1-3. New FWCD antennas

## 6.2. RADIATIVE DIVERTOR PROGRAM

The work on the radiative divertor program in FY93 has been a combination of experimental effort and engineering conceptual design. Divertor heat flux reduction with D<sub>2</sub> and neon puffing was demonstrated. In the case of D<sub>2</sub> puffing shown in Fig. 6.2-1, there is a delayed heat flux reduction and an increase in the core electron density. These discharges show good confinement, which is unaffected by gas puffing. Preliminary feedback experiments (gas valve on and off because the feedback gain was high) were performed to control both the heat flux and density rise. In the case of neon puffing, shown in Fig. 6.2-2, the divertor heat flux decreases immediately, and the core

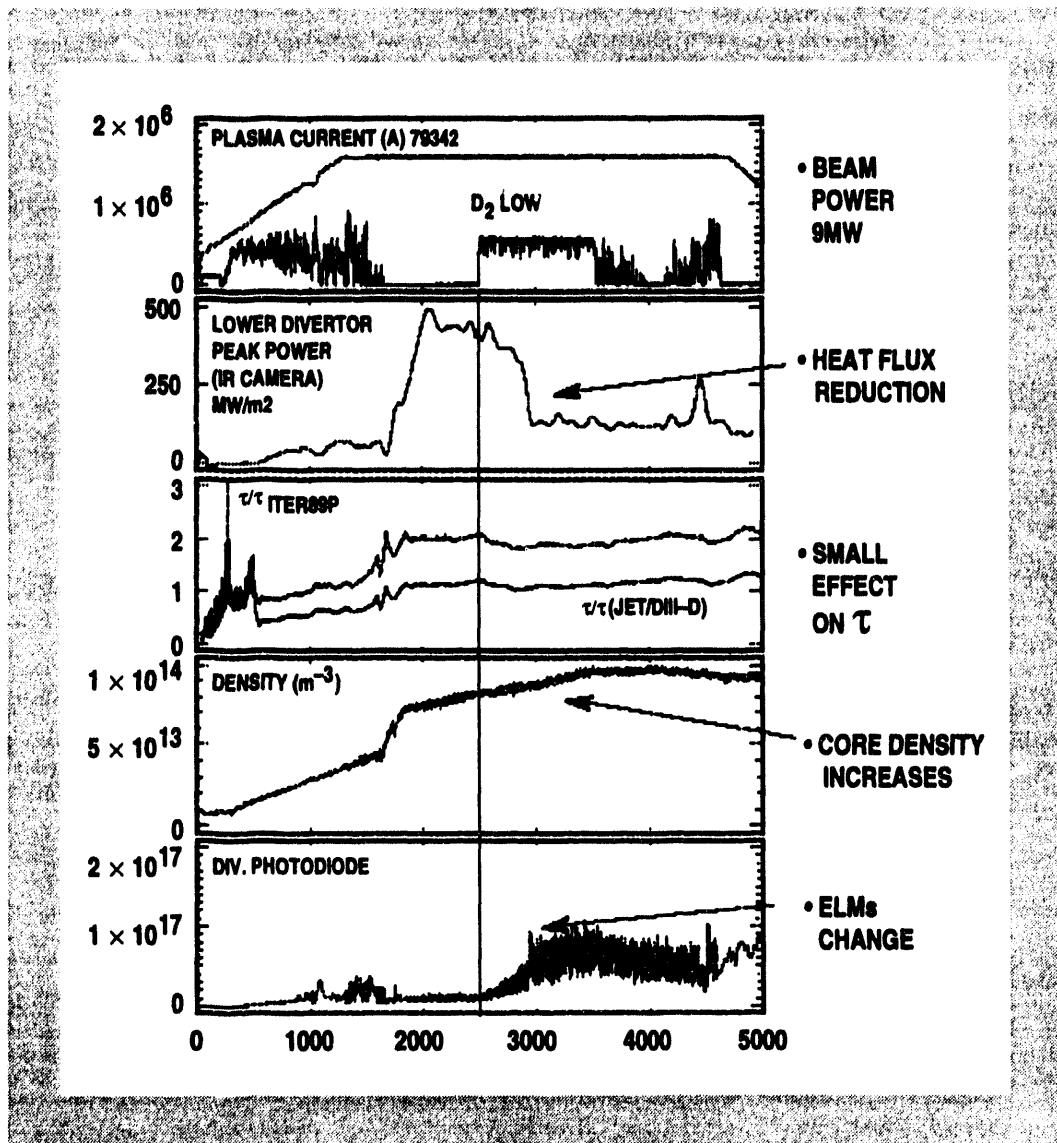


Fig. 6.2-1. D<sub>2</sub> puffing reduces divertor heat flux while increasing core density

neon as measured by charge exchange recombination remains constant and does not accumulate. The neon injection changes the ELM behavior, but the average confinement time is only slightly reduced. The core neon radiates at the plasma edge, and may in fact be beneficial to reduce the radiated power to the scrape off layer, but in present experiments, there is no control over the ratio of core to divertor radiation. Modeling suggests that the neon leaks around the divertor region to the plasma midplane where it is easier to penetrate into the core plasma.

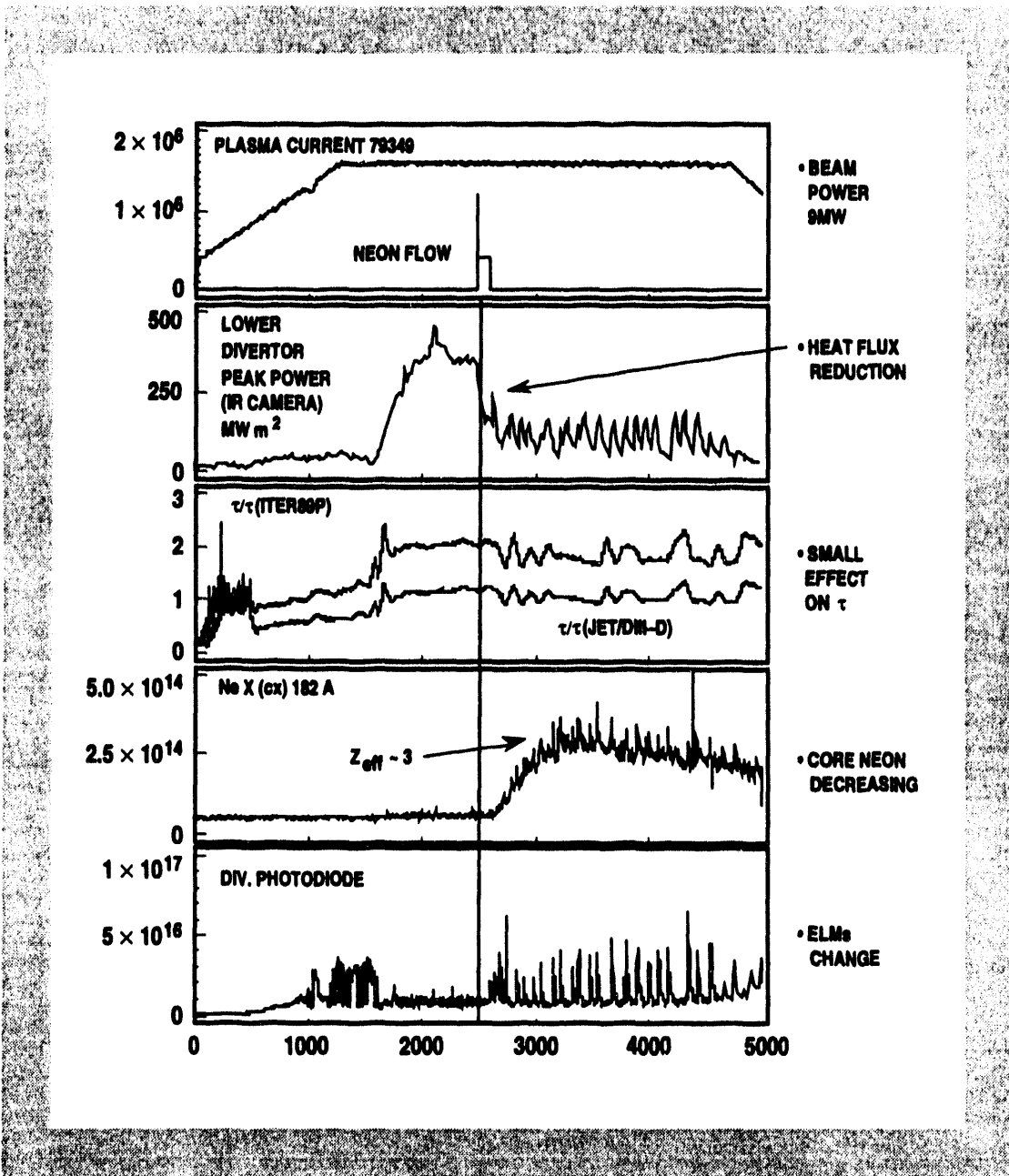


Fig. 6.2-2. Neon puffing reduces divertor heat flux with only small effect on confinement but increases core  $Z_{eff}$

Confinement experiments were also performed to determine the effect of shape on confinement. These experiments were very important for the radiative divertor design, as they determined the shape that was consistent with high confinement advanced tokamak discharges. As shown in Fig. 6.2-3, the shape depends strongly on the triangularity  $\delta$ , and less on the elongation  $\kappa$ . The first discharge considered, with  $\delta = 0.5$ , showed a factor of three less in the confinement figure-of-merit  $\beta\tau$  than the normal VH-mode plasma with  $\delta = 0.9$ . There are some advantages from the diagnostic standpoint for the low triangularity design, as there is an access port directly below the X-point in Fig. 6.2-3. On the other hand, the normal VH-mode shape has an X-point so close to the floor that there is no room for a divertor structure. For this reason, a lower elongation case  $\kappa = 1.6$ , was considered. This discharge has somewhat reduced absolute parameters because the plasma current is reduced, but in normalized parameters, the performance is similar. Preliminary analysis of the diagnostic access for this shape was done and determined that capabilities are similar to the existing DIII-D diagnostic set. For this reason, a shape similar to that in Fig. 6.2-3 was picked for the baseline design case. This case will be examined in detail in the models and the neutral transport and impurity shielding will be calculated.

Preliminary physics and engineering conceptual design based on the divertor designs in the DIII-D proposal (GACP 221-043) and shown in Fig. 6.2-4. This is a very flexible design, which includes pumping at both the inner and outer strike point, biasing, and a slot-like structure to minimize the communication between the divertor and core plasma. Our plan over the next year is to more fully develop this design, and test the concept with modeling.

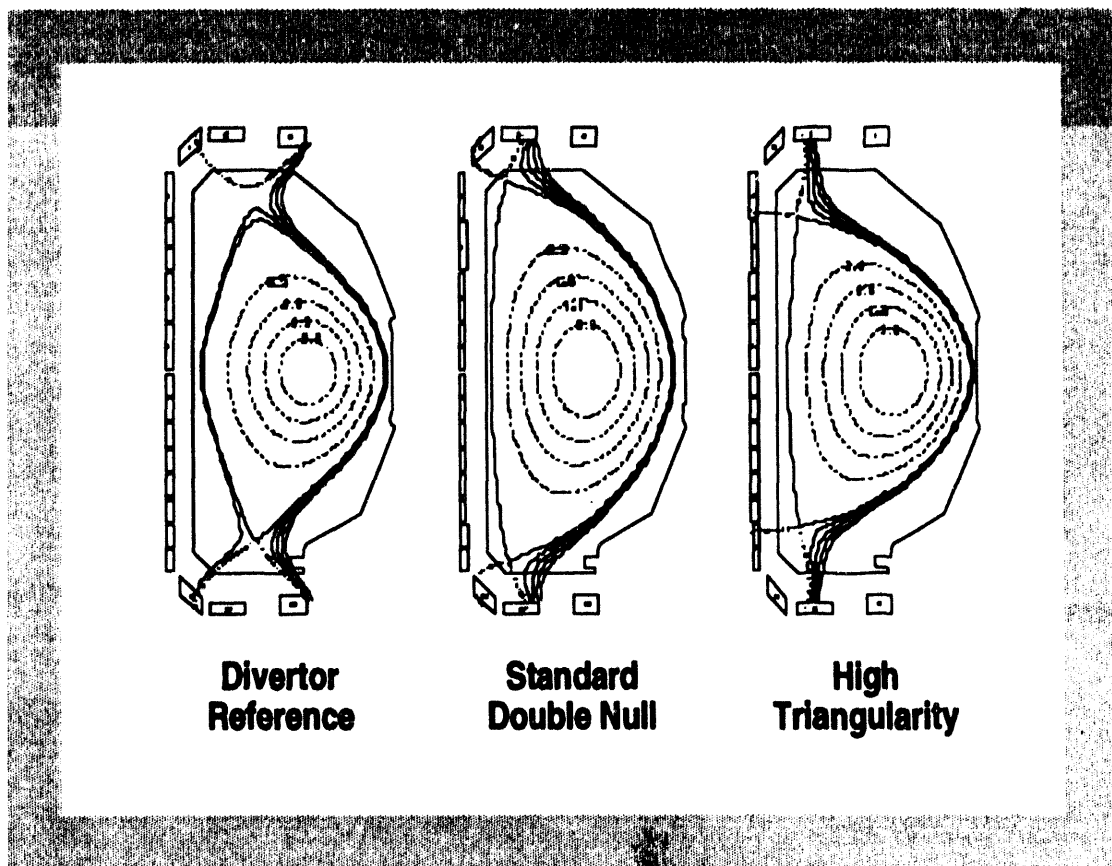
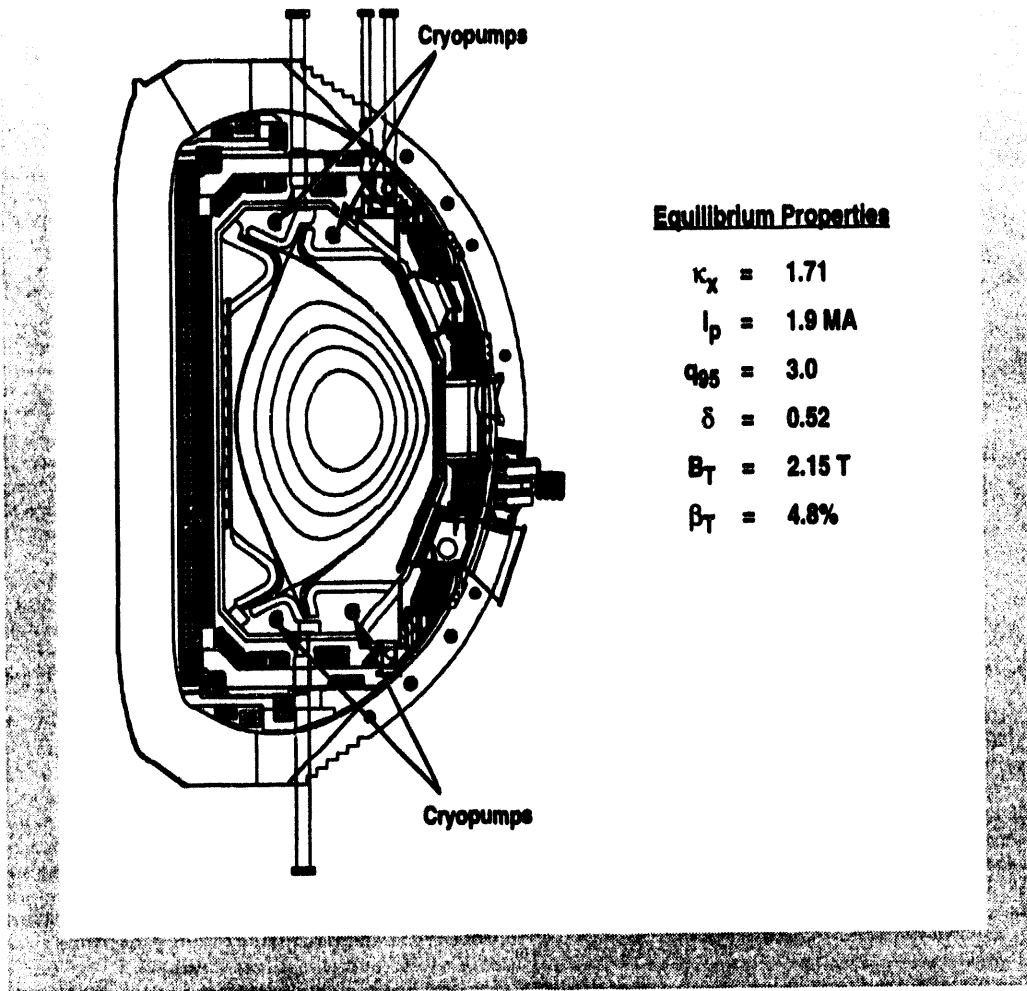


Fig. 6.2-3. Shape studies show that confinement and plasma performance increase with triangularity



#### Equilibrium Properties

$$\kappa_x = 1.71$$

$$I_p = 1.9 \text{ MA}$$

$$q_{95} = 3.0$$

$$\delta = 0.52$$

$$B_T = 2.15 \text{ T}$$

$$\beta_T = 4.8\%$$

Fig. 6.2-4. Preliminary conceptual design of a plasma radiative divertor and operational features

### 6.3. 110 GHz ECH SYSTEM

Electron cyclotron resonance is "nature's way of heating electrons." Provided that plasmas are sufficiently high in electron temperature and not too high in density, damping of either the fundamental frequency or the second harmonic is strong and highly localized to the resonant magnetic field in the plasma. For DIII-D with axial toroidal field of up to 2.1 T, second harmonic ECH at 110 GHz allows strong absorption at higher plasma density and thus beta and serves as a test for fundamental heating at 4 T for TPX and ITER.

The DIII-D radio frequency (rf) heating program is targeted to address specific needs not being considered on other devices and fosters DIII-D programmatic goals in the areas of confinement improvement, high beta operation, and long-pulse operation. A unique application of the DIII-D ECH system is to raise the temperature and beta of the electron component so that the damping of the traveling fast wave is strengthened. The symbiotic improvement by ECH in efficiency of current drive by fast waves is crucial as a key tool for the DIII-D Advanced Tokamak program

to develop a very high confinement, high normalized beta steady-state commercial power plant. The localized second harmonic ECH allows fast waves to drive off-axis current in a very controlled manner, independent of plasma density and temperature unlike lower hybrid current drive. It is expected that 10 MW of ECH 110 GHz with 8 MW of fast waves at 120 MHz will drive 2 MA of noninductive plasma current at 5% volume-averaged beta in DIII-D.

The first phase of the ECH program is to develop and operate a system with 2 MW at 110 GHz for up to 10 s. The ECH system consists of four Varian 500 kW gyrotrons to generate 110 GHz microwave power with pulse widths up to 10 s. (An alternate system under development is to use 1 MW gyrotrons from Russia.) Low-loss transmission systems transmit this power to the DIII-D tokamak. In FY93, the project directed its efforts to validate the design of the waveguide components and to investigate the mode purity of the gyrotron output. While the project waited for Varian to resolve the technical problems in developing a long pulse 500 kW gyrotron, the short pulse gyrotron SN#1 was used to investigate the performance of the U of W mode converter as an alternate to the GA mode converter, and issues related to the mode purity of the gyrotron. Mode purity testing using the University of Wisconsin mode converter indicated that the output of the U of W mode converter behaves the same as the GA mode converter with a large fraction ( $\approx 20\%$ ) of the power being unconvertible to the  $HE_{11}$  mode. Since the University of Wisconsin mode converter operates on a different principal than the GA one, the results support the assumption that the gyrotron is not producing a pure  $TE_{15,2}$  mode, but has a large fraction of its power in off modes.

A 1 MW 110 GHz gyrotron with an internal mode converter was ordered from GYCOM, a Russian company. This gyrotron is based upon designs that have worked quite well at 140 GHz. The changes, in addition to a slightly lower frequency, are a higher power (1 MW vs 500 kW) level and a longer pulse length (10 s vs a few seconds). The gyrotron window to be supplied is rated 750 kW for 2 seconds. In the future when a 1 MW cw window is developed the gyrotron can be retro-fitted.

## 7. SUPPORT SERVICES

### 7.1. QUALITY ASSURANCE

Fusion Quality Assurance (QA) engineers, inspectors, and support personnel maintained a high level of activity during 1993. Significant projects supported were the Advanced Divertor Program, the Divertor Material Exposure System, the DIII-D Graphite Tile Upgrade Project, the Fast Wave Current Drive Antenna for the Ion Cyclotron RF Heating System, the Electron Cyclotron Heating System, and the Neutral Beam Injector System.

#### 7.1.1. DESIGN SUPPORT

1. Using theodolites, transits, and mirrors, provided as-built measurements to the Thompson Diagnostics Group to design an interference-free laser path.
2. Measured as-built attitudes of three DIII-D diagnostic ports for the Fusion Design Group.
3. Measured the relationship of the 180° R-O port to the new work platform for input into the CAD system.
4. Provided accurate measurements of film tracings from the Russian high resolution spectrometer.
5. Reverse-engineered cryogenic valve details for the Fusion Design Group.
6. Measured the as-built configuration of the 0° R-O port and submitted the results to the Fusion Design Group.
7. Reviewed and approved all DIII-D design drawings, specifications, procedures, and procurement requisitions. Participated in design reviews and chaired the Material Review Board (MRB).

#### 7.1.2. INSPECTION SUPPORT

1. The majority of Quality Control (QC) activities during the year involved receiving and source inspections of purchased and fabricated material, parts, subassemblies, and assemblies. Inspection activity was particularly heavy for the DIMES Project, the ADP, the Graphite Tile Upgrade Project, the neutral beam system repair and the fast wave antenna project
2. The fast wave antenna also required extensive in-process and final source inspections at the suppliers' facilities. Fusion QA personnel interacted with Oak Ridge National Laboratory (ORNL) to resolve several design problems, and problems with production specifications. Intensive liaison between GA QA, the customer, and our suppliers prevented several situations from developing into cost and schedule burdens.
3. Fusion QC participated in an investigation to determine the reasons for a loss of preload in the DIII-D Toroidal Field Coil. Several shim bags and a missing wedge were determined to be the cause of the problem.

QC also performed hardness tests, ultrasonic NDE tests, chemical and physical tests of high strength bolts, characterized weld distortions, witnessed hydro and air pressure tests, assisted the Operations Group in measuring the location of DIII-D bumper limiters with respect to the inner wall tiles, performed visual and dimensional inspections of the 525 MVA motor-generator thrust bearings, load tested the ICRH Final Power Amplifier (FPA) lifting fixture, performed borescope inspections and verified machine setups prior to machining operations.

### **7.13. TOOLING/LAYOUT/ALIGNMENT SUPPORT**

1. Accurately measured and readjusted the 210° Neutral Beam Source Isolation Valve paddle stop screw heights.
2. Fabricated two sets of special tooling which will be used to measure beamline subsidence and attitude.
3. Completed the quarterly column and footing subsidence tasks, and the semi-annual pit wall crack inspections.
4. Verified proper location (centering) of the ECH Gyrotrons in their magnet/cryostat.
5. Developed an inspection technique and fabricated tooling to measure an internal radius in the DIII-D x-ray diode calibration fixture.
6. Assisted Fusion Engineering with the alignment of the DIMES transport tubes.
7. Performed a series of measurements inside the DIII-D vacuum vessel to document the radial location of the fast wave antenna and adjacent outer wall graphite tiles.

### **7.14. QA SYSTEM IMPROVEMENTS**

Doe Order 5700.6C was recently made a requirement in GA's Fusion contract with the DOE. As a consequence, GA is developing a new Fusion QA Manual (FQAM), a set of Fusion Engineering Procedures (FEP) and a series of implementing work instructions (e.g., the DIII-D Work Procedures Manual (WPM)). This action represents a major change in the way GA's Fusion Group addresses Quality Assurance, in that for the first time GA will adopt the order's requirements for a graded QA approach, continuous improvement program, and internal/external assessments. In the spirit of continuous improvement and the graded approach concept, DIII-D project personnel are the major contributors to the new QAM.

### **7.15. OTHER SUPPORT**

1. Fusion QA/QC personnel conducted the quality hoisting and rigging equipment inspection.
2. They also monitored numerous high consequence lifts in accordance with DOE Hoisting and Rigging Manual requirements with no adverse incidents.
3. Fusion QC personnel upgraded the CORDAX Coordinate Measuring Machine (CMM) to the latest software and firmware versions. Improvements include automatic probe compensation, faster screen draw, expanded operator prompting, enhanced ANSI functions, and automatic ANSI reporting. This upgrade package should reduce CMM inspection time by about 20%.

## **7.2. PLANNING AND CONTROL**

The Planning and Control Group supported operation and maintenance of the DIII-D facility. Planning and control provided long-term program planning, as well as day-to-day scheduling (cost control, preparation of Field Work Proposals and Cost and Fee Proposals), processing of purchase requests, expediting and reporting of status. These support activities are essential to the performance of the program within prescribed budgets and schedules. These planning activities (budget, schedule, resource) enabled us to maximize the utilization of available resources for accomplishment of program goals and were extremely important in planning and replanning of scope, budget, and schedule with fluctuating funding levels.

Major planning activities during FY93 included the 4 MW ICH upgrade, vessel outer wall tiles, diagnostic upgrades, liquifier procurement and installation, machine operations and maintenance, and a major five-month vent.

## **7.3. ENVIRONMENT SAFETY AND HEALTH**

### **7.3.1. FUSION AND DIII-D SAFETY**

The Fusion safety program provides for the safe operation of the DIII-D facility and for a safe working environment for employees and visitors. Special programs address high voltage and high current, high vacuum systems, ionizing radiation, microwave radiation, cryogenics and the use of power equipment and machine tools. The "DIII-D Safety Procedures for Facility and Equipment Operation" contains policies and procedures that specify safety rules and procedures that must be adhered to while working at the DIII-D site. Fusion works closely with GA's Licensing, Safety and Nuclear Compliance organization in areas such as health physics, industrial hygiene, environmental permitting and industrial safety.

Fusion has established a Safety Committee in accordance with company policy as a means of focusing on and addressing both the numerous safety issues faced daily and longer range safety needs and goals. The Fusion Safety Committee is comprised of Fusion representatives from various Departments within the Fusion group, including top management, supervisors and technicians. The safety Committee chairman is the DIII-D Program Director and the assistant chairman is the Fusion Safety Officer. The Safety Committee meets twice a month to address safety activities and concerns of the Fusion group such as: hazardous work requests, radiation work authorizations, accident/incident reports, near misses, equipment malfunctions, accident avoidance programs, supervisor involvement, training, inspections, access control procedures and high voltage hazards. The Safety Committee also solicits specialized help from any one of the five Fusion Safety Subcommittees during reviews of lasers, electrical systems, vacuum systems, the use of cryogens or the use of chemicals.

In addition to the Fusion Safety Committees oversight of activities at DIII-D, two individuals are dedicated full-time for onsite "preventive" safety involvement. Their activities include writing and reviewing procedures, developing and conducting special training classes, conducting inspections and follow-up, interfacing and coordinating with GA's Licensing, Safety and Nuclear Compliance organization and providing continuous oversight to assure compliance with established safety policies, procedures, and regulations.

The DIII-D Emergency Response Team consists of individuals involved directly with maintenance and operation of the DIII-D equipment. They are trained in CPR, first aid, SCBA and the use of fire extinguishers, evacuation and crowd control and facility familiarization. The team can respond within seconds to provide immediate assistance until the company Emergency Medical Technicians (EMTs) arrive.

Safety Inspections are conducted throughout the year to promote an active Hazard Prevention Program. The inspections are conducted by a combination of Fusion, GA Licensing Safety and Nuclear Compliance personnel and outside consultants.

A report is provided to the Fusion Safety Committee where corrective action assignments are made. DIII-D inspections include:

<u>Inspection</u>	<u>Frequency</u>
Site Inspection (GA Personnel)	Monthly
Electrical Consultant	Yearly
CAL/OSHA Consulting Service	Yearly
Insurance Carrier Inspection	Yearly (Multiple)
S.D. City Fire Department CEDMAT	Yearly
GA Safety Committee Hazards Survey	Yearly
DOE-SF Safety Review Inspection	Every 2 years

The Fusion Safety Officer is responsible for tracking the progress of all discrepancies and ensuring resolution.

All new employees and collaborators must go through a thorough and comprehensive safety indoctrination by the Fusion Safety Officer and Pit Coordinator. They are informed of the specific potential hazards that are present daily at DIII-D and the special safety precautions and rules that apply, with specific emphasis on the areas where they will be working. Subcontractors also receive a similar indoctrination.

## **7.3.2. FY93 SAFETY**

### **7.3.2.1. Training**

Training is all-important to the safety of both personnel and equipment. Due to the complexity of the DIII-D site and its operation, numerous safety training classes are conducted. Subjects of the classes include, but are not limited to: confined space entry, back injury prevention, radiological safety, laser safety, hazard communication, cryogenic safety, crane and forklift operation, lockout/tagout, the national electrical code, machine shop tool usage and basic industrial safety requirements.

The Fusion Safety Officer attended the National Safety Council Annual Conference on Safety and Health.

The yearly DIII-D Emergency Response Team training sessions were presented by the GA Emergency Services Department in a joint training effort with the Fusion Safety Department. They include the following: Facility Familiarization Training; Fire Extinguisher Training; Hydrant Hook-Up Training; SCBA Training; CPR Training.

A fire and emergency evacuation drill was conducted by GA Emergency Services Department which exercised the DIII-D Emergency Response Team as well as the emergency preparedness of all DIII-D personnel. A CPR training class was also provided for all electrical technicians.

The "Working Safely and Effectively in the DIII-D Pit" training class was presented to the Fusion employees who work in the DIII-D pit. This class is mandatory for all employees who are working in the DIII-D pit with retraining required once a year.

Numerous Confined Space Entry Classes were provided prior to and during the vent to enable the safe entry into the DIII-D vessel and other confined spaces. Every individual who enters any confined space must have attended this one-hour training class that is good for one year. At the close of FY93, we had 111 confined space trained individuals.

A six-hour radiation training course was offered to all new DIII-D employees and Job Shoppers to fill the Health Physics/Nuclear Regulatory Commission (NRC) radiation training requirements. Three radiation refresher courses were also given by the Fusion Safety Officer to all Fusion employees who have previously had the complete course and only needed the yearly update.

Hazard Communication Training was offered by GA's Industrial Hygiene Department covering Material Safety Data Sheets, container labeling and hazard identification.

A presentation on the safe use and handling of cryogenic materials used at DIII-D was presented to technicians, supervisors, and other users of cryogenics.

A crane operator training class was held on the safe operation of a crane and the correct way to attach various slings and shackles.

The new Stationary Power Tool training program is now complete and is in full operation. The program requires that each individual have the proper training on the safe use of each stationary power tool prior to operation.

During FY93, 45 new employees and long-term visitors received a safety indoctrination from the Fusion Safety Officer.

### **7.3.2.2 Inspections**

As stated above, a number of DIII-D inspections occurred during the year. In addition to these, the following inspections were conducted. A DOE Multidiscipline Safety Review audit was conducted by representatives from DOE/SF. A comment made by one DOE/SF representative was "I think if I were to give you a DOE type word rating, I would give you an EXCELLENT," All identified problem areas have been addressed.

Slings, shackles, and all lifting equipment are inspected and load tested as per the requirements in the DOE Hoisting and Rigging manual.

A representative from American Nuclear Insurers toured the DIII-D facility to inspect and check for unusual fire hazards and other areas that might put the facility at risk. A chemical inspection and inventory was conducted of the entire DIII-D facility, cataloging all hazardous substances. Missing Material Safety Data Sheets (MSDSs) were requested and have now been cataloged for employee access in the Safety Library and the Fusion Safety Office. These data sheets have also been cataloged in the computer database system for easy reference and back up.

### 7.3.2.3. Other Activities

As a result of an accident involving a Japanese scientist at Lawrence Livermore National Laboratory (LLNL) in February 1992, the U.S. DOE and Japan formed a Joint Working Group. The U.S./Japan Joint Working Group (JWG), led by Steve Rossi of the Office of Fusion Energy, met at the DOE headquarters in Germantown, Maryland in October 1992 and in Tokyo and Mito City, Japan in January 1993 to discuss the issues of safety of inter-institutional collaborations. The group consists of five U.S. and five Japanese safety representatives from national laboratories, private contractors and universities. The Fusion Safety Officer represents both GA and the U.S. industrial contractors.

The Fusion Safety Officer also visited the University of Wisconsin for two days in an interlaboratory safety assessment/collaboration visit.

The DIII-D Safety Committee Membership was reviewed, brought up to date, and temporary rotating members were replaced by new members. This committee met a total of 24 times. Listed below are some of the tasks that were accomplished:

1. Reviewed and approved 21 HWAs after appropriate recommendations and changes by the Safety Committee and select Safety Subcommittees.
2. Reviewed three incidents that involved no injury, three minor first aid incidents and four accidents that required minor off-site medical treatment.
3. Reviewed the monthly inspection discrepancy reports of the DIII-D site. These include a request from the Fusion Safety Officer for the CAL/OSHA Industrial Hygiene consultation services, an Electrical Consultant Inspection, a GA Hazard Survey Inspection, monthly Fusion Safety Committee inspections, daily walk-around inspections, and follow-up visits from the San Diego Fire Marshal's Hazardous Materials Inspection Team and the DOE Multidisciplinary Review Committee. In all, a total of 548 safety discrepancies were noted, and at the close of FY93, all of these discrepancies had been corrected.

As a consequence of a DOE safety review, an extensive program is underway to install shields on all rotating water pump and motor shafts so that openings from the top or sides to the exposed shaft are one-half inch or less. These modifications are being made to manufacturers' standard pump hardware.

### 7.3.3. RADIATION SAFETY

The State of California, NRC, and DOE set criteria for the maximum radiation exposures for the general public and employees. [Refer to "Radiation Aspects of DIII-D," by Project Staff; J. Kim, J.L. Luxon (eds.), February 1989.] Section 30268 of the State of California regulations state: No user shall possess sources of radiation in such a manner as to create in any uncontrolled area, from such sources, radiation levels which could cause any individual to receive a dose to the whole body in excess of:

1. Two (2) millirem in any hour.
2. One hundred (100) millirem in any seven consecutive days.
3. Five hundred (500) millirem in any one year. (The State of California limit will decrease from 500 to 100 millirem per year in 1994.)

GA operates DIII-D according to the general requirement that the exposure of the public to radiation be kept as low as reasonably achievable (ALARA). In the spirit of this goal, GA and DOE now operate DIII-D at a guideline of 20 mRem/yr, at the DIII-D site boundary, with a DOE administrative allocation of 5 mRem/quarter. An important consideration is the radiation level experienced by members of the staff, either in carrying out device operations or in working in the facility, especially near or in the tokamak after operations in the presence of residual radiation due to activation of device materials. All GA DIII-D personnel, visitors, collaborators, and contractors who are in the DIII-D facility for more than 18 hr/qtr during operations are classified as radiation workers. They receive radiation training and carry radiation badges during operations. The present limiting criteria is that worker exposure be less than 1250 mRem/qtr. The DIII-D program presently applies a limit of 300 mRem/qtr for individuals. The two most restrictive conditions for DIII-D are the exposure of individuals who work in the vessel for prolonged periods of time and the site accumulated radiation at the boundary limit.

Radiation levels for all proposed DIII-D experiments are estimated and approved in accordance with the ALARA principal before authorization is given to conduct any experiment. The actual site boundary exposure in 1993 was 6.8 mRem.

In DIII-D operation through 1993, the highest D-D neutron rate produced was  $5.8 \times 10^{15}$  neutrons/s, and the largest number of neutrons produced on a single shot was  $5.7 \times 10^{15}$  neutrons. For the present DIII-D radiation shield,  $1.5 \times 10^{17}$  neutrons is the equivalent of 1 mRem at the site boundary. The highest site-boundary radiation rate produced is 0.037 mRem/s, and the maximum site radiation produced per shot was 0.038 mRem.

The neutron and gamma radiation produced at DIII-D is constantly monitored during operations at the site boundary with the level kept below 20 mRem per year. Personnel dosimeters are worn by all individuals while on the DIII-D site and if entrance into the machine pit is required between shots, an alarming dosimeter is worn in addition to the TLD badge. Prior to unrestricted machine pit access, the pit is surveyed and the areas requiring monitoring before entry are cordoned off until radiation levels fall below the DIII-D procedural control limits. Workers in the vessel also carry alarming dosimeters and each entry is controlled, monitored, and recorded.

## 7.4. VISITOR AND PUBLIC INFORMATION PROGRAM

Tours of the DIII-D facilities are open to organizations and institutions interested in fusion development (colleges, schools, government agencies, manufacturers, and miscellaneous organizations). These tours are conducted on a noninterference basis and are arranged through the DIII-D tour coordinator whose responsibilities include security, arranging tour guides, and scheduling tours. During the year, 1583 people toured DIII-D to give a total of 11,051 during the last nine years.

## 8. CONTRIBUTION TO ITER PHYSICS R&D

The DIII-D program continues to make substantial contributions to the ITER Physics R&D Program. During the interim period before the newly established ITER Engineering Design Activity is fully formed, the U.S. ITER Home Team has identified a summary list of key issues for ITER Physics R&D. These are shown in Table 8-1. The planned divertor program will contribute considerably to the first three issues. Experiments are planned to optimize power and particle exhaust, and helium transport. Modeling of these divertor experiments has become a key element of the divertor program. The DIMES program will address the *in-situ* testing of divertor wall materials (Issue 4). The DIII-D program continues an active effort to characterize and model disruptions with the goal of providing a strong design basis for next generation machines although this effort is lessened due to funding restraints (Issue 5). The confinement program is focused on the understanding of enhanced confinement modes and the ability to sustain them in time (Issue 6). Key  $\alpha$ -particle stability issues

**TABLE 8-1  
ITER PHYSICS R&D NEEDS**

- 1 **Demonstrate a divertor configuration with adequate power and particle exhaust capability for ITER.** This remains the most prominent and demanding physics issue. The head loads predicted for established divertor configurations are too high for reliable engineering designs.
- 2 **Demonstrate adequate fueling and helium exhaust in this configuration.** In addition to demonstrating power and particle exhaust handling, a divertor configuration must be capable of central fueling and exhaust of impurities including helium ash.
- 3 **Demonstrate models to extend divertor results in existing experiments to ITER.** Modeling is separately specified to clearly identify the need to develop adequate models for the divertor.
- 4 **Demonstrate appropriate divertor materials in-situ to handle the power exhaust with low plasma impurity content.** Candidate materials for the high heat flux region of the divertor will need to be tested and characterized in a tokamak environment.
- 5 **Demonstrate the ability to control or avoid disruptions.** The development of regimes of disruption-free operation will continue to be an important challenge for ITER.
- 6 **The scaling of a suitable long-pulse confinement mode to D-T operation in ITER.** It will be essential to understand which confinement modes ITER will operate in and to understand how to maintain stable confinement levels in that mode.
- 7 **Ascertain the role of  $\alpha$ -particle effects on confinement and stability in ignited plasmas.** The understanding of  $\alpha$ -particle effects will be one of the key areas of physics understanding in the ITER operating regimes.
- 8 **Develop suitable long-pulse current drive scenarios for ITER.** This capability is not crucial until several years into the operating life of ITER. No accepted candidate exists at this time and the ability to implement any proposed scheme could be highly impacted by decisions made during the engineering design phase.

TAE modes) are studied by the losses of energetic beam-induced  $\alpha$ -particles from the deuterium plasmas (Issue 7). There is an ongoing focus on the development of current drive scenarios focused on fast wave current drive (Issue 8). This will be considerably strengthened in FY94 by the increase in the fast wave power from 2 MW to 6 MW.

The DIII-D program is renowned for its strong contributions to the ITER program. This results from both the appropriation of the DIII-D device to study many other issues and an active awareness of ITER needs and issues in the DIII-D program. Key ITER relevant results in the past year include the better understanding of the plasma divertor configuration including the use of divertor cryopumping to demonstrate density control in divertor plasmas. Divertor cryopumping was also used to demonstrate helium pumping from diverted H-mode plasmas demonstrating the particle confinement times which when normalized to the energy confinement are near those needed for a burning plasma. A strong effort has also been undertaken to better diagnose and model the divertor region and to benchmark these models against DIII-D data. Detailed studies of the role of plasma shape in determining confinement and stability are providing essential answers for next generation devices. A separation of the current and density dependence of H-mode confinement was demonstrated for the first time using divertor pumping to control the density. Considerable progress was also made on the characterization of vertical displacement events, in order to allow these events to be properly scaled to ITER.

In total the DIII-D program has contributed to nearly all of the ITER issues. Progress on ITER physics R&D issues identified during the CDA was reported to ITER and a substantial set of reports were made. Table 8-2 summarizes the contributions of each area by country and device. It can be seen that DIII-D contributed in most areas.

TABLE 8-2  
ITER PHYSICS R&D CONTRIBUTIONS

ITER PHYSICS R&D CONTRIBUTIONS  
31-Mar-93



Contributors

No.	Topic	E1 JET	E2 AEA Culham	E3 CCRM Varennes	E4 CEA Cadarache	E5 CEMAT(CRPP *)	E6 ENEA Frascati	E7 FOM Maastricht	E8 IPP Garching	E9 IPP Garching	E10 IPP Garching	E11 KFA/ERM-IOMS *)	E12 NFRNL *)	S1 T-15, T-10, TO-2	S2 T-10, TO-2	S3 TVO	S4 SPRUT, LENTA	S5 T-10, T-15, TUMAN-3	S6 TUMAN-3, T-10, FT-1, FT-2	S7 T14	S8 T-3M-2	S9 TUMAN-3	J1 DMR-D	L2 MTX	U5 PBX-M	U6 IFTR	U7 TEXT	U8 U. Wisc.	U9 Other
1.1	Divertor and scrape-off layer expts	X	X	X	X	X	X	X	X	X	X	X	X	X	X	X	X	X	X	X	X	X	X	X	X	X	X	X	
1.1a	Divertor power load profiles																						X						
1.1b	Impact of divertor geometry variation																						X						
1.1c	Hot spots on plasma facing comp.																						X						
1.1d	Edge plasma effects of heating and CD																						X						
1.1e	Impact of fuelling																						X						
1.1f	ELMS and other edge transients																						X						
1.2	Edge impurity radiation and transport	X	X	X					X														X						X
1.2a	Radiating plasma edge layers											X										X							X
1.3	Helium and hydrogen exhaust			X	X							X						X				X							X
1.4	Divertor and startup optimization			X	X	X			X			X										X							
1.5	Plasma-facing materials characterization			X	X							X					X					X							
1.5a	Wall conditioning methods								X		X											X		X	X	X	X	X	
1.5b	Wall conditioning between discharges										X											X							
1.6	Alternative divertor concepts																												
2.1	Disruptions characterization	X	X				X	X	X	X	X											X			X	X	X	X	
2.1a	Disruption-produced runaways													X									X			X			
2.1b	Disruption w. soft current quench																						X			X			
2.2	Plasma motion during disruptions	X							X								X					X							
2.3	Disruption avoidance and control	X	X				X	X	X	X	X																		
2.3a	Identification of pre-disruptive state													X															X
2.4	Char. of beta-limiting phenomena	X		X	X	X	X	X	X	X													X			X	X	X	
2.4a	Profile effects on the beta limit																						X			X	X	X	
2.4b	Inductive equilibrium profiles																						X			X	X	X	
2.4c	MHD impact on high beta ops																						X			X	X	X	
2.4d	Fast ion impact on high beta ops.																						X		X	X	X	X	
2.5	Density limit			X					X	X								X				X		X	X	X	X	X	
3.1	H-mode SS operation							X	X	X	X	X					X					X		X	X	X	X	X	
3.1a	Confinement scalings			X																			X						
3.1b	Plasma particle transport																								X	X	X	X	
3.1c	Momentum transport																												
3.2	Control of MHD activity		X																				X	X					
3.3	Transport mechanisms	X	X	X	X	X	X	X	X	X	X	X					X					X		X	X	X	X	X	
3.3a	Plasma turbulence																									X	X	X	
4.1	Long pulse operation	X					X				X																		
4.1a	Bootstrap current			X					X																X	X	X	X	X
4.1b	LNCD	X	X	X	X	X												X							X	X	X	X	
4.1c	FWCD	X													X								X			X	X	X	
4.1d	ECCD		X																										
4.1e	NBCD																												X
4.1f	Advanced CD techniques																												X
4.2	Startup optimization		X	X	X	X	X	X	X	X																			X
4.2a	LH current removal																												
4.3	Shutdown optimization			X					X																				
4.4	Control of fast ions w. IC waves	X									X																		
4.5	Pellet ablation physics				X		X	X	X	X								X											
4.5a	Compact toroid injection			X																									X
5.1	Fast ion single-particle physics	X	X									X												X		X	X	X	
5.1a	Fast ion ripple losses																								X	X	X	X	
5.2	Fast ion collective effects	X	X	X	X	X																		X	X	X	X	X	
5.3	DT plasmas and alpha heating													X															X

\*) CEMAT Madrid  
CRPP Lausanne  
KFA Jülich  
ERM-IOMS Brussels  
NFR Göteborg  
RNL Riga

## 9. TPX SUPPORT

During FY93, the DIII-D group contributed to the TPX preconceptual design effort primarily in the areas of development of operations plans, analysis of error fields and development of error field specifications, and a field error correcting coil (FECC), and specification of divertor diagnostics. In addition, a number of formal and informal workshops were held at GA. Most of the work done directly in support of TPX was carried out during the first half of FY93, in preparation for the TPX Conceptual Design Review, which took place in March. There were a number of contributions to portions of the project documentation, including the System Design Descriptions (SDD) and the Physics Design Description (PDD). Also, there has been a continuing dialog between TPX and the DIII-D program. Experimental results from DIII-D are communicated on a regular basis to the TPX team. These results have had a significant impact on development of the TPX design. In addition, the DIII-D program has carefully considered the physics R&D needs of TPX in development of the DIII-D experimental plan.

Work was continued on the development of an initial TPX operating plan which meets the requirements of maximal progress toward achieving the initial goals of steady-state, advanced plasma operation, while providing reduced activation during the first two years, so that the first major maintenance period can be done hands-on. A four year plan of physics studies and an associated neutron production profile were prepared. Subsequently, the plan was modified to incorporate a phased program of hardware upgrades and enhancements. The revised plan included upgrades in three categories: in support of the plasma control and advanced tokamak development aspects of the TPX mission, in support of the power and particle control and divertor development goals, and to extend the operating capabilities of the TPX tokamak. The first upgrades to be introduced (at the end of the third year) will be an improvement in the lower hybrid rf system and an improved current profile diagnostics for enhancing the current profile control capabilities. At the same time, a pellet injector and an active control coil system is called for. At the end of the fifth year, a major upgrade of the divertor configuration is planned.

A study of the impact of magnetic field errors on the TPX plasma equilibrium was undertaken. As seen in DIII-D and other tokamaks, toroidal magnetic asymmetries resulting from small variations in coil placement can limit the range of plasma operating space through the development of magnetic islands and the inhibition of plasma rotation. Specifications were provided for the field error tolerance of the TPX tokamak, and requirements developed for TPX field error correcting coils.

A detailed definition of the required diagnostics for the TPX divertor was developed, in addition to specifications for access to the divertor region for diagnostic measurements. Work was also done on the incorporation of plasma diagnostics into the divertor structure. A draft plan for diagnostics for both divertor physics and divertor operations in TPX was submitted for inclusion in the TPX System Design Description document.

In October, an informal workshop was held at GA on the question of analysis and control of plasma equilibria, particularly with regard to vertical stability. Various analysis techniques, possible control schemes, and instrumentation requirements were discussed. In June, GA hosted a workshop on "Stabilization of the External Kink and Other MHD Issues", at the request of the TPX program management and the US DOE. The workshop consisted of a day and a half of invited talks, followed by panel discussions and working group meetings. The purpose was to bring together theorists and experimentalists in order to assess our current understanding of the external kink

instability at high beta and its stabilization by passive or active means, and to outline R&D needed for TPX and other future devices. The workshop was extremely successful, in that it brought together the theoretical and experimental communities, and developed a clear statement of future research needs. The theory was clearly presented, including new results on the influence of cold plasma edge resistivity and toroidicity. The experimental results were comprehensively reviewed and found to be generally consistent with the more complete theory. Discussions of the prospects for MHD feedback, and illustrations of the capabilities of simulation codes enhance the prospect for designing future tokamaks with significantly higher disruptive beta limits.

## 10. COLLABORATIVE EFFORTS

### 10.1. DIII-D COLLABORATION PROGRAMS OVERVIEW

Although the major part of the fusion research which is carried out on DIII-D is performed by General Atomic scientists under General Atomic management, in the last few years DIII-D has become a type of national fusion research users facility with 40 institutions participating. The total number of national and international collaborators on DIII-D in FY93 for long-term assignments was 50. In addition, 200 persons made visits of three weeks or longer to DIII-D. Through its national and international collaboration programs GA is playing a major role in the worldwide advancement of fusion research towards the goal of a fusion power reactor. Our collaboration with the DOE national laboratories has brought new recognition to our program and broadened its scope. Our international collaborations have helped the U.S. to maintain its role as a strong partner in the ITER project.

The recent increase in our collaboration with Russian fusion research institutes and scientists has helped maintain an active Russian fusion program as well as providing GA and the U.S. fusion program to expand DIII-D relevant research.

The DIII-D collaboration programs have contributed to the results presented in the previous sections of this report and are discussed in more detail in the following.

### 10.2. JAPAN ATOMIC ENERGY RESEARCH INSTITUTE (JAERI)

JAERI scientists continued to participate in the DIII-D program. They contributed to and learned from the DIII-D experiments in the area of VH-mode, divertor pumping, rf current drive and diagnostics. These activities were direct benefit to the DIII-D, JT-60U, and JFT-2M programs.

Work on the VH-mode studies in DIII-D found appreciable difference in the edge flow shear and density turbulence caused by a small amount of neon gas puff. Even about 1% neon was enough to prevent the development of shear flow and therefore VH-mode. These results are in some sense consistent with 1992 results in which the nickel was a dominant impurity and indicating significant role of impurities on VH-mode. Analysis of the MHD activity at the VH-mode termination shows the development of a non-symmetric mode structure with high frequency component which might be related to some kind of singularity inherent to the machine. Contributions were made to the MIST impurity transport code, operation and several simulation analyses were done for the preparation of the DIII-D experiments. Participation included the initial cryopump experiment in DIII-D and the initial FWCD experiment with new Faraday shield in DIII-D.

In addition, JAERI physicists visited DIII-D for the purpose of the technical discussions and information exchanges on ray tracing and current drive code, 110 GHz ECH, 60 GHz ECH transfer, DIMES, ECE, x-ray, and to study the multipulse YAG-laser Thomson scattering of DIII-D.

### 10.3. LAWRENCE LIVERMORE NATIONAL LABORATORY

Lawrence Livermore National Laboratory (LLNL) personnel participated in both the edge physics and advanced tokamaks areas on DIII-D in FY93. Contributions were made to the Remote Experimental Site development. After the shutdown of the MTX experiment at LLNL, the GA collaboration was expanded in FY93. There are now about 16 physicists in the collaboration; roughly half are located in San Diego, and the other half commute between LLNL and GA. There are also an engineer and three technicians located in San Diego working on the collaboration.

LLNL work in the edge physics and divertor area has included both experiments and modeling. One focus in the area of divertor experiments this year has been radiative divertor experiments; these are in support of the radiative divertor design. Both  $D_2$  and neon puffing experiments have been performed; divertor heat flux reduction of factors of 3-5 have been observed. In the case of  $D_2$  injection, the core density rises, and in the case of neon injection, the core  $Z_{eff}$  rises. New divertor structures are being explored to minimize these effects.

Several new diagnostics were proposed in FY93: a divertor interferometer, a divertor Thomson Scattering system, and an Edge MSE system. These systems are being tracked through the new 93.01 set of procedures for diagnostic construction. The divertor interferometer (Fig. 10.3-1) is a 250 GHz system which will measure the line-averaged

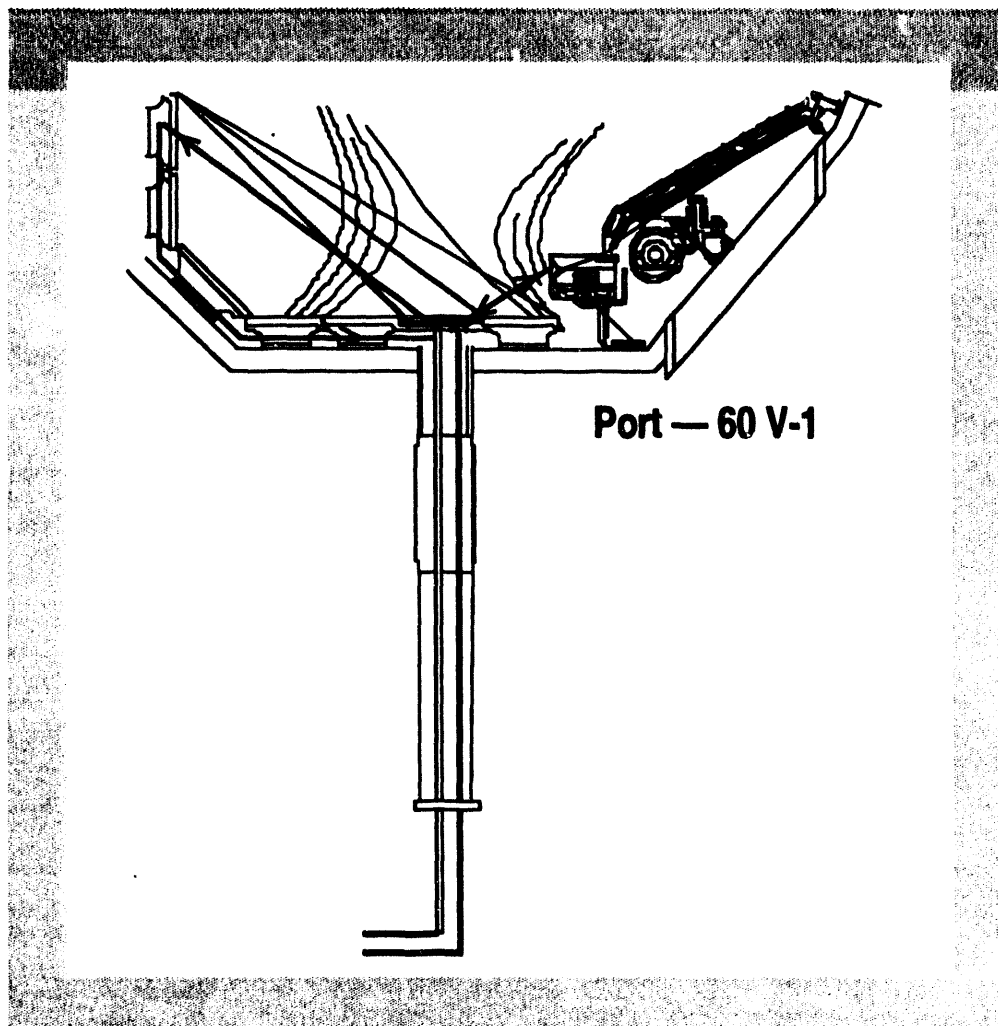


Fig. 10.3-1. Divertor interferometer views

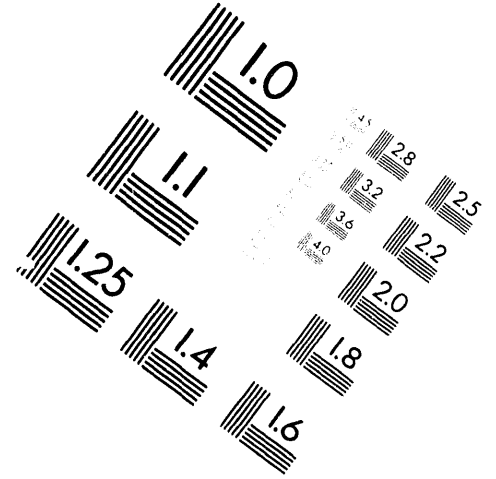
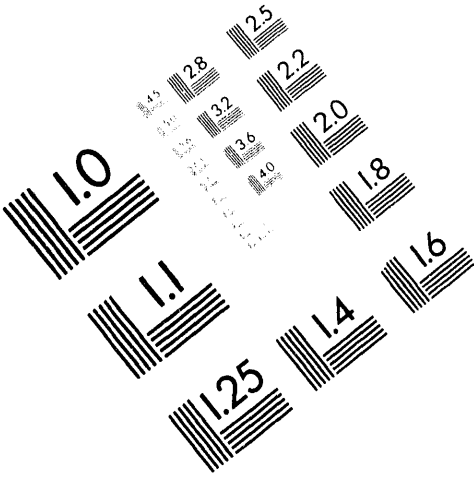


**AIM**

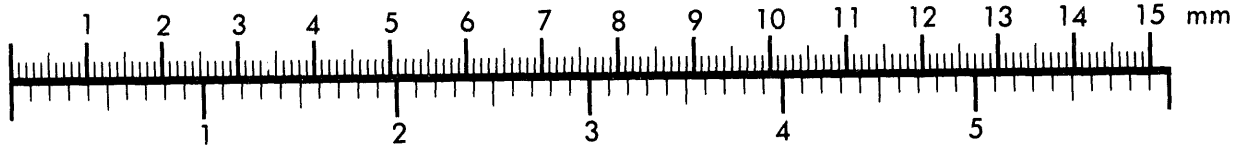
**Association for Information and Image Management**

1100 Wayne Avenue, Suite 1100  
Silver Spring, Maryland 20910

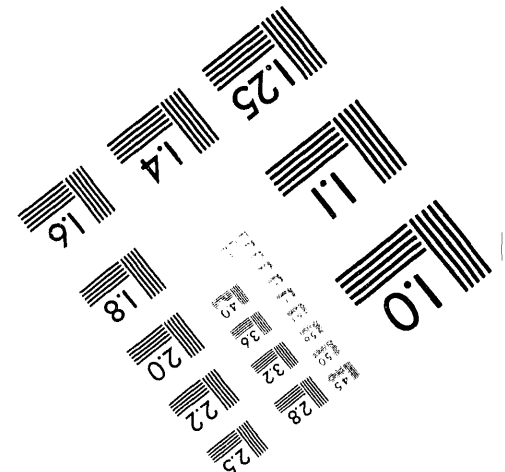
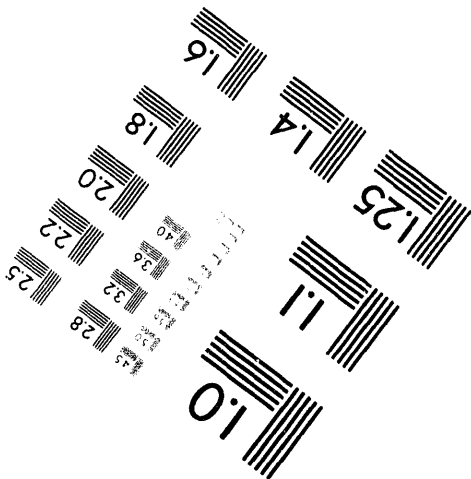
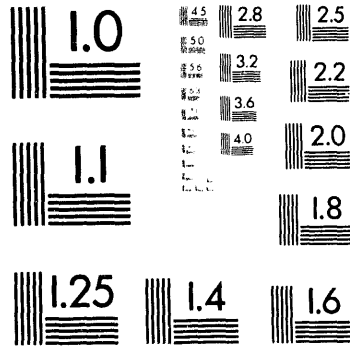
301/587-8202



Centimeter



Inches



MANUFACTURED TO AIM STANDARDS  
BY APPLIED IMAGE, INC.

**2 of 2**

density across each leg of the divertor; this diagnostic will be very important in the study of high density (MARFE-like) structures in the divertor region. The divertor Thomson Scattering system (Fig. 10.3-2) is an extension of the existing core Thomson Scattering system and will involve a close collaboration between GA and LLNL, i.e., GA will provide the core laser and LLNL will duplicate the existing detection system. This diagnostic will take two years to construct, due to funding limitations, but is scheduled for installation before the planned date for the Radiative Divertor Program.

In the area of modeling, UEDGE simulations of the DIII-D Scrape-off layer (SOL) were compared with detailed data from the experiment. Improvements in the code (see the boundary modeling section of this report) have enabled

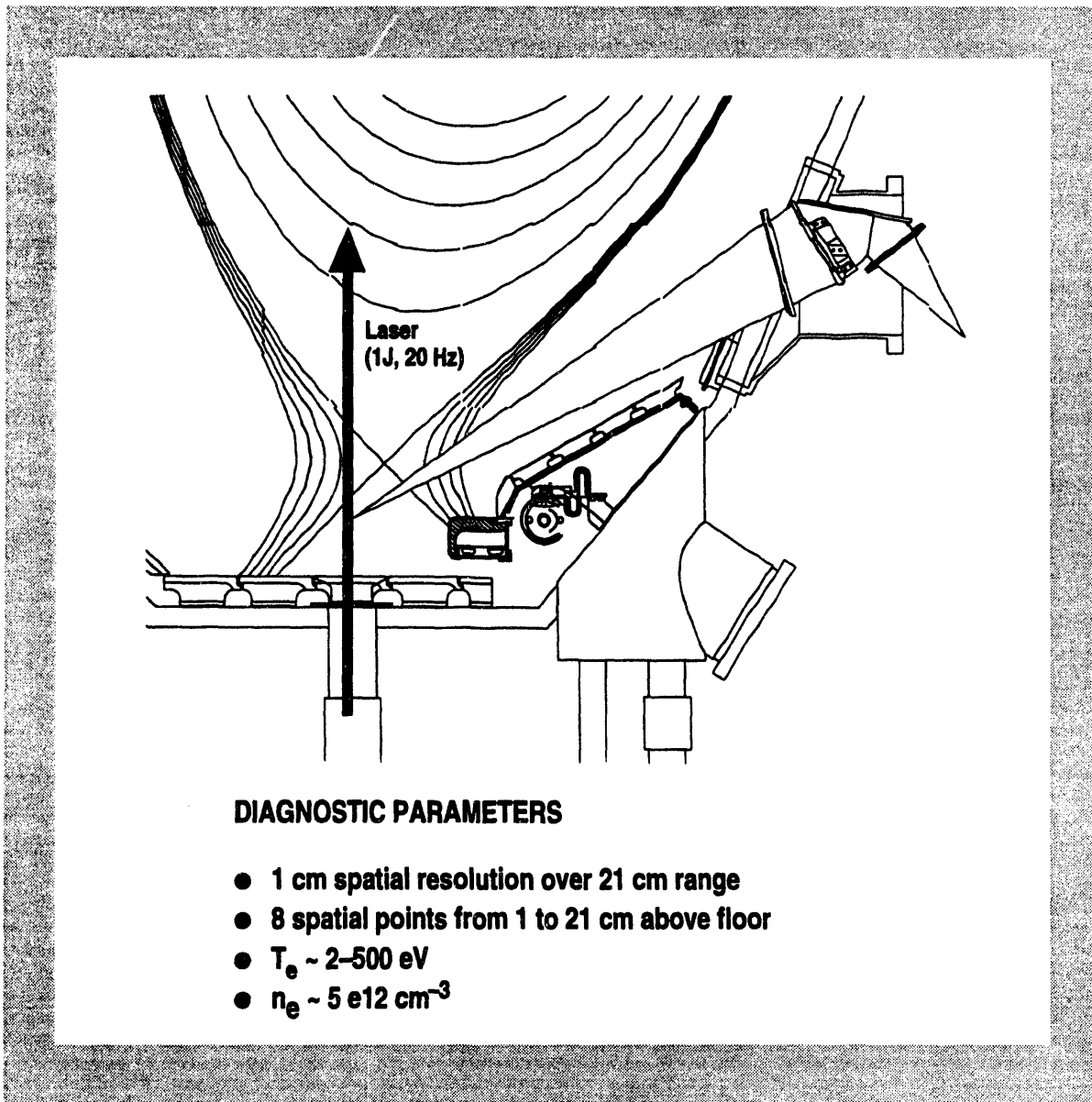


Fig. 10.3-2. Divertor Thomson scattering

obtaining results which simultaneously match the midplane profiles of density and temperatures, and the amplitude and shape of the outer divertor power profile. Much higher power flux is calculated at the inner strike point than is measured. The discrepancy is attributed to the lack of impurity radiation near the inner strike point in the simulation. The experiment indicates most of the power flowing to that inside is radiated in a region above the plate. Using the post processor developed this year, consistency is obtained between the calculated and measured  $H\alpha$  emission for the photo diode views near the inner and outer strike point. However, the experimental results typically indicate much higher emission in the private flux region than obtained in the simulation.

During the past year the boundary database has been significantly expanded. Effort was coordinated with the edge physics group at JET to define a set of boundary relevant data to include in a joint DIII-D/JET boundary database. Many, but not all, of the plasma parameters in this joint data set already existed in the DIII-D database. The BNDY database was expanded to include all of the joint plasma parameters. In addition, a file format was worked out to ease sharing data between the two machines. Finally, the number of time slices in the BNDY database was greatly enlarged during the past year.

UEDGE-generated plasma parameters were established for both the 20 cm and 40 cm reference radiative divertor configurations. A single-null configuration was examined with a calculational mesh which extends to the flux surface which lies 2 cm outside the separatrix at the outside midplane; the plasma characteristics were found to be sensitive to the assumed boundary conditions with this narrow domain. To avoid this sensitivity, a domain was used which extends to the 4 cm flux surface. Since an upper null point exists between the 2 cm and 4 cm flux surfaces, the plasma is modeled as a symmetric double-null with the broader computational domain.

The sensitivity of the plasma profile was explored to the anomalous perpendicular transport coefficients and found that the divertor power profile obtained in the 40 cm configuration becomes much narrower than has been seen experimentally when the thermal diffusivity obtained in UEDGE validation runs is used with shorter X-point to divertor distances. This suggests the thermal diffusivity depends on the X-point height.

Hydrogenic neutral transport modeling for DIII-D was done with the DEGAS code. The effort focused on supporting the Radiative Divertor Program. To that end two generic single-null equilibrium shapes were looked at, one with a 20 cm X-point to strike point distance, and the other with a 40 cm distance. Using a UEDGE plasma solution with a 2 cm SOL domain, DEGAS simulations of the neutral propagation were done for a variety of baffle configurations. These included close fitting conformal slots around the UEDGE plasma, completely open geometries with the DIII-D vacuum vessel as the only boundary, a "Gas Bag" geometry with a single baffle from the vacuum vessel toward the X-point, and a partially open geometry with an angled wall boundary closer to the plasma than the actual vacuum vessel. The results were compared in terms of the total ionization rate of neutrals in the plasma core (inside the separatrix) and the profiles of the neutral atomic density poloidally from the divertor plate to the X-point. The close fitting conformal slot gave the greatest reduction in ionization current to the core as expected and reduced the neutral density half way up the slot by up to two orders of magnitude over the open configuration.

LLNL involvement in the advanced tokamak effort on DIII-D has been concentrated in two areas, high  $\beta_p$  confinement experiments and development of the Motional Stark Effect (MSE) diagnostic to measure the current profile. High  $\beta_p$  plasmas may be attractive for advanced tokamak scenarios for two principle reasons. First, they have large bootstrap current fractions and therefore modest auxiliary power requirements are needed for steady-state current drive. Second, they exhibit improved performance, thus allowing operation at lower current which can lead

to smaller reactors. In earlier experiments, a high  $\beta_p$  configuration, was established which spontaneously ended with a weak collapse in beta due presumably to profile evolution to MHD unstable conditions.

During FY93 experiments were conducted in high  $\beta_p$  plasmas with the intention of increasing both the poloidal beta and the duration of this configuration. The goals of our experiments were 1) to explore the long pulse evolution of the current profile and 2) to study the effect on stability and confinement by using current ramps to alter the edge current density. In these experiments, operation was at low current, 0.4–0.8 MA, H-mode plasmas with neutral beam injection of 3–10 MW. Over resistive time scales the plasma current profile broadened and central  $q$  increased as shown in Fig. 10.3–3(a). The figure shows the radial and temporal dependence of integral  $q$  surfaces as obtained from EFIT calculations of plasma equilibria using magnetic loop and eight channel MSE diagnostics. Poloidal betas of up to 3.5, were achieved with the high  $\beta_p$  duration extending for the entire duration of neutral beam injection without a beta collapse. For the equilibria obtained experimentally, the MHD stability was consistent with the stability predicted by the GATO code.

With  $q_0 > 2$ , a change in the MHD character was observed from predominantly  $m/n = 2/1$  to  $m/n = 3/1$  modes and eventually to a state without detectable MHD fluctuations. Correlated with the disappearance of fluctuations, the plasma density increased a factor two in the core as shown in Fig. 10.3–3(b). Ideal MHD calculations showed stability against ballooning modes during the density rise. The improved central confinement was evident from the centrally peaked current and density profiles measured. The increase in core pressure gradient drove large bootstrap currents which ultimately caused a decrease of  $q_0$ , the re-appearance of fluctuations, and the termination of the improved confinement. Bootstrap current fractions of up to 80% were achieved along with the global energy confinement improvement of about 30% over H-mode.

Also observed during the low current experiments was an inferred prompt loss of neutral beam injected fast ions (typically ~50% at 0.4 MA). These losses are not well understood, but the large fast ion banana orbits at low current possibly play a role.

For current ramp experiments the total current was ramped down from 0.8 to 0.4 MA. Several important results were obtained. Following completion of the ramp for a time period of about 0.4 s, corresponding to about 5 to 6  $\tau_E$ , enhanced values of  $\beta_p$ , normalized toroidal beta, and energy confinement were obtained at high  $\ell_i$  ( $\beta_p$  up to 5.2,  $\beta_N \approx 3.5$ ,  $\tau_E/\tau_{ITER-89P} \approx 2.6$ , and  $\ell_i$  up to 2.4). During both the ramp and the improved confinement phases fast ion losses were also low (~10%), about equal to that measured before the ramp. The loss then increased coincident with an observed onset of high frequency fluctuations. More experimental data is required to understand these results, but it indicates that fluctuations may enhance transport of fast ions at low plasma current. Future experiments are planned to obtain the enhanced mode at higher current where the fast ion losses are smaller and energy confinement is expected to increase. While this enhanced confinement state was achieved, a critical element to extending and improving this behavior is control of the current profile, including the development of real-time control.

During the FY93 experiments on DIII-D, the eight channel MSE instrument provided reliable current profile measurements. Improvements in optics (low Faraday rotation glass) and calibration (shrinking plasma across chords) were implemented during this time [D. Wróblewski, Phys. Rev. Lett. **71** (1993) 859]. To improve both the prospects for real time current density measurement and control, as well as the for the quality of equilibrium and stability analyses, we have begun an upgrade of the MSE diagnostic to 16 channels. An error analysis study was performed using the EFIT equilibrium code to better understand the way in which MSE measurements constrain the equilibrium solution. Based on this study, it was concluded that additional channels, improved radial resolution, and improvements in calibration would all contribute to better equilibrium reconstructions.

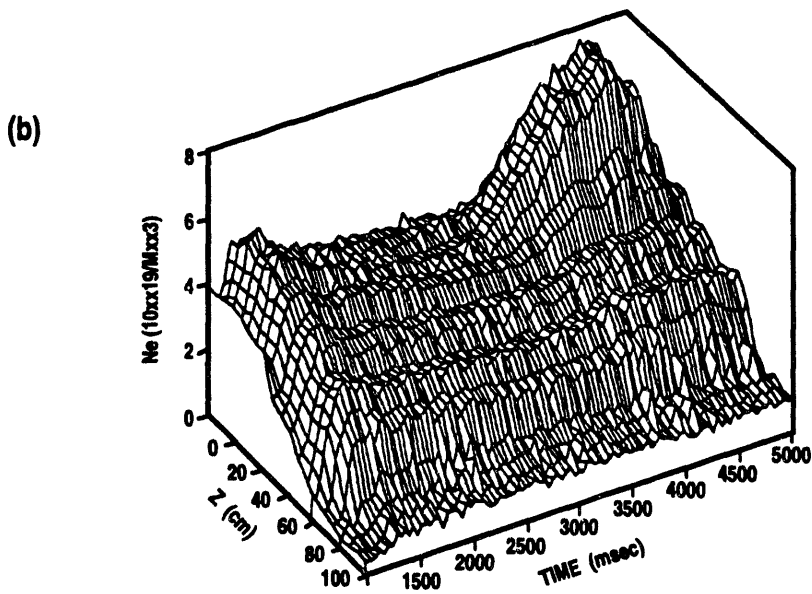
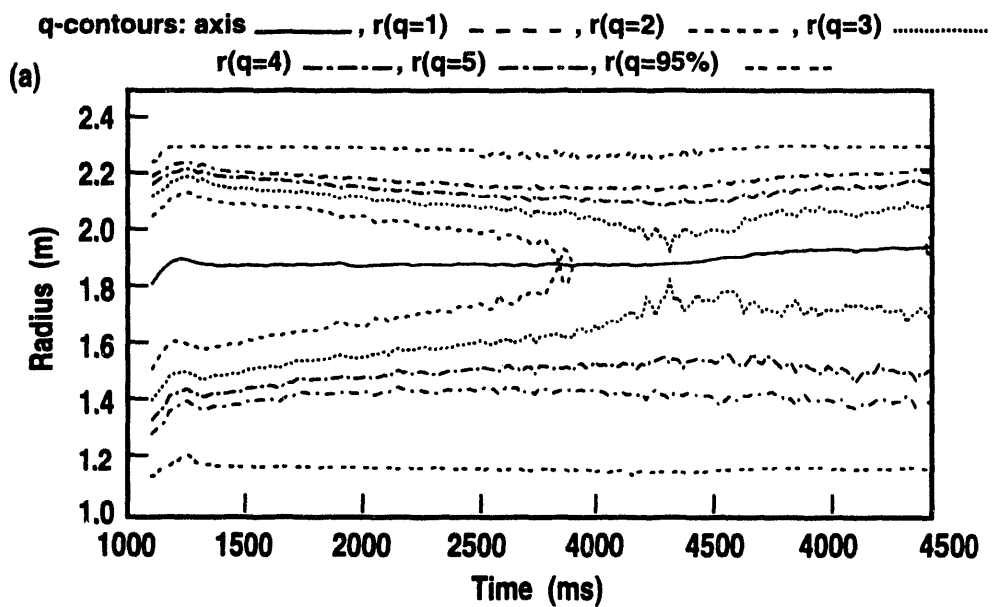


Fig. 10.3-3. High  $\beta_p$  discharge evolution showing a) the radial and temporal dependence of integral  $q$  surfaces and b) the enhancement of core density, correlated with turnoff of MHD fluctuations at 3360 ms.

Therefore, an upgrade was designed to the existing MSE instrument shown in Fig. 10.3-4, which adds eight additional channels in the outer portion of the plasma ( $R = 195\text{--}230$ ) while relocating the existing eight channels to view only the center of the plasma ( $R = 155\text{--}195$ ). The new channels are obtained from a completely different viewing geometry which improves the radial resolution in this region to 2-4 cm. The new system requires a turning mirror to collect light, which can introduce unwanted polarization effects. Significant effort has gone into the design of a multilayer dielectric mirror that minimizes these effects. In addition, the new system has vacuum compatible polarizers built into a movable shutter that will allow in-situ calibrations during plasma operation. The design of the Edge MSE upgrade is complete, with installation scheduled for March 1994.

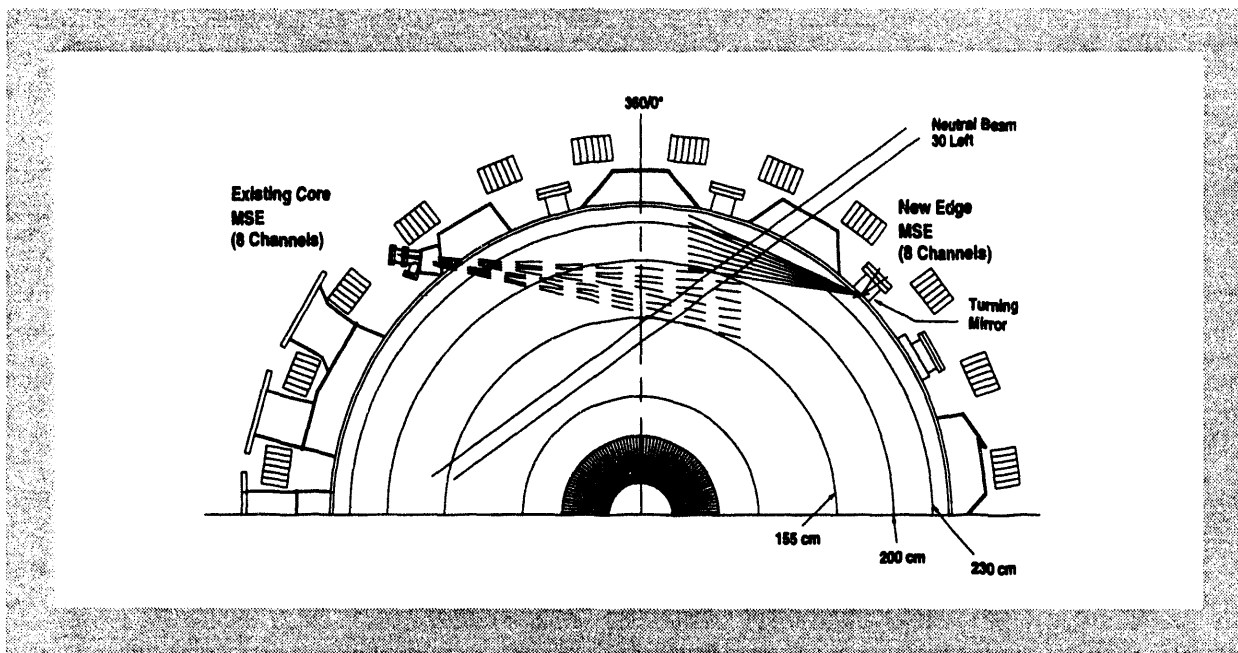


Fig. 10.3-4. Layout of 16 channel MSE instrument, showing eight new edge channels and eight reconfigured central channels.

## 10.4. OAK RIDGE NATIONAL LABORATORY

The ORNL collaboration during the past year includes work in the areas of the Advanced Divertor Program, boundary physics, FWCD, high beta operation, and pellet injection, in addition to hardware preparations of the ORNL pellet injector and FWCD antenna.

### 10.4.1. ADVANCED DIVERTOR AND BOUNDARY PHYSICS PROGRAM

Considerable progress has been made in the study of helium transport and exhaust on DIII-D during FY93. This includes improvements in diagnostic capabilities and calibration, planning and execution of experiments to study helium transport, and the analysis of the obtained data. In the diagnostic area, a modified penning gauge was installed in the divertor baffle region of DIII-D and has been used extensively to monitor the helium partial pressure in this region during dedicated helium transport experiments. Also, improvements have been made in the techniques to calibrate the CER system, allowing more accurate reconstruction of the helium density profiles. The most

significant experiment conducted during FY93 in this area was devoted to characterizing helium transport properties of ELMing H-mode plasmas as the plasma current and injected power were systematically varied. Simulation of this data via MIST was used to determine the helium diffusivity  $D_{He}$  and pinch velocity in the various plasma conditions. Energy transport analysis of data from the same discharges using the energy transport code ONETWO has also been done to determine the local thermal conductivity  $\chi_{eff}$ . The obtained  $D_{He}/\chi_{eff}$  can then be used as a measure of helium particle confinement relative to energy confinement in these discharges. Results of this analysis suggests that  $D_{He}/\chi_{eff}$  is insensitive to changes in plasma current (see Fig. 10.4-1) but increases strongly with increasing injected power or ELM frequency (see Fig. 10.4-2)

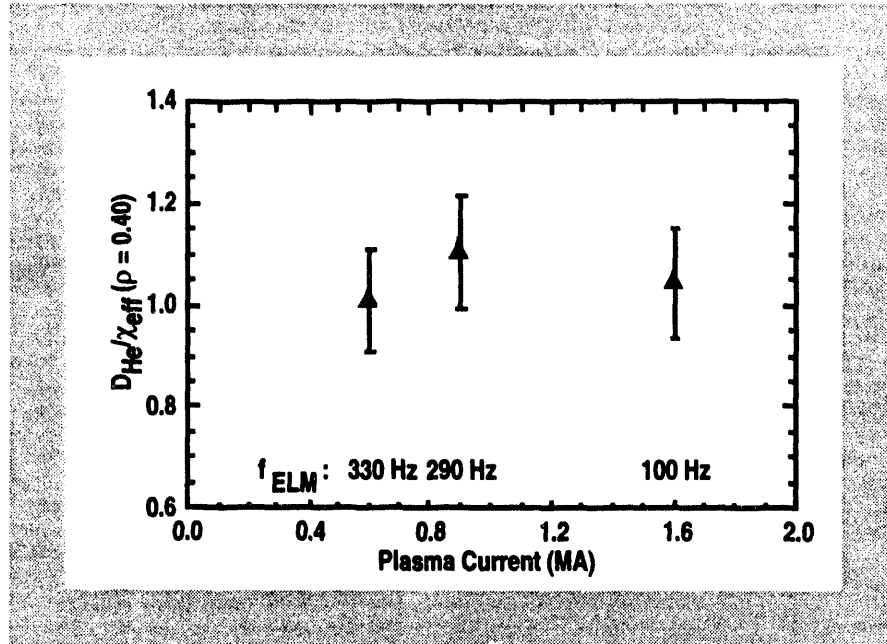


Fig. 10.4-1. Variation of  $D_{He}/\chi_{eff}$  with plasma current ( $P_{NBI}$  fixed at 10 MW).

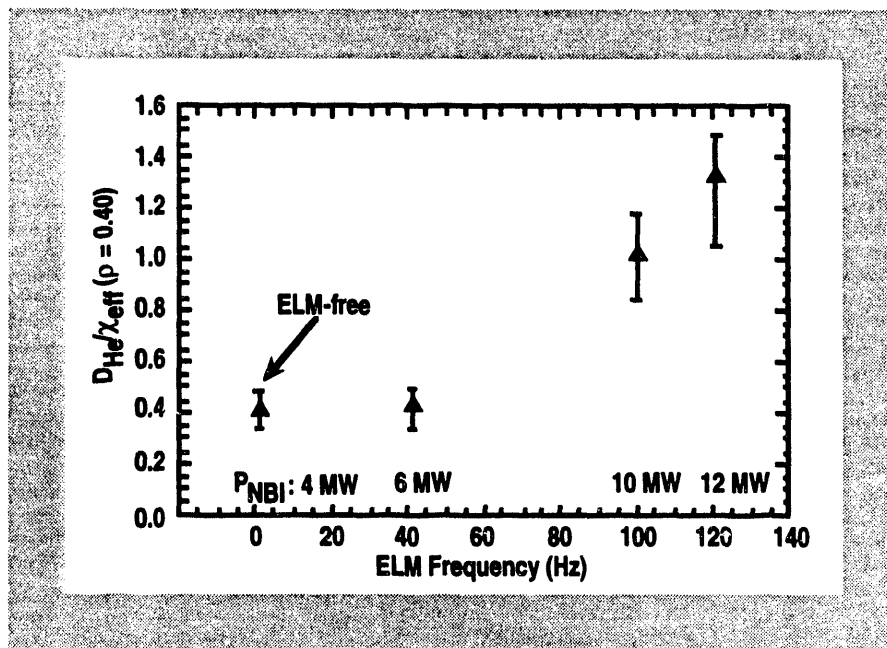


Fig. 10.4-2. Variation of  $D_{He}/\chi_{eff}$  with ELM frequency ( $I_p$  fixed at 1.5 M).

On October 8, 1993, the first He exhaust experiments were performed on DIII-D using Ar frost on the ADP to pump helium. These results were very encouraging for the next step fusion devices, like ITER.

Without He pumping the Helium density after the gas puff rises and comes to a constant level in  $\approx 100$  ms, which indicates that the helium recycling coefficient is approximately one. When the He pumping is turned "on", the He density is observed to drop and  $\approx 70\%$  of the He is removed from the core plasma ( $\rho \approx 0.3$ ) in  $\approx 2$  seconds. This discharge has an ELM frequency during the pumping phase of about 200 Hz. The decay of the He density during pumping permits the determination of the Helium confinement time in the vacuum vessel, namely  $\tau_{\text{He}}^* = 2.4$  seconds. The energy confinement time  $\tau_E$  was found to be about 170 ms. This yields a ratio of  $\tau_{\text{He}}^*/\tau_E \approx 14$ , which is a current measure of the "goodness" of a fusion reactor. Current reactor modeling codes indicate that this ratio  $\tau_{\text{He}}^*/\tau_E$  should be  $\leq 7-15$ , which is a strong indication that ELMing H-mode discharges are probably acceptable for a reactor, at least from a Helium removal standpoint. The discharge shown here has an ELM frequency of only  $\approx 00$  Hz. Higher frequency or "grassy" ELMs are expected to improve the Helium removal and therefore one can expect further improvements in the ratio of  $\tau_{\text{He}}^*/\tau_E$  at higher ELM frequencies. Indeed, it looks promising for efficient He removal in ELMing H-mode discharges.

First experiments were performed on June 2 to assess the effects of divertor pumping on the SOL and divertor parameters. In these experiments, the outer divertor strike-point position was scanned to allow for a variation of the particle exhaust rate. This way particle exhaust rates between 5 and 50 Torr-L/s were achieved after the H-mode transition, without gas puffing. Neutral beam fueling was approximately 5-10 Torr-L/s. Resulting core plasma density reductions up to factors of nearly two were observed. Qualitatively, the observed changes in the divertor parameters were as expected, i. e. lower neutral pressure, lower plasma density, higher electron temperature, and higher divertor heat flux. Significant progress has also been made in upgrading the b2.5 code to include a particle balance in the presence of the biasing ring and divertor baffle, as well as an, upgraded the atomic physics model.

#### 10.4.2 ORNL FAST WAVE CURRENT DRIVE PROGRAM

The final design review of the new long-pulse fast wave current drive (FWCD) antennas was held at ORNL on January 28, 1993 at which time the design was approved with no major changes. Two antennas are being built for the midplane ports at the  $0^\circ$  and  $180^\circ$  toroidal locations. Each antenna will be capable of launching up to 4 MW of rf power at frequencies between 30 and 120 MHz into the DIII-D plasma for pulse lengths of 10 s. In combination with the existing four-element FWCD array, the expected driven current is about 1 MA. A drawing of the new antennas is shown in Fig. 10.4-3.

FWCD experiments were conducted on DIII-D with the existing four-strap antenna with the new single-tiered, tilted, B<sub>4</sub>C-coated Faraday shield at  $0^\circ$  and  $180^\circ$  phasing. Power levels up to 1.6 MW were obtained, and energies of 3.7 MJ were injected in a single pulse. During one run the plasma current was ramped down during the shot to maximize the noninductive current during the rf pulse. There were shots at low current which appeared to have complete noninductive current drive.

Operation with both the normal and reversed direction of toroidal magnetic field was obtained. The power limits were approximately the same for both directions, despite the fact that the single-tier, B<sub>4</sub>C-coated Faraday shield has slanted elements to align with the normal direction of field lines at the antenna location.

A prototype antenna decoupler for high power operation was installed and worked flawlessly. The antenna phasing was changed in  $90^\circ$  increments of four successive shots while maintaining a good match at the transmitter without adjustment of any stub tuner elements.

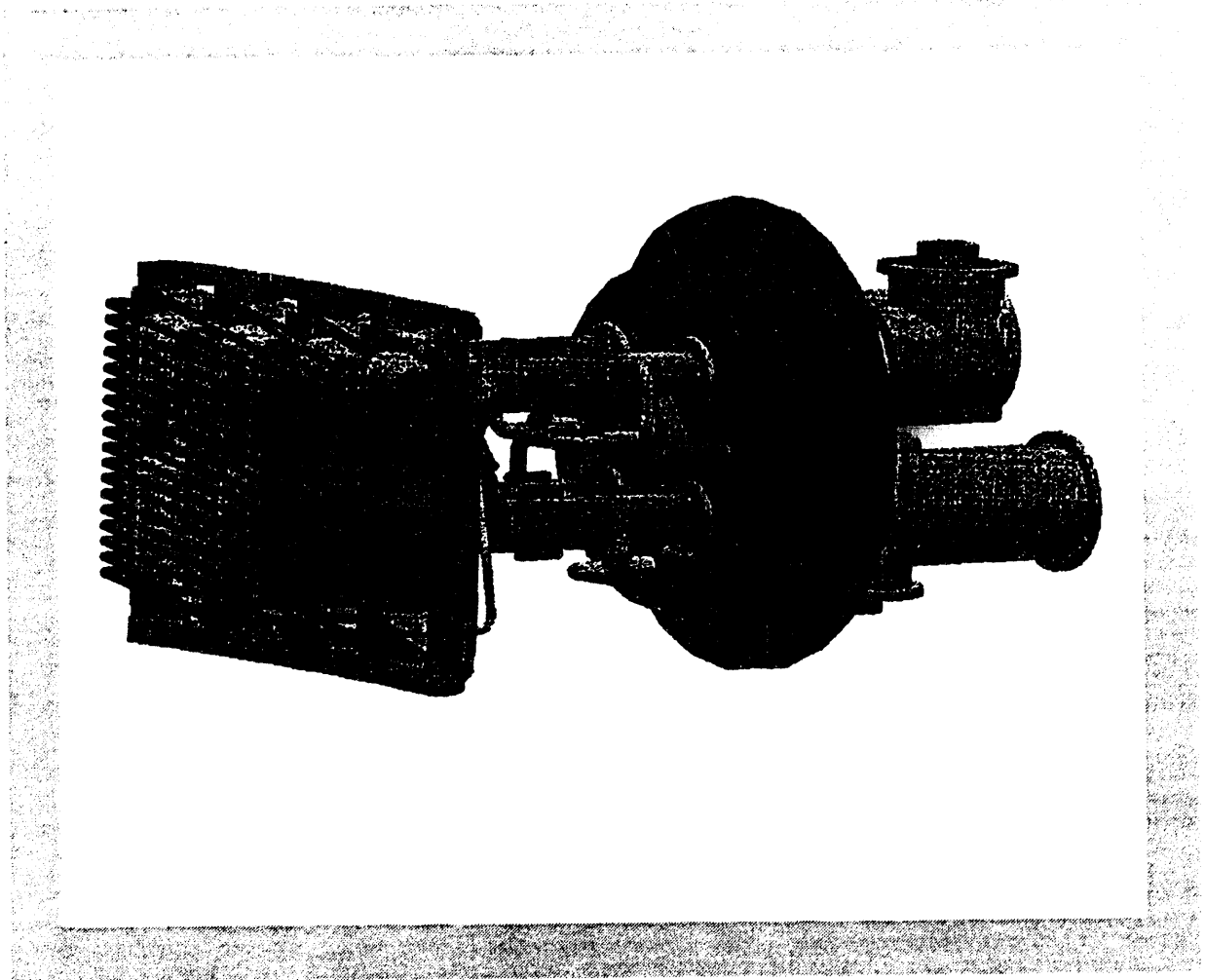


**Fig. 10.4-3. ORNL fast wave current drive antenna**

### **10.4.3 PELLET INJECTOR PROGRAM**

Work on the pellet injector project for DIII-D continued through 1993. The primary goals of the experiments using the injector are continuous fueling inside the separatrix with the pumped divertor and increased plasma performance (PEP mode) as found on JET. The injector will be the three barrel, repeating pneumatic injector installed on the JET tokamak in 1987. The configuration to be used on DIII-D has three barrels: a 1.8 mm, a 2.7 mm, and a 4 mm. The injector is capable in injecting one hundred 1.8 mm pellets at a 10 Hz repetition rate and a speed of up to 1.1 km/s. The larger barrels will probably be run in single shot mode. Deuterium will be used for the pellets and helium for the propellant gas.

The injector and injection line are being tested at ORNL. A photo is shown in Fig. 10.4-4. The 2.7 mm line has been tested at up to 1 Hz. The 1.8 mm line has been tested successfully at up to 10 Hz. The 4 mm has also been tested in single shot mode, but the pellets were found to be larger than expected. A new nozzle is being fabricated to reduce the volume of these pellets closer to the specified size.

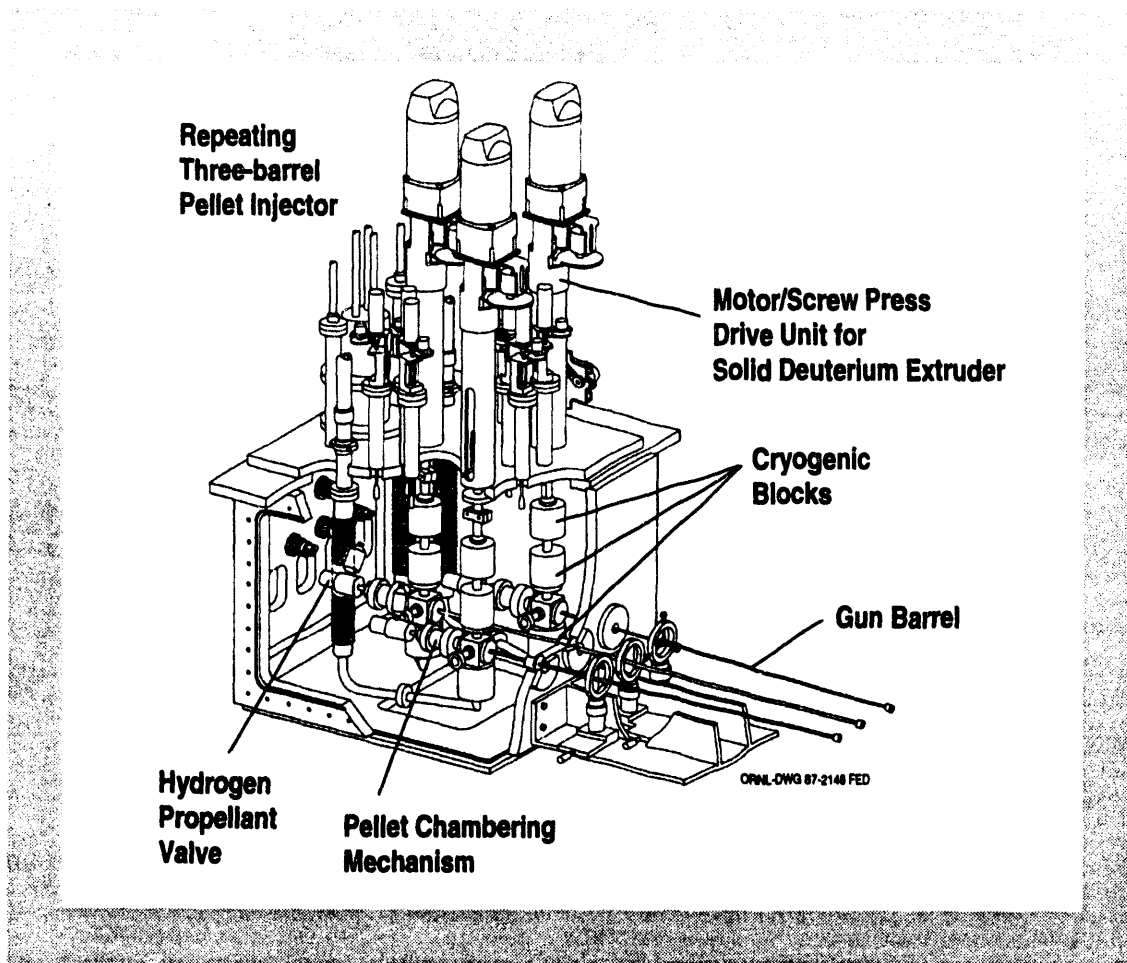


Fig. 10.4-4. ORNL pellet injector to be installed on DIII-D.

## 10.5. UCLA/SANDIA

UCLA contributes to the overall DIII-D program in two distinct ways: first, by bringing to DIII-D specific areas of UCLA institutional strength, especially in the fields of turbulence measurement and analysis, advanced millimeter-wave diagnostic systems and edge probe measurements. Second, by supporting the DIII-D research program via full participation in the planning, execution and analysis of experiments on DIII-D, including programmatic aspects.

Other contributions are to the overall U.S. fusion program, as DIII-D is an ideal machine on which to develop and demonstrate reactor relevant diagnostic systems, and to the University teaching role through student research projects.

At present, UCLA has responsibility for all the mm-wave and FIR turbulence diagnostic systems on DIII-D, and has a joint effort with Sandia National Laboratories on edge probe measurements. Specific systems installed on the machine are inboard and outboard (high/low field side) fixed frequency reflectometers, a frequency tunable correlation reflectometer, profile measurement reflectometers at two toroidal locations, a new reflectometer system specifically designed to measure and detect the electrostatic component of the ICRF waves used for heating and

current drive, a multichannel heterodyne FIR scattering system, and, with Sandia, a reciprocating Langmuir probe array. These systems have been used to support a wide range of experiments on DIII-D, and the most important results obtained during the year are outlined below:

### 10.5.1. EDGE TURBULENCE AND L-H TRANSITION PHYSICS

Significant progress has been made by the UCLA/Sandia collaboration in this area with the reciprocating probe array. Probe measurements have confirmed the formation of a narrow layer of negative (inward) radial electric field  $E_r$  during the L-H transition (Fig. 10.5-1). The high spatial resolution of the probe permits the width of this layer to be determined accurately. The layer is only 0.8 cm wide, or about 1-2 ion poloidal gyroradii. Suppression of electrostatic turbulence and steepening of the density and electron temperature profiles are simultaneously observed in the sheared  $E_r$  layer. Previously, similar data from CER, reflectometry, and Thomson scattering was used to infer that the sheared  $E_r$  layer suppressed the electrostatic turbulence and therefore reduced transport, which in turn led to steepening of the plasma profiles. The reciprocating probe, however, has the unique capability to measure the correlated density and potential fluctuations, allowing the convective particle and heat transport to be determined (Fig. 10.5-2). These new measurements provided the first direct confirmation of the reduction in plasma transport (both particle and heat) in the electric field shear layer across the L-H transition by a factor of about 10, predominantly as a result of the reduction in fluctuation levels.

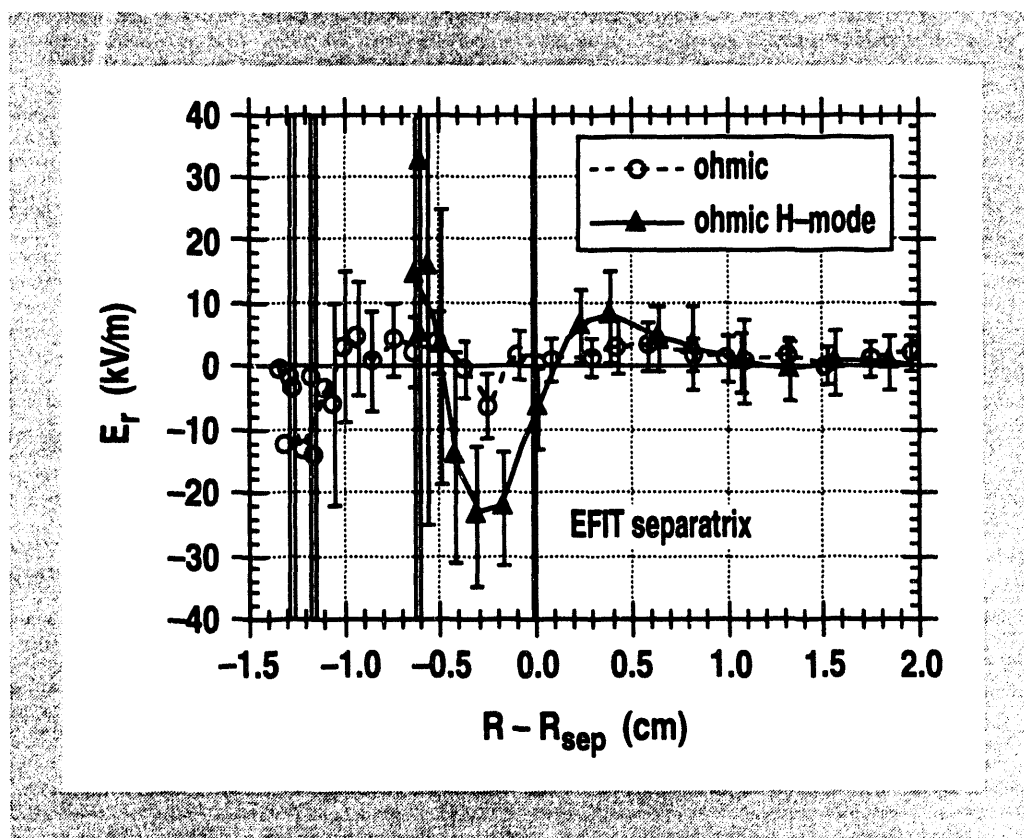


Fig. 10.5-1. Comparison of the radial electric field measured by the reciprocating Langmuir probe using the measured floating potential and  $T_e$  profiles for ohmic (open circles) and ohmic-sustained H-modes (solid triangles). A narrow region of negative (radially inward)  $E_r$  develops at the separatrix in the H-mode.

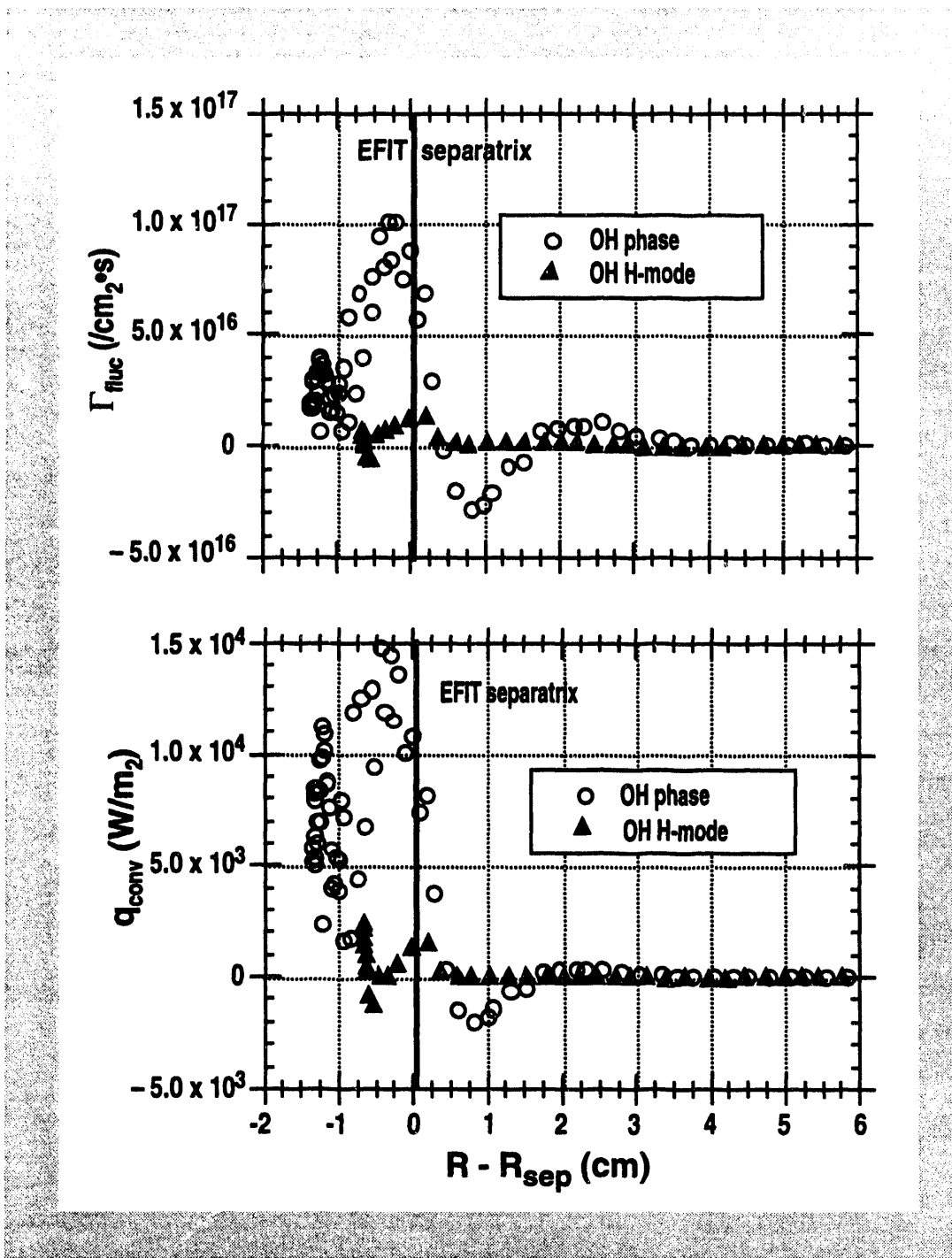


Fig. 10.5-2. Radial profiles of the turbulent particle and convective heat fluxes in the DIII-D boundary for OH and OH-sustained H-modes. Both perpendicular transport fluxes are reduced a factor of 10.

### 10.5.2. CORE TURBULENCE MEASUREMENTS

The most notable developments in this field are associated with VH-mode operation. One possible explanation for the transition to VH-mode operation from H-mode is that interior transport is reduced because of a reduction in turbulence levels in the core, caused by increased shear in  $E_r$ . This picture is supported by internal fluctuation measurements using the FIR scattering system, which indicate reduced core turbulence from H- to VH-mode operation. This decrease is both spatially and temporally correlated with increased shear in the radial electric field (as deduced from CER measurements), in agreement with theory. Moreover, obtaining VH-mode operation is associated with the suppression of so called momentum transfer events (MTEs), which are evidenced by strong internal bursts of fluctuations. The suppression of these MTEs as seen by the FIR scattering system is a signature of VH-mode operation.

### 10.5.3. SOL CHARACTERIZATION AND SCALING

The dependence of the scrape-off layer width on discharge conditions (shape, confinement mode, current, density, etc.), is important for evaluating the design of the proposed DIII-D Radiative Divertor, as well as the ITER and TPX divertors. The UCLA/Sandia probe collaboration has investigated the scaling of the SOL width, represented by the characteristic decay length for the density  $\lambda_n$ , as a function of plasma current  $I_p$ , toroidal magnetic field  $B_t$ , and connection length to the divertor target plates. The density decay lengths obtained in lower single null (LSN) divertor discharges for several confinement modes increase with SOL connection length to the divertor target plates for each mode. The ordering of the density decay lengths is  $\lambda_n$  in L-mode  $\approx 2 \times \lambda_n$  in ohmic  $\approx \lambda_n$  in ELM-free H-mode. The SOL plasma is enhanced in both ELMing H-modes and DND discharges, with  $\lambda_n$  1.5-2 times as large as the ELM-free H-mode values in Fig. 10.5-1. Figure 10.5-3 shows a comparison of the SOL density profile for LSN and DN L-mode discharges with  $I_p = 1.3$  MA. Such enhanced scrape-off layers affect the penetration probabilities of impurities generated at the wall, and can improve core plasma performance.

### 10.5.4. DENSITY PROFILE MEASUREMENTS

Density profile measurements via reflectometry have been resumed, with the objective of demonstrating routine and reliable operation, important for future devices such as TPX and ITER, and providing information for RF wave coupling studies. It is also planned to compare and contrast several competing reflectometer techniques on DIII-D by making use of the flexible hardware configuration installed on the machine. Measurements can be performed at two distinct toroidal locations, one, in collaboration with ORNL, at the FWCD antenna, and another displaced by  $45^\circ$  on the midplane. First results, using an improved digital phase extraction algorithm and a broadband frequency sweep technique are encouraging. An example, showing that the edge H-mode transport barrier can be clearly resolved, and excellent agreement with multipoint Thomson data, is shown in Fig. 10.5-4.

### 10.5.5. INTERNAL RF WAVE MEASUREMENTS

RF heating and current drive plays a large role in current tokamak experiments, is very important for the success of the advanced tokamak research at DIII-D, and is planned for future devices such as ITER and TPX. While many features of RF wave propagation have been validated experimentally, there are still important unresolved questions, and also a need for internal measurements with good spatial resolution. As reflectometry has very good radial

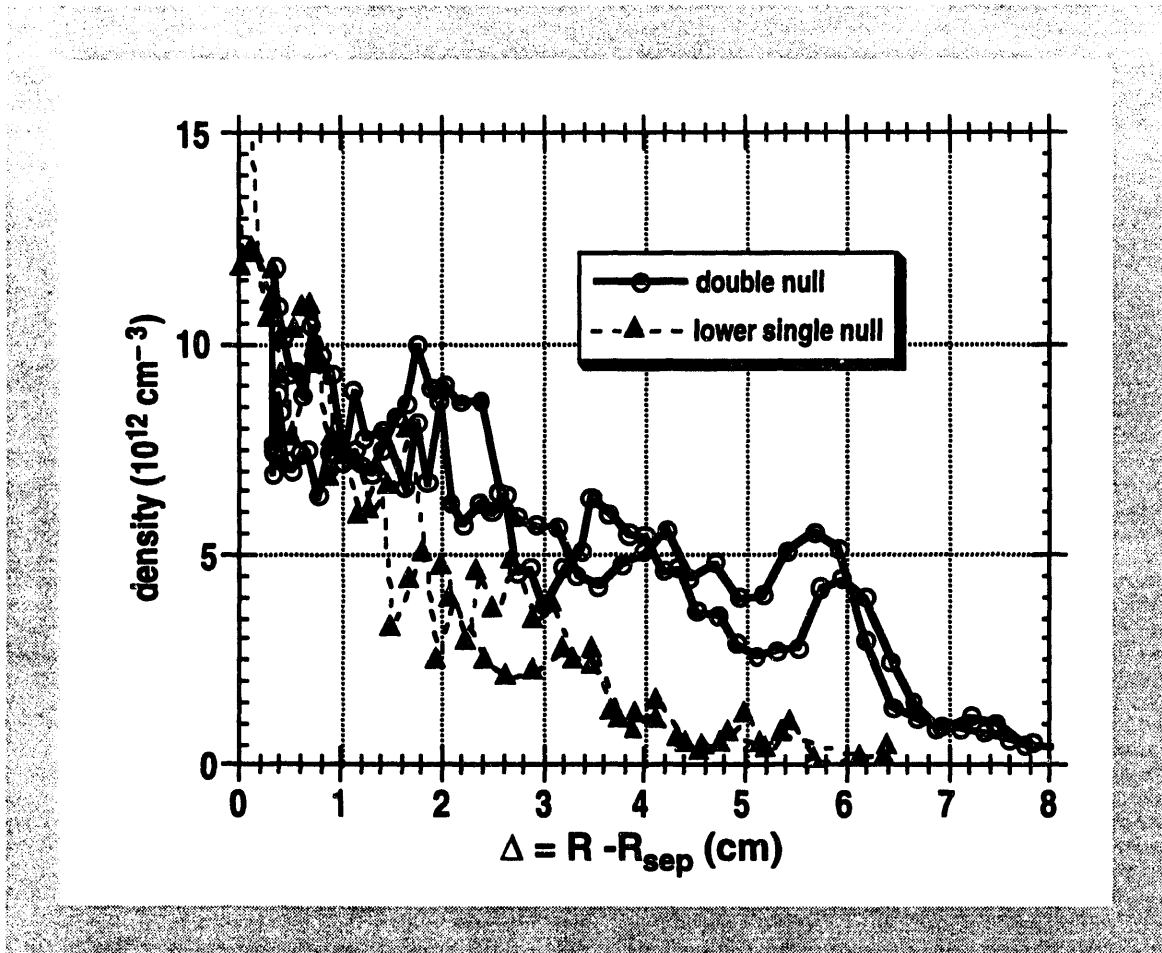


Fig. 10.5-3. Comparison of SOL density profiles for lower single-null (filled triangles) and double-null (open circles) divertor L-mode discharges with  $I_p = 1.3$  MA. The SOL is substantially broader in the DN case.

resolution (order of cm), a reflectometer system especially designed to measure fluctuations at the fast wave frequency (60 MHz) was installed on DIII-D. The first measurements from this system are very encouraging: fluctuations associated with the FW are clearly seen, with no spurious pickup. An example of local internal FW amplitude as monitored by this system is shown in Fig. 10.5-5. This is the first demonstration of RF wave detection via reflectometry, and opens up the prospect of much improved local monitoring of RF wave heating and current drive experiments.

## 10.6. INTERNATIONAL COLLABORATIONS

GA's International Collaboration Program continues to provide a broad source of innovative new ideas and opportunities which support the DIII-D research program. Major collaborations are underway with JET in England and JT-60U in Japan. In addition to the benefits gained from DIII-D staff assignments in these laboratories, foreign scientists visiting GA have made significant contributions to the DIII-D program goals.

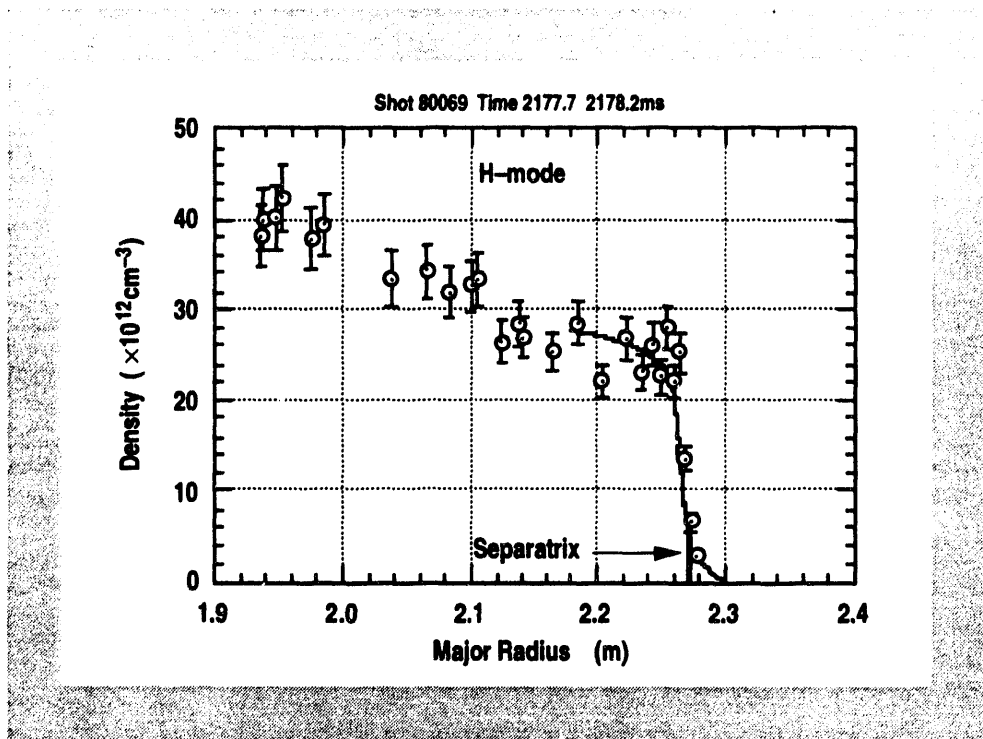


Fig. 10.5-4. H-mode density profile (single sweep). Comparison between Thomson scattering and FM reflectometry

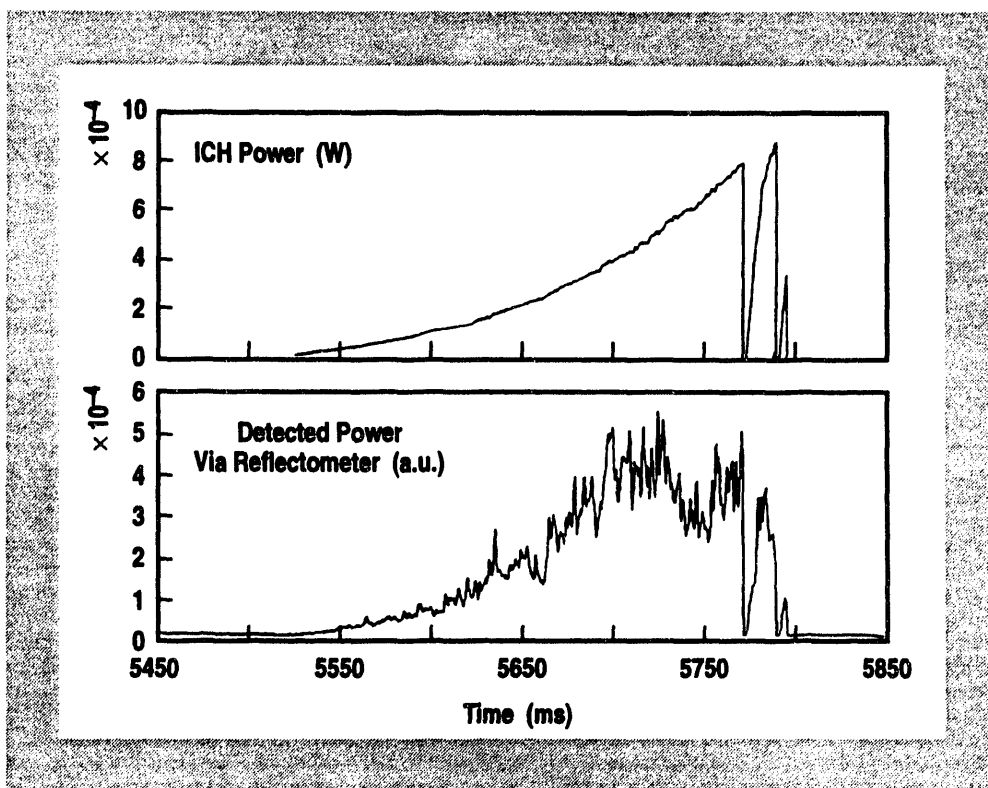


Fig. 10.5-5. FW power versus time and detected power via reflectometer

Contributions to the DIII-D program goals were made by: P. Ghendrih (1 year assignment) from Tore Supra working on effects of Marfes on divertor operation, Jorg Winter (2 week exchange) from TEXTOR working on experiments for in situ boronization of vessel walls, K. Makino (3 month assignment) from Kyushu University working on particle control and noninductive current drive, T. Hatae (2 month assignment) from JAERI working on multipulse Thomson scattering, R. Khayrudinov (3 month assignment) from the Troitsk Institute working on disruption studies, O. Sauter (1 year assignment) from Switzerland developing a Fokker-Planck code, and Y. Martin (1 year assignment) from Switzerland working on charge exchange recombination (CER).

A summary of the progress made by DIII-D staff members in support of the International Collaboration Program is given below.

### 10.6.1. JET

A comparison was made between the JET discharges identified as VH-mode, and the DIII-D VH-mode discharges. They appear to exhibit similar physics (second stable edge and shear stabilization of turbulence), but appearing in the opposite order to that seen in DIII-D. Initial conditions at the L-H transition were identified as a probable controlling factor, and this behavior was later at least partially duplicated in DIII-D. This collaboration may become as fruitful as the previous JET/DIII-D H-mode energy confinement scaling.

A joint GA/JET boundary physics database is under development and work continued on the joint H-mode database. GA personnel contributed to converting EFTT to run on JET and on the design of the JET Mark II pumped divertor which included designing a friction test rig, design of the MK II mounting clamps and the MK II diagnostics integration.

### 10.6.2. ASDEX-U/W7 STELLARATOR

During a collaboration at ASDEX-Upgrade (September 1992 through December 1992), a high temporal resolution spectroscopic diagnostic was designed, constructed and implemented for the outside divertor plates of ASDEX-Upgrade using a fast scanning framing camera. This diagnostic provided 2-D images of the interaction between the plasma and divertor plates on a millisecond timescale and was able to reveal fast divertor plasma phenomena.

At Garching, a program was continued of Tokamak-Stellarator comparisons started during the Summer 1992 Exchange. This involved working to develop an experiment to feed ohmic current into the W7 Stellarator during strong off-axis RF heating. A transition to a Tokamak state with strong profile consistency thus verifying toroidal current as its cause is hypothesized. A second project involved development of ballooning mode formulations for microstability and turbulence simulations in Stellarators.

### 10.6.3. TORE SUPRA

At Cadarache a theoretical project was begun to investigate the possibility of transport "action at a distance". As a result, a new type of 2-D inhomogeneous turbulence code is under development to look for action at a distance.

As part of a collaboration, on the workstations at Cadarache, rf wave absorption and current drive simulations were made for both lower-hybrid and fast waves. These simulations use a novel statistical approach to calculate the wave propagation and absorption in the multipass regime [K. Kupfer, D. Moreau, and X. Litaudon, Phys. Fluids B, Vol. 5, 4391 (1993)].

#### 10.6.4. JT-60U

A collaboration was held at JAERI with the primary purpose to study the relation between toroidal rotation speed, error fields and the sawtooth crash. The ideas proposed for JT-60U and JFT-2M were based on work done on the DIII-D tokamak. In DIII-D it was found that significant changes in the sawtooth behavior occurred when relatively large error fields were introduced. In DIII-D the error field and the rotation velocity are coupled in that as the error field is increased the rotation velocity decreases (via magnetic braking). In both JT-60U and JFT-2M tangential neutral beams pointed in both directions (counter to the plasma current and with the plasma current) are installed. In principle these beams can be used to control the rotation velocity independent (more or less) of the error fields. Further, both of the Japanese machines have toroidally asymmetric coils that can be used to introduce error fields. The results from experiments performed on JT-60U and JFT-2M can be summarized as follows: 1) DIII-D and JFT-2M show clearly that fast crash, no precursor, ideal sawtooth crashes are produced at low rotation velocity and high error field, while slow crash, resistive sawtooth crashes are favored at high rotation velocity or low error field. 2) JT-60U and JFT-2M show that low rotation velocity alone or high error field alone is not sufficient to produce ideal type crashes. 3) The model developed to explain the DIII-D results qualitatively fits the data from the Japanese machines but important problems with the model remain.

Discussions were held at JT-60U on the interpretation of data on the effects of error on locked modes. The sources of error fields on JT-60U were investigated and recommendations on better magnetic diagnostics for detecting locked modes, measuring PF-coil irregularities and a possible correcting coil were made to the hosts.

#### 10.6.5. GAMMA-10

A collaboration with the Gamma-10 x-ray group on silicon x-ray detectors for tokamaks was initiated. The collaboration will include characterization of the DIII-D x-ray detectors by the Gamma-10 group, a test of new detector types developed by the Gamma-10 group on DIII-D and, in the long term the joint development of improved x-ray detectors and techniques for tokamak plasmas.

#### 10.6.6. T-10

The joint research program between DIII-D at General Atomics and T-10 at the Kurchatov Institute continued during CY93. Four General Atomics scientists participated in the fall T-10 campaign on high power electron cyclotron heating and current drive and five T-10 staff members and one member of the Latvian Center for Knowledge visited General Atomics and the DIII-D facility. The results of the 1992 T-10 campaign, during which second harmonic ECCD experiments were conducted at power levels up to 1 MW, were analyzed using the General Atomics codes TORAY and CQL3D. Current drive efficiencies were determined, a nonlinear enhancement of the efficiency at the highest power levels was studied and the effects of sawteeth and the internal electric fields during ECCD were calculated to contribute to understanding of the current drive process. A highlight of the joint research activity on T-10 and DIII-D was the exchange of diagnostic hardware and expertise between the two experiments. During the fall operational campaign on T-10, a Michelson interferometer, provided by GA, for measurement of the electron cyclotron emission spectrum over the frequency range 100-1000 GHz was installed to provide profiles of electron temperature and an indication of the presence of a suprathermal component of the electron velocity distribution function during injection of EC power. A complete operating system was written for this equipment and preliminary operation in synchronism with the plasma discharges was achieved. In the other direction, the x-ray spectrometer on DIII-D was completely revamped to include a three element detector system and advanced ultra high speed electronics provided through the Kurchatov Institute.

Another major activity was the upgrade of the data acquisition and archival system for T-10. With DOE support, GA provided a hard disk system, a netserver computer and network software to the computer support group of the Plasma Physics Division of the Kurchatov Institute. This activity was nearly completed during 1993, with the installation of Ethernet lines and network capability for data sharing throughout the division. During the fall campaign, this capability was exercised not only to follow the progress of the T-10 experiments, but also to produce extensive calculational results using the transport code ASTRA to model the electric field behavior during the sawtooth instability under the influence of high power injection at the electron cyclotron frequency. The relaxation of restrictions on direct access to the Internet from Russia in mid December permitted GA researchers in Moscow to log in to the GA computer system directly for the first time and will in the future, through remote login made possible by the network capability, permit sharing of data and calculational capability to become efficient and routine.

The preliminary results of the fall 1993 campaign were demonstration of suppression of MHD activity near the density and  $q$  limits by ECH and the study of ECCD at higher power levels above 1 MW where nonlinear effects may be important. Both of these areas of investigation bear directly on the viability of ECH as a constituent of the program plan for the next generation of tokamak experiments such as ITER. General Atomics participants were fully integrated into the T-10 experimental group and submitted proposals for off-axis heating and current ramp experiments which had been added to the T-10 experimental plan but not completed by the end of the year.

#### **10.6.7. TRINITI (RUSSIA)**

Under GA's subcontract with the TRINITI Laboratory, the DINA code for modeling the resistive magnetohydrodynamic evolution of plasmas in DIII-D was applied to studying plasma behavior during disruptions and during dynamic shaping experiments, with the ultimate objective in the latter case of testing plasma control algorithms offline. The code was upgraded to simulate the interaction of halo currents with the vessel wall during vertical displacement events; its entire structure was documented; and its input/output was reworked to make the code more user friendly for GA personnel.

In the area of materials research, pyrolytic boron carbide coatings developed in Russia were shown to possess outstanding durability under plasma bombardment, even at power levels approaching those predicted in ITER. In comparison with the amorphous coating pursued in the U.S., the crystalline B<sub>4</sub>C coating from Russia exhibited superior bonding to a graphite substrate and significantly higher erosion resistance.

#### **10.6.8. TEXTOR**

Specific accomplishments include the following: 1) the development of coating fabrication process parameters for three different boron carbide plus silicon carbide (B<sub>4</sub>C + SiC) reaction-sintered coating compositions (5, 10, and 20 atom-percent silicon); 2) the coating of specimens for electron-beam and ion-beam testing at KFA, using precursor coatings with compositions of 69 wt.% B<sub>4</sub>C + 31 wt.% SiC (10 atom-% Si) — in a related program, specimens with coatings of the same composition were also prepared for testing at Trinit, Russia (ion beam tests of these specimens have been conducted; encouraging results were obtained).

The B<sub>4</sub>C-SiC coatings developed have multiphase microstructures and are comprised of B<sub>4</sub>C, SiC, and graphite phases. Specimens to be evaluated at KFA have adherent, low-porosity, uniform-thickness coatings with nominal coating thicknesses between 200 and 600 nm. The substrate materials used to fabricate the KFA test specimens consist of Ringsdorfwerke EK 98 graphite, and Le Carbon Lorraine felt-type AEROLOR A05 carbon-fiber-

reinforced carbon (CFC). The coatings were applied by depositing precursor layers of powder/binder mixtures on the substrates and then rapidly heating to a nominal temperature of 2260°C. The coatings are comprised of two microstructural layers: 1) a graded penetration (conversion) layer of B<sub>4</sub>C and SiC within the substrate, and 2) a surface layer, whose microstructure is the result of the reaction-sintering process, and consists of sintered B<sub>4</sub>C particles (remnants of the precursor coating material) and graphite particles contained in an eutectic-formed matrix of B<sub>4</sub>C and SiC.

## 11. FY93 PUBLICATIONS

- Alikaev, V.V., Yu. V. Esipchuk, A.Ya. Kislov, G.E. Notkin, K.A. Razumova, and The T-10 Team, C.B. Forest, J. Lohr, T.C. Luce, and R.W. Harvey, "Second Harmonic ECCD on T-10," in Bull. 35th Annual American Physical Society Meeting, November 1-5, 1993, St. Louis, Missouri, (Abstract) Vol. 38, 2069.
- Allais, F., and T.E. Evans, "A Method for Resolving Inconsistencies Between the Two Fluid MHD Equations and Maxwell's Equations," in Bull. 35th Annual American Physical Society Meeting, November 1-5, 1993, St. Louis, Missouri, (Abstract) Vol. 38, 1925.
- Allen, S.L., D.N. Hill, A.W. Hyatt, M.A. Mahdavi, T.W. Petrie, G.D. Porter, M.E. Rensink, T. Rognlien, M.J. Schaffer, D.L. Sevier, J.P. Smith, and R.D. Stambaugh, "Design of a Radiative Divertor for DIII-D," in Bull. 35th Annual American Physical Society Meeting, November 1-5, 1993, St. Louis, Missouri, (Abstract) Vol. 38,
- Austin, M.E., R.F. Ellis, R.A. James, and T.C. Luce, "Measurement of 3rd Harmonic Electron Cyclotron Emission on DIII-D," in Bull. 35th Annual American Physical Society Meeting, November 1-5, 1993, St. Louis, Missouri, (Abstract) Vol. 38, 1936.
- Baker, D.R., R.J. Groebner, and K.H. Burrell, "Between Shot Analysis of DIII-D CER Data Using a Neural Network," in Bull. 35th Annual American Physical Society Meeting, November 1-5, 1993, St. Louis, Missouri, (Abstract) Vol. 38, 2070.
- Baker, D.R., R.J. Groebner, and K.H. Burrell, "A Neural Network for the Analysis of DIII-D Charge Exchange Recombination Data," to be published in Nucl. Fusion; General Atomics Report GA-A21260 (1993).
- Baxi, C.B., and W. Obert, "Transient Thermal Analysis of Cryocondensation Pump for JET," to be published in Proc. International Cryogenic Engineering Conference, July 12-16, 1993, Albuquerque, New Mexico; General Atomics Report GA-A20941 (1993).
- Baxi, C.B., and The GA Divertor Team, "Evaluation of Helium Cooling for Fusion Divertors," to be published in Proc. of International Society for Optical Engineering at High Heat Flux Session, July 11-16, 1993; General Atomics Report GA-A21035 (1993).
- Baxi, C.B., and H. Falter, "A Model for Analytical Performance Prediction of Hypervapotron," to be published in Proc. IAEA Technical Committee Meeting on Fusion Studies, September 13-17, 1993, Los Angeles, California; General Atomics Report GA-A21448 (1993).

- Brooks, N.H., D.L. Hillis, A.M. Howald, S. Tugarinov, M.R. Wade, and W.P. West, "Impurity Spectroscopy of the Divertor Region in DIII-D," in Bull. 35th Annual American Physical Society Meeting, November 1-5, 1993, St. Louis, Missouri, (Abstract) Vol. 38, 2059.
- Burrell, K.H., T.H. Osborne, R.J. Groebner, and C.L. Rettig., "The Role of Electric Field Shear Stabilization of Turbulence in the H-Mode to VH-Mode Transition in DIII-D," in Proc. 20th European Conference on Controlled Fusion and Plasma Heating, Lisbon, Portugal, 1993, (European Physical Society, Petit-Lancy, Switzerland, 1993) Vol. 17C, Part I, p. 27; General Atomics Report GA-A21308 (1993).
- Burrell, K.H., "Role of the Radial Electric Field in the Transition from L- to H- to VH-mode in the DIII-D Tokamak," in Bull. 35th Annual American Physical Society Meeting, November 1-5, 1993, St. Louis, Missouri, (Abstract) Vol. 38, 1958.
- Campbell, G.L., J.R. Ferron, E. McKee, A. Nerem, et al., "New DIII-D Tokamak Plasma Control System," in Proc. 17th Symp. on Fusion Technology, September 14-18, 1992, Rome, Italy, Vol. 2, p. 1017; General Atomics Report GA-A21036 (1992).
- Campbell, G.L., K.M. Schaubel, and J.J. Harris, "DIII-D Cryogenics Control System Status," in Proc. 15th Symp. on Fusion Engineering, IEEE (Hyannis, Massachusetts, October 11-15, 1993) to be published; General Atomics Report GA-A21414 (1993).
- Carlstrom, T.N., P. Gohil, J.G. Watkins, and K.H. Burrell, "Reduced H-Mode Power Thresholds for D\* into D<sup>+</sup> in Boronized DIII-D," in Bull. 35th Annual American Physical Society Meeting, November 1-5, 1993, St. Louis, Missouri, (Abstract) Vol. 38, 2063.
- Caroliopio, E.M., H.H. Duong, W.W. Heidbrink, R.J. La Haye, and H.E. Mynick, "Helical Fields for Burn Control and Alpha Ash Removal," in Bull. 35th Annual American Physical Society Meeting, November 1-5, 1993, St. Louis, Missouri, (Abstract) Vol. 38, 2063.
- Cary, W.P., J.C. Allen, R.I. Pinsker, and C.C. Petty, "ICRF System Data Acquisition and Real Time Control Using a Micro Computer System," to be published in Proc. 15th Symp. on Fusion Engineering, IEEE (Hyannis, Massachusetts, October 11-15, 1993); General Atomics Report GA-A21429 (1993).
- Chiu, S.C., "Full Wave Simulations of DIII-D FWCD Results and Comparison with Ray Tracing," in Bull. 35th Annual American Physical Society Meeting, November 1-5, 1993, St. Louis, Missouri, (Abstract) Vol. 38, 2068.
- Chiu, S.C., C.F. Karney, Y.R. Lin-Liu, and T.K. Mau, "The Efficiency of Fast Wave Current Drive for a Weakly Relativistic Plasma," in Proc. of 10th Top. Conf. on Radio Frequency Power in Plasmas, Boston, Massachusetts, 1993, Vol. 289, p. 305; General Atomics Report GA-A21254 (1993).
- Coda, S., M. Porkolab, K.H. Burrell, and T.N. Carlstrom, "Edge Fluctuation Measurements by Phase Contrast Imaging on DIII-D," in Bull. 35th Annual American Physical Society Meeting, November 1-5, 1993, St. Louis, Missouri, (Abstract) Vol. 38, 2064.

- Coda, S., "Measurements of Edge Fluctuations by Phase Contrast Imaging on DIII-D," in Proc. 20th European Conference on Controlled Fusion and Plasma Heating, Lisbon, Portugal, 1993, (European Physical Society, Petit-Lancy, Switzerland, 1993) Vol. 17C, Part III, p. 1179; General Atomics Report GA-A21316 (1993).
- DeBoo, J.C., H. St. John, J.R. Ferron, and S.J. Thompson, "Comparison of Critical Temperature Gradient Transport Model Simulations With a Temporally Evolving Current Ramp Discharge in DIII-D," in Bull. 35th Annual American Physical Society Meeting, November 1-5, 1993, St. Louis, Missouri, (Abstract) Vol. 38, 2065.
- deGrassie, J.S., F.W. Baity, R.C. Callis, D.J. Hoffman, et al. "Fast Wave Current Drive System Design for DIII-D," in Proc. 17th Symp. on Fusion Technology, September 14-18, 1992, Rome, Italy, Vol. 1, p. 457; General Atomics Report GA-A21043 (1992).
- deGrassie, J.S., "Simulation of Enhanced Tokamak Performance on DIII-D Using Fast Wave Current Drive," in Proc. 20th European Conference on Controlled Fusion and Plasma Heating, Lisbon, Portugal, 1993, (European Physical Society, Petit-Lancy, Switzerland, 1993) Vol. 17C, Part II, p. 647; General Atomics Report GA-A21312 (1993)
- deGrassie, J.S., R.I. Pinsker, C.B. Forest, C.C. Petty, J.R. Ferron, Y.R. Lin-Liu, and F.W. Baity, "Real Time Computer for the DIII-D Fast Wave RF System," in Bull. 35th Annual American Physical Society Meeting, November 1-5, 1993, St. Louis, Missouri, (Abstract) Vol. 38, 2069
- deGrassie, J.S., W.P. Cary, R.W. Callis, and D.B. Remsen, "4 MW Upgrade to the DIII-D Fast Wave Current Drive System," to be published in Proc. 15th Symp. on Fusion Engineering, IEEE (Hyannis, Massachusetts, October 11-15, 1993); General Atomics Report GA-A21318 (1993).
- DIII-D Team, "Recent DIII-D Results," in Proc. 14th International Conference on Plasma Physics and Controlled Nuclear Fusion Research, September 30 through October 7, 1992, Wurzburg, Germany; Vol. I, p. 41; General Atomics Report GA-A21089 (1992).
- Doyle, E.J., W.A. Peebles, R.A. Moyer, et al., "Comparison of Edge Turbulence Measurements at the L-H Transition on DIII-D," paper presented at the 1993 Annual Meeting of the Division of Plasma Physics, in Bull. 35th Annual American Physical Society Meeting, November 1-5, 1993, St. Louis, Missouri, (Abstract) Vol. 38, 1937.
- Doyle, E.J., C.L. Rettig, K.H. Burrell, P. Gohil, R.J. Groebner, T.K. Kurki-Suonio, R.J. La Haye, R.A. Moyer, T.H. Osborne, W.A. Peebles, R. Philipona, T.L. Rhodes, T.S. Taylor, and J.G. Watkins., "Turbulence and Transport Reduction Mechanisms in the Edge and Interior of DIII-D H-Mode Plasmas," Plasma Phys. and Contr. Nucl. Research 1992, (International Atomic Energy Agency, Vienna, 1993) Vol. 1, 235.
- Duong, H.H., W.W. Heidbrink, E.J. Strait, T.W. Petrie, R. Lee, R.A. Moyer, and J. Watkins, "Loss of Energetic Beam Ions During TAE Instabilities," Nucl. Fusion 33 (1993) 749; General Atomics Report GA-A21038 (1993).

- Evans, T.E., C.J. Lasnier, D.N. Hill, A.W. Leonard, S.I. Lippmann, T.W. Petrie, R. Maingi, A.M. Howald, R.D. Wood, R.A. Moyer, M.J. Schaffer, J.G. Watkins, D.M. Thomas, and J.W. Cuthbertson, "Measurements of Nonaxisymmetric Effects in the DIII-D Scrape-Off Layer and Divertor," in Bull. 35th Annual American Physical Society Meeting, November 1-5, 1993, St. Louis, Missouri, (Abstract) Vol. 38, 2060.
- Ferron, J.R., "User's Manual for the DAD-1 Data Acquisition Daughter Board for the SuperCard-2," General Atomics Report GA-A21236 (1993).
- Ferron, J.R., "User's Manual for the XDC-1 Digitizer Controller," General Atomics Report GA-A21247 (1993).
- Ferron, J.R., L.L. Lao, T.S. Taylor, Y.B. Kim, E.J. Strait, and D. Wroblewski, "Improved Confinement and Stability in the DIII-D Tokamak Obtained Through Modification of the Current Profile," Phys. Fluids B 5, 2532 (1993); General Atomics Report GA-A21151 (1993).
- Ferron, J.R., T.S. Taylor, L.L. Lao, T.H. Osborne, E.J. Strait, A.D. Turnbull, D. Wroblewski, and G. Garstka, "The Effect of Edge Current Density on Confinement and Kink Mode Stability in H-Mode and VH-Mode Discharges," in Bull. 35th Annual American Physical Society Meeting, November 1-5, 1993, St. Louis, Missouri, (Abstract) Vol. 38, 2061.
- Finkenthal, D.F., M.R. Wade, D.L. Hillis, J.T. Hogan, W. Mandel, W.P. West, K.H. Burrell, R.J. Groebner, and R.P. Seraydarian, "Determination of He Density Profiles Using Charge Exchange Recombination Spectroscopy on the DIII-D Tokamak," in Bull. 35th Annual American Physical Society Meeting, November 1-5, 1993, St. Louis, Missouri, (Abstract) Vol. 38, 2071.
- Forest, C.B., "Inductive Effects During Second Harmonic Current Drive Experiments on T-10," in Proc. 10th Top. Conf. on Radio Frequency Power in Plasmas, 1993, Boston, Massachusetts, (American Institute of Physics, New York, 1994) Vol. 289, p. 238; General Atomics Report GA-A21293 (1993).
- Forest, C.B., K. Kupfer, C.C. Petty, R.I. Pinsker, R.W. Harvey, and Y.R. Lin-Liu, "The Effect of Sawteeth Activity on Noninductively Driven Current Profiles," in Bull. 35th Annual American Physical Society Meeting, November 1-5, 1993, St. Louis, Missouri, (Abstract) Vol. 38, 2068.
- Garstka, G.D., J.R. Ferron, T.S. Taylor, L.L. Lao, T.H. Osborne, E.J. Strait, A.D. Turnbull, and D. Wroblewski, "Transport Analysis of High- $\ell_i$  H-Mode Discharges in the DIII-D Tokamak," in Bull. 35th Annual American Physical Society Meeting, November 1-5, 1993, St. Louis, Missouri, (Abstract) Vol. 38, 2007.
- Gohil, P., K.H. Burrell, R.J. Groebner, J. Kim, and R.P. Seraydarian, "The Parametric Dependence of the Spatial Structure of the Radial Electric Field in the DIII-D Tokamak," in Bull. 35th Annual American Physical Society Meeting, November 1-5, 1993, St. Louis, Missouri, (Abstract) Vol. 38, 2063.
- Gohil, P., K.H. Burrell, E.J. Doyle, and R.J. Groebner, "The Phenomenology of the L-H Transition in the DIII-D Tokamak," submitted for publication in Nucl. Fusion; General Atomics Report GA-A21265 (1993).

- Gohil, P., K.H. Burrell, E.J. Doyle, R.J. Groebner, T.H. Osborne, and C.L. Rettig, "The Role of the Radial Electric Field in Confinement and Transport in H-Mode and VH-Mode Discharges in the DIII-D Tokamak," in Proc. Workshop on Local Transport Studies in Fusion Plasma, August 30 through September 3, 1993, Varenna, Italy; General Atomics GA-A21415 (1993).
- Gootgeld, A.M., "Impact of Environmental Regulations on Control of Copper Ion Concentration in the DIII-D Cooling Water System," to be published in Proc. 15th Symp. on Fusion Engineering, IEEE (Hyannis, Massachusetts, October 11-15, 1993); General Atomics Report GA-A21440 (1993).
- Greenfield, C.M., B. Balet, K.H. Burrell, J.G. Cordey, J.C. DeBoo, N. Dellyanakis, E.J. Doyle, G.L. Jackson, S. Konoshima, D.P. O'Brien, L. Porte, C.L. Rettig, T.H. Osborne, A.C.C. Sips, G.M. Staebler, P.M. Stubberfield, and T.S. Taylor, "Comparison of the VH-Mode in DIII-D and JET," in Bull. 35th Annual American Physical Society Meeting, November 1-5, 1993, St. Louis, Missouri, (Abstract) Vol. 38, 1937.
- Groebner, R.J., D.R. Baker, K.H. Burrell, and H. St. John, "Implementation of a Neural Net in Least Squares Analysis of Charge Exchange Recombination Data," in Bull. 35th Annual American Physical Society Meeting, November 1-5, 1993, St. Louis, Missouri, (Abstract) Vol. 38, 2070.
- Groebner, R.J., "An Emerging Understanding of H-Mode Discharges in Tokamaks," Phys. Fluids B 5, 2343 (1993); General Atomics Report GA-A21128 (1992).
- Harris, J.J., and G.L. Campbell, "DIII-D Neutral Beam Control System Operator Interface," to be published in Proc. 15th Symp. on Fusion Engineering, IEEE (Hyannis, Massachusetts, October 11-15, 1993); General Atomics Report GA-A21423 (1993).
- Harris, T.E., and G.L. Campbell, "Operational Upgrades to the DIII-D 60 GHz Electron Cyclotron Resonant Heating System," to be published in Proc. 15th Symp. on Fusion Engineering, IEEE (Hyannis, Massachusetts, October 11-15, 1993); General Atomics Report GA-A21439 (1993).
- Harvey, R.W., C.B. Forest, O. Sauter, J. Lohr, and Y.R. Lin-Liu, "Modification of Electrical Conductivity in T-10 by Electron Cyclotron Heating," in Proc. 10th Top. Conf. on Radio Frequency Power in Plasmas, 1993 Boston, Massachusetts (American Institute of Physics, New York, 1994) Vol. 289, p. 169; General Atomics Report GA-A21292 (1993).
- Harvey, R.W., "Electron Cyclotron Current Drive for Tokamak Reactors," in Bull. 35th Annual American Physical Society Meeting, November 1-5, 1993, St. Louis, Missouri, (Abstract) Vol. 38, 2051.
- Harvey, R.W., M.R. O'Brien, V.V. Rozhdestvenski, T.C. Luce, M.G. McCoy, G.D. Kerbel, "Electron Cyclotron Emission From Non-Thermal Tokamak Plasmas," Phys. Fluids B 5, 446 (1993).
- Hassam, A.B., "Poloidal Rotation of Tokamak Plasmas at Super Poloidal-Sonic Speeds," in Bull. 35th Annual American Physical Society Meeting, November 1-5, 1993, St. Louis, Missouri, (Abstract) Vol. 38, 1925.
- Heidbrink, W.W., R.J. Barron, M.S. Chu, E.J. Strait, and A.D. Turnbull, "Relative Stability of Alfvén Gap Modes," in Bull. 35th Annual American Physical Society Meeting, November 1-5, 1993, St. Louis, Missouri, (Abstract) Vol. 38, 2067.

- Heidbrink, W.W., E.J. Strait, M.S. Chu, and A.D. Turnbull, "Observation of Beta-Induced Alfvén Eigenmodes in the DIII-D Tokamak," *Phys. Rev. Lett.* **71**, 855 (1993); General Atomics Report GA-A21191 (1993).
- Heidbrink, W.W., H.H. Duong, J. Manson, E. Wilfrid, C. Oberman, and E.J. Strait, "The Nonlinear Saturation of Beam-Driven Instabilities: Theory and Experiment," *Phys. Fluids B* **5**, 2176 (1993); General Atomics Report GA-A21168 (1993).
- Henline, P.A., "Use of Open Systems for Control, Analysis, and Data Acquisition of the DIII-D Tokamak," to be published in *Proc. 15th Symp. on Fusion Engineering, IEEE* (Hyannis, Massachusetts, October 11-15, 1993); General Atomics Report GA-A21403 (1993).
- Hill, D.N., A.H. Futch, A.W. Leonard, M.A. Mahdavi, et al., "The Effect of ELMs on Edge Plasma Scaling in DIII-D," *J. Nucl. Materials* **196-198** (1992) 204; General Atomics Report GA-A20962 (1992).
- Hill, D.N., T.W. Petrie, S.L. Allen, J.W. Cuthbertson, C.J. Lasnier, and A.W. Leonard, "A Comparison Between Double-Null and Single-Null Radiative Divertor," in *Bull. 35th Annual American Physical Society Meeting, November 1-5, 1993, St. Louis, Missouri, (Abstract) Vol. 38*, 2060.
- Hill, D.N., T.W. Petrie, S.L. Allen, N.H. Brooks, D. Buchenauer, J. Cuthbertson, T.E. Evans, R.A. Jong, C.J. Lasnier, A.W. Leonard, S.I. Lippmann, M.A. Mahdavi, R. Maingi, R.A. Moyer, G.D. Porter, J.G. Watkins, W.P. West, and R. Wood, "Variation of Divertor Plasma Parameters With Divertor Depth for H-Mode Discharges in DIII-D," in *Proc. 20th European Conference on Controlled Fusion and Plasma Heating, Lisboa, Portugal, 1993, (European Physical Society, Petit-Lancy, Switzerland, 1993) Vol. 17C, Part II, p. 643*; General Atomics Report GA-A21311 (1993).
- Hinton, F.L., "Effect of Orbit Squeezing on Poloidal Rotation in Tokamaks," in *Bull. 35th Annual American Physical Society Meeting, November 1-5, 1993, St. Louis, Missouri, (Abstract) Vol. 38*, 2064.
- Hinton, F.L., J. Kim, Y.B. Kim, A. Brizard, and K.H. Burrell, "Poloidal Rotation Near the Edge of a Tokamak Plasma in H-Mode," *Phys. Rev. Lett.* **72**, 1216 (1994); General Atomics Report GA-A21469 (1993).
- Hollerbach, M.A., R.L. Lee, J.P. Smith, and P.L. Taylor, "Upgrade of the DIII-D Vacuum Vessel Protection System," to be published in *Proc. 15th Symp. on Fusion Engineering, IEEE* (Hyannis, Massachusetts, October 11-15, 1993); General Atomics Report GA-A21417 (1993).
- Holtrop, K.L., "Operation of DIII-D With All-Graphite Walls," to be published in *Proc. 40th Symp. and Topical Conference of the American Vacuum Society, November 15-19, 1993, Orlando, Florida*; General Atomics Report GA-A21487 (1993).
- Hong, R., A.P. Colleraine, D.H. Kellman, J. Kim, et al., "Enhancement of DIII-D Neutral Beam System for Higher Performance," in *Proc. 17th Symp. on Fusion Technology, September 14-18, 1992, Rome, Italy*; General Atomics Report GA-A21034 (1992).
- Hong, R., "Efficiency of Arc Discharge and Beam Extraction of the DIII-D Neutral Beam Ion Source," to be published in *Proc. 15th Symp. on Fusion Engineering, IEEE* (Hyannis, Massachusetts, October 11-15, 1993); General Atomics Report GA-A21391 (1993).

- Hsieh, C, M.S. Chu, J.C. DeBoo, R.R. Dominguez, L.L. Lao, R.E. Stockdale, and T.S. Taylor, "Nonlinear Heat Conduction in Tokamaks," in Bull. 35th Annual American Physical Society Meeting, November 1-5, 1993, St. Louis, Missouri, (Abstract) Vol. 38, 2065.
- Hyatt, A.W., R.J. La Haye, T.H. Jensen, J.T. Scoville, D.R. Baker, and R.J. Groebner, "Applied Magnetic Island Experiments in DIII-D," in Bull. 35th Annual American Physical Society Meeting, November 1-5, 1993, St. Louis, Missouri, (Abstract) Vol. 38, 2062.
- Ikezi, H., and R.I. Pinsky, "Studies of Fast Waves by B-Probe Array in DIII-D," in Bull. 35th Annual American Physical Society Meeting, November 1-5, 1993, St. Louis, Missouri, (Abstract) Vol. 38, 2068.
- Jackson, G.L., C.M. Greenfield, T. Hodapp, K.L. Holtrop, S. Konoshima, M.A. Mahdavi, J.C. Phillips, T.S. Taylor, W.P. West, and J. Winter, "Particle Control During VH-Mode Discharges with an All-Graphite Wall," in Bull. 35th Annual American Physical Society Meeting, November 1-5, 1993, St. Louis, Missouri, (Abstract) Vol. 38, 2062.
- James, R.A., "High  $\beta_p$  Experiments on DIII-D Using Inductive Current Ramps," in Bull. 35th Annual American Physical Society Meeting, November 1-5, 1993, St. Louis, Missouri, (Abstract) Vol. 38, 2066.
- Kellman, D.H., J. Busath, and R. Hong, "Measurement of Electron Temperature and Density in the DIII-D Neutral Beam Ion Source Arc Chamber," to be published in Proc. 15th Symp. on Fusion Engineering, IEEE (Hyannis, Massachusetts, October 11-15, 1993); General Atomics Report GA-A21398 (1993).
- Kessler, D.N., R. Hong, D.H. Kellman, and J.C. Phillips, "Investigation of Collisional Effects Within the Bending Magnet Region of a DIII-D Neutral Beamline," to be published in Proc. 15th Symp. on Fusion Engineering, IEEE (Hyannis, Massachusetts, October 11-15, 1993); General Atomics Report GA-A21428 (1993).
- Kim, J., K.H. Burrell, P. Gohil, R.J. Groebner, Y.B. Kim, H.E. St. John, R. Seraydarian, and M.R. Wade, "Rotation Characteristics of Main Ions and Impurity Ions in H-Mode Tokamak Plasma," to be published in Nucl. Fusion; General Atomics Report GA-A21332 (1993).
- Kim, J., K.H. Burrell, R.J. Groebner, P. Gohil, F.L. Hinton, Y.B. Kim, W. Mandl, R.P. Seraydarian, and M.R. Wade, "Main Ion Rotation Measurement and Its Implications on H-Mode Theories," in Bull. 35th Annual American Physical Society Meeting, November 1-5, 1993, St. Louis, Missouri, (Abstract) Vol. 38, 1937.
- Konoshima, S., T.H. Osborne, G.L. Jackson, W.P. West, C.M. Greenfield, R.D. Wood, D. Whyte, H. Ogawa, R.J. La Haye, E.J. Strait, T.N. Carlstrom, C.L. Rettig, E.J. Doyle, R.T. Snider, G.M. Staebler, and the DIII-D Team, "Effect of Impurities During VH-Mode Discharges and VH-Mode Termination in DIII-D," in Bull. 35th Annual American Physical Society Meeting, November 1-5, 1993, St. Louis, Missouri, (Abstract) Vol. 38, 2062.
- Kupfer, K., "Statistical Approach to Multipass Absorption for Fast Wave Current Drive in Tokamaks," in Bull. 35th Annual American Physical Society Meeting, November 1-5, 1993, St. Louis, Missouri, (Abstract) Vol. 38, 2105.

- Kupfer, K., "Statistical Approach to LHCD Modeling Using the Wave Kinetic Equation," 93 RF Meeting; General Atomics Report GA-A21258 (1993).
- Kurki-Suonio, T., K.H. Burrell, R.J. Groebner, R. Philipona, and C.L. Rettig, "Transport and Fluctuations in the Interior of the DIII-D Plasmas," to be published in Nucl. Fusion (1993); General Atomics Report GA-A21017 (1992).
- La Haye, R.J., C.M. Greenfield, R.J. Groebner, A.W. Hyatt, T.H. Osborne, C.L. Rettig, and J.T. Scoville, "Role of Core Toroidal Rotation Shear on Turbulence and Transport in the Improved Confinement VH-Mode of DIII-D," in Bull. 35th Annual American Physical Society Meeting, November 1-5, 1993, St. Louis, Missouri, (Abstract) Vol. 38, 2062.
- La Haye, R.J., C.M. Greenfield, R.J. Groebner, A.W. Hyatt, L.L. Lao, T.H. Osborne, C.L. Rettig, and J.T. Scoville, "Role of Core Toroidal Rotation Shear on Turbulence and Transport in the Improved Confinement Regimes of the DIII-D Tokamak," in Proc. Workshop on Local Transport Studies in Fusion Plasmas, August 30 through September 3, 1993, Varenna, Italy; General Atomics Report GA-A21431 (1993).
- La Haye, R.J., "Role of Core Toroidal Rotation on the H-Mode Radial Electric Field Shear, Turbulence, and Confinement as Studied by Magnetic Braking in the DIII-D Tokamak," Phys. Plasmas 1, 373 (1994); General Atomics Report GA-A21229 (1993).
- La Haye, R.J., "Limits on  $m = 2$ ,  $n = 1$  Error Field Induced Locked Mode Instability in TPX With Typical Sources of Poloidal Field Coil Error Field and a Prototype Correction Coil, 'C-Coil'," General Atomics Report GA-A21167 (1992).
- La Haye, R.J., R.J. Groebner, A.W. Hyatt, and J.T. Scoville, "Effect of Magnetic Braking of the Plasma Rotation on the H-Mode Radial Electric Field and Energy Confinement in the DIII-D Tokamak," Nucl. Fusion 33, 349 (1993); General Atomics Report GA-A20782 (1992).
- Lao, L.L., J.R. Ferron, T.S. Taylor, V.S. Chan, et al., "Regimes of Improved Confinement and Stability in DIII-D Obtained Through Current Profile Modifications," to be published in Proc. 14th International Conference on Plasma Physics and Controlled Nuclear Fusion Research, September 30 through October 7, 1992, Wurzburg, Germany; General Atomics Report GA-A21053 (1992).
- Lao, L.L., J.R. Ferron, T.S. Taylor, K.H. Burrell, V.S. Chan, M.S. Chu, J.C. DeBoo, E.J. Doyle, C.M. Greenfield, R.J. Groebner, R. James, E.A. Lazarus, T.H. Osborne, H. St. John, E.J. Strait, S.J. Thompson, A.D. Turnbull, D. Wroblewski, H. Zohm, and The DIII-D Team, "High Internal Inductance Improved Confinement H-Mode Discharges Obtained With an Elongation Ramp Technique in the DIII-D Tokamak," to be published in Phys. Rev. Lett.; General Atomics Report GA-A21061 (1993).
- Lao, L.L., R.J. La Haye, D.R. Baker, K.H. Burrell, J.R. Ferron, A.W. Hyatt, G.L. Jackson, E.A. Lazarus, T.H. Osborne, C.L. Rettig, E.J. Strait, T.S. Taylor, and D. Wroblewski, "Role of Rotational Shear on Confinement Enhancement in High  $\ell_i$  H-Mode Discharges," in Bull. 35th Annual American Physical Society Meeting, November 1-5, 1993, St. Louis, Missouri, (Abstract) Vol. 38, 1936.

- Lazarus, E.A., and The DIII-D Team, "Dependence of  $\beta \cdot \tau$  on Plasma Shape in DIII-D," in Proc. 20th European Conference on Controlled Fusion and Plasma Heating, Lisbon, Portugal, 1993, (European Physical Society, Petit-Lancy, Switzerland, 1993) Vol. 17C, Part I, p. 95; General Atomics Report GA-A21306 (1993)
- Lazarus, E.A., A.W. Hyatt, T.H. Osborne, and The DIII-D Team, "A Comparison of Performance for Various Plasma Shapes in DIII-D," in Bull. 35th Annual American Physical Society Meeting, November 1-5, 1993, St. Louis, Missouri, (Abstract) Vol. 38, 1936.
- Lee, R.L., M.A. Hollerbach, K.L. Holtrop, A.G. Kellman, P.L. Taylor, and W.P. West, "Surface Impurity Removal from DIII-D Graphite Tiles by Boron Carbide Grit Blasting," to be published in Proc. 15th Symp. on Fusion Engineering, IEEE (Hyannis, Massachusetts, October 11-15, 1993); General Atomics Report GA-A21426 (1993).
- Leonard, A.W., C.J. Lasnier, M.E. Fenstermacher, D.N. Hill, R.A. Jong, and T.W. Petrie, "Power Flow in the SOL and Divertor Plasmas of DIII-D," in Bull. 35th Annual American Physical Society Meeting, November 1-5, 1993, St. Louis, Missouri, (Abstract) Vol. 38, 2059.
- Lin-Liu, Y.R., "Transport Simulation Study of High  $\ell_i$  H-Mode Sustained by Fast Wave Current Drive on DIII-D" in Bull. 35th Annual American Physical Society Meeting, November 1-5, 1993, St. Louis, Missouri, (Abstract) Vol. 38, 2065.
- Lippmann, S.I., G.T. Sager, P.B. Parks, G.M. Staebler, and W.P. West, "Initial Studies Using a Monte Carlo Impurity Code on DIII-D," in Bull. 35th Annual American Physical Society Meeting, November 1-5, 1993, St. Louis, Missouri, (Abstract) Vol. 38, 2061.
- Lohr, J., and Tony Wong, "Cutoff of Electron Cyclotron Emission as a Probe of Density Fluctuations in the Core of a Tokamak," in Bull. 35th Annual American Physical Society Meeting, November 1-5, 1993, St. Louis, Missouri, (Abstract) Vol. 38, 2069.
- Lohr, J., et al., "On the Second Harmonic Electron Cyclotron Resonance Heating and Current Drive Experiments on T-10 and DIII-D," in Proc. of 8th Joint Workshop on EC Emission and EC Heating, Gut Ising, Max Planck IPP Garching, 1993, Vol. II, p. 497; General Atomics Report GA-A21107 (1993).
- Lohr, J., "Enhanced Confinement Regimes and Control Technology in the DIII-D Tokamak," Plasma Physics and Controlled Fusion Summer School, St. Petersburg, 1993, to be published; General Atomics Report GA-A21342 (1993).
- Luce, T.C., C.C. Petty, R. Prater, R.W. Harvey, et al., "Recent Results From the 60 GHz Inside Launch ECH System on the DIII-D Tokamak," to be published in Proc. 8th Joint Workshop on Electron Cyclotron Emission and Electron Cyclotron Resonance Heating, October 18-21, 1992, Garching, Federal Republic of Germany; General Atomics Report GA-A21134 (1992).
- Luce, T.C., C.B. Forest, M.A. Makowski, C.C. Petty, W.H. Meyer, and C. Janicki, "Evidence for Coupled Transport During Off-Axis ECH," in Proc. Workshop on Local Transport Studies in Fusion Plasmas, August 30 through September 3, 1993, Varenna, Italy; General Atomics Report GA-A21413 (1993).

- Luce, T.C., C.B. Forest, M.A. Makowski, C.C. Petty, W.H. Meyer, and C. Janicki, "Evidence for Coupled Transport During Off-Axis ECH," in Bull. 35th Annual American Physical Society Meeting, November 1-5, 1993, St. Louis, Missouri, (Abstract) Vol. 38, 2065.
- Mahdavi, M.A., S.L. Allen, T.E. Evans, D.N. Hill, et al., "Applications of Divertor Biasing to the Next Generation Tokamaks," General Atomics Report GA-A21064 (1992).
- Mahdavi, M.A., J.R. Ferron, A.W. Hyatt, R.J. La Haye, G.L. Laughon, M. Leh, R. Maingi, M.M. Menon, P.K. Mioduszewski, K.M. Schaubel, M.J. Schaffer, D.P. Schissel, J.T. Scoville, J.P. Smith, R.D. Stambaugh, and M.R. Wade, "Application of Divertor Cryopumping to H-Mode Density Control in DIII-D," to be published in Proc. 15th Symp. on Fusion Engineering, IEEE (Hyannis, Massachusetts, October 11-15, 1993); General Atomics Report GA-A21501 (1993).
- Mahdavi, M.A., J.R. Ferron, R. Maingi, M.M. Menon, M.J. Schaffer, D.P. Schissel, M.R. Wade, and The DIII-D Advanced Divertor Group, "Active Density Control in DIII-D H-Mode Plasmas," in Proc. 20th European Conference on Controlled Fusion and Plasma Heating, Lisbon, Portugal, 1993, (European Physical Society, Petit-Lancy, Switzerland, 1993) Vol. 17C, Part II, p. 747; General Atomics Report GA-A21304 (1993).
- Maingi, R., P.K. Mioduszewski, J.W. Cuthbertson, et al., "Effect of Particle Exhaust on SOL and Divertor Plasma Parameters in DIII-D," paper presented at the 1993 Annual Meeting of the Division of Plasma Physics, abstract published in Bull. 35th Annual American Physical Society Meeting, November 1-5, 1993, St. Louis, Missouri, (Abstract) Vol. 38, 2059.
- Makariou, C.C., R.E. Stockdale, T.N. Carlstrom, C.-L. Hsieh, and G. Bramson, "New Thomson Scattering Laser Control for DIII-D," to be published in Proc. 15th Symp. on Fusion Engineering, IEEE (Hyannis, Massachusetts, October 11-15, 1993); General Atomics Report GA-A21427 (1993).
- Makowski, M.A., T.A. Casper, E.J. Strait, and A.D. Turnbull, "MHD Analysis of High  $\beta_p$  DIII-D Discharges," in Bull. 35th Annual American Physical Society Meeting, November 1-5, 1993, St. Louis, Missouri, (Abstract) Vol. 38, 2066.
- Mandl, W., M.R. Wade, and K.H. Burrell, "Absolute Measurement of Ion Density Profiles as a Function of Time With Charge Exchange Spectroscopy," in Bull. 35th Annual American Physical Society Meeting, November 1-5, 1993, St. Louis, Missouri, (Abstract) Vol. 38, 2071.
- McHarg, Jr., B.B., "Access to DIII-D Data Located in Multiple Files and Multiple Locations," to be published in Proc. 15th Symp. on Fusion Engineering, IEEE (Hyannis, Massachusetts, October 11-15, 1993); General Atomics Report GA-A21404 (1993).
- Menon, M.M., C.B. Baxi, G.L. Campbell, K.L. Holtrop, A.W. Hyatt, G.J. Laughon, R. Maingi, C.C. Makariou, M.A. Mahdavi, E.E. Reis, M.J. Schaffer, K.M. Schaubel, J.T. Scoville, J.P. Smith, R.D. Stambaugh, and M.R. Wade, "Performance Characteristics of the DIII-D Advanced Divertor Cryopump," to be published in Proc. 15th Symp. on Fusion Engineering, IEEE (Hyannis, Massachusetts, October 11-15, 1993); General Atomics Report GA-A21412 (1993).

- Mett, R.R., E.J. Strait, and S.M. Mahajan, "Damping of Toroidal Alfvén Modes in DIII-D," submitted to *Phys. Fluids B*; General Atomics Report GA-A21343 (1993).
- Moyer, R.A., J.G. Watkins, G. Tynan, et al., "Turbulent Particle Transport and the L-H Transition," paper presented at the 1993 Annual Meeting of the Division of Plasma Physics, abstract published in *Bull. 35th Annual American Physical Society Meeting*, November 1-5, 1993, St. Louis, Missouri, (Abstract) Vol. 38, 2063.
- Osborne, T.H., K.H. Burrell, M.S. Chu, J.C. DeBoo, E.J. Doyle, C.M. Greenfield, R.J. Groebner, G.L. Jackson, S. Konoshima, L.L. Lao, C.L. Rettig, G.M. Staebler, E.J. Strait, T.S. Taylor, A.D. Turnbull, D. Wroblewski, and the DIII-D Team, "The Effect of Plasma Shape on VH-Mode Energy Confinement in DIII-D," in *Bull. 35th Annual American Physical Society Meeting*, November 1-5, 1993, St. Louis, Missouri, (Abstract) Vol. 38, 2061.
- Osborne, T.H., K.H. Burrell, T.N. Carlstrom, M.S. Chu, J.C. DeBoo, E.J. Doyle, P. Gohil, C.M. Greenfield, R.J. Groebner, G.L. Jackson, Y.B. Kim, S. Konoshima, R.J. La Haye, L.L. Lao, S.I. Lippmann, C.L. Rettig, R.D. Stambaugh, G.M. Staebler, H. St. John, E.J. Strait, T.S. Taylor, S.J. Thompson, A.D. Turnbull, J. Winter, and D. Wroblewski, "Confinement and Stability of VH-Mode Discharges in the DIII-D Tokamak," submitted for publication to *Nucl. Fusion*; General Atomics Report GA-A21182 (1992).
- Petrach, P.M., A.R. Rouleau, R.D. McNulty, D. Patrick, and J. Walin, "Upgrade of DIII-D Toroidal Magnetic Field Power Supply Controls," to be published in *Proc. 15th Symp. on Fusion Engineering, IEEE* (Hyannis, Massachusetts, October 11-15, 1993); General Atomics Report GA-A21445 (1993).
- Petrie, T.W., and The DIII-D Physics Group, "Radiative Divertor Experiments in DIII-D," in *Bull. 35th Annual American Physical Society Meeting*, November 1-5, 1993, St. Louis, Missouri, (Abstract) Vol. 38, 2071.
- Petty, C.C., T.C. Luce, and R.I. Pinsky, "Gyro-Bohm-Like Transport Scaling With Central RF Heating on the DIII-D Tokamak," in *Bull. 35th Annual American Physical Society Meeting*, November 1-5, 1993, St. Louis, Missouri, (Abstract) Vol. 38, 1938.
- Petty, C.C., "Inward Transport of Energy During Off-Axis Heating on the DIII-D Tokamak," accepted for publication in *Nucl. Fusion*; General Atomics Report GA-A21234 (1993).
- Petty, C.C., "Dimensionally Similar Discharges With Central RF Heating on the DIII-D Tokamak," in *Proc. of 10th Top. Conf. on Radio Frequency Power on Plasmas, 1993*, Boston, Massachusetts, (American Institute of Physics, New York, 1994) Vol. 289, p. 165; General Atomics Report GA-A21257 (1993).
- Phelps, D.A., F. Durodie, and C.P. Moeller, "An Externally Tunable Feedback Controlled TWA," in *Bull. 35th Annual American Physical Society Meeting*, November 1-5, 1993, St. Louis, Missouri, (Abstract) Vol. 38, 2069.
- Phillips, J.C., "Implementation of a Quasi-Realtime Display of DIII-D Neutral Beam Heating Waveforms," to be published in *Proc. 15th Symp. on Fusion Engineering, IEEE* (Hyannis, Massachusetts, October 11-15, 1993); General Atomics Report GA-A21446 (1993).

- Phillips, J.C., C.B. Baxi, and R. Hong, "Investigation of the Heat Handling Capabilities of DIII-D Neutral Beamline Internal Components," to be published in Proc. 15th Symp. on Fusion Engineering, IEEE (Hyannis, Massachusetts, October 11-15, 1993); General Atomics Report GA-A21409 (1993).
- Pinsker, R.I., C.C. Petty, M.J. Mayberry, M. Porkolab, and W.W. Heidbrink, "Observation of Parametric Decay Correlated With Edge Heating Using an Ion Bernstein Wave Antenna on DIII-D," Nucl. Fusion **33**, 777, (1993); General Atomics Report GA-A20820 (1993).
- Pinsker, R.I., "Review of Tokamak Experiments on Direct Electron Heating and Current Drive with Fast Waves," in Proc. 10th Top. Conf. on Radio Frequency Power on Plasmas, 1993, Boston, Massachusetts, (American Institute of Physics, New York, 1994) Vol. 289, p. 179; General Atomics Report GA-A21286 (1993).
- Pinsker, R.I., C.C. Petty, J.S. deGrassie, C.B. Forest, H. Ikezi, Y.R. Lin-Liu, T.C. Luce, M. Porkolab, R. Prater, F.W. Baity, R.H. Goulding, D.J. Hoffman, D.W. Swain, and The DIII-D Group, "Recent Results from the DIII-D Fast Wave Current Drive Experiment," in Bull. 35th Annual American Physical Society Meeting, November 1-5, 1993, St. Louis, Missouri, (Abstract) Vol. **38**, 2068.
- Pinsker, R.I., F.W. Baity, W.P. Cary, R.H. Goulding, and C.C. Petty, "Experimental Test of a Two-Port Decoupler in the DIII-D Fast Wave Current Drive System," to be published in Proc. 15th Symp. on Fusion Engineering, IEEE (Hyannis, Massachusetts, October 11-15, 1993); General Atomics Report GA-A21498 (1993).
- Prater, R., "FWCD and ECCD Experiments on DIII-D," to be published in Proc. International Atomic Energy Research Agency Technical Committee on Radio Frequency Launchers for Current Drive, Naka, Japan; General Atomics Report GA-A21418 (1993).
- Prater, R., "Noninductive Current Drive Experiments on DIII-D, and Future Plans," to be published in Fusion Engineering and Design; General Atomics Report GA-A21525 (1993).
- Prater, R., R.A. James, C.C. Petty, R.I. Pinsker, M. Porkolab, F.W. Baity, S.C. Chiu, J.S. deGrassie, R.H. Goulding, R.W. Harvey, D.J. Hoffmann, H. Ikezi, H. Kawashima, Y.R. Lin-Liu, T.C. Luce, and V. Trukhin, "Current Drive With Fast Waves, Electron Cyclotron Waves, and Neutral Injection in the DIII-D Tokamak," Plasma Physics and Controlled Fusion **35**, A53 (1993); General Atomics Report GA-A21003 (1992).
- Politzer, P.A., "Long-Time Evolution of High  $\beta_p$  Plasmas With Improved Stability and Confinement," in Bull. 35th Annual American Physical Society Meeting, November 1-5, 1993, St. Louis, Missouri, (Abstract) Vol. **38**, 1883.
- Project Staff, "DIII-D Research Operations Annual Report to the U.S. Department of Energy October 1, 1991 through September 30, 1992," General Atomics Report GA-A21186 (1993).
- Project Staff, "Plan for Operation of DIII-D Facilities and Related Research," General Atomics Report GA-A21363 (1993).

- Reis, E., I. Almajan, C.B. Baxi, M.M. Menon, et al., "Design and Analysis of the Cryopump for the DIII-D Advanced Divertor," in Proc. 17th Symp. on Fusion Technology, September 14-18, 1992, Rome, Italy; General Atomics Report GA-A21016 (1992).
- Reis, E.E., E. Chin, A.W. Hyatt, and K. Redler, "Structural Analysis of the TPX Plasma Facing Components," to be published in Proc. 15th Symp. on Fusion Engineering, IEEE (Hyannis, Massachusetts, October 11-15, 1993); General Atomics Report GA-A21407 (1993).
- Remsen, D.B., D.A. Phelps, J.S. deGrassie, W.P. Cary, and R.I. Pinsker, "Feedback Controlled Hybrid Fast Ferrite Tuners," to be published in Proc. 15th Symp. on Fusion Engineering, IEEE (Hyannis, Massachusetts, October 11-15, 1993); General Atomics Report GA-A21381 (1993).
- Rensink, M.E., S.L. Allen, A.H. Futch, D.N. Hill, M.A. Mahdavi, and G.D. Porter, "Particle Transport Studies for Single-Null Divertor Discharges in DIII-D," Phys. Fluids B 5, 2165 (1993); General Atomics Report GA-A20510 (1992).
- Rettig, C.L., W.A. Peebles, K.H. Burrell, R.J. La Haye, E.J. Doyle, R.J. Groebner, and N.C. Luhmann, Jr., "Microturbulence Damping Mechanisms in the DIII-D Tokamak,," Phys. Fluids B 5, 2428 (1993).
- Rettig, C.L., W.A. Peebles, K.H. Burrell, E.J. Doyle, R.J. Groebner, N.C. Luhmann, Jr., and R. Philipona, "Edge Turbulence Reduction at the L-H Transition in DIII-D," Nucl. Fusion 33, 643 (1993).
- Riggs, S.P., and R. Hong, "Beam Species Mix as a Function of DIII-D Neutral Beam Ion Source Operation Parameters," to be published in Proc. 15th Symp. on Fusion Engineering, IEEE (Hyannis, Massachusetts, October 11-15, 1993); General Atomics Report GA-A21437 (1993).
- Sager, G.T., S.I. Lippmann, P.B. Parks, and W.P. West, "Transport Modeling in the Monte Carlo Impurity Code," in Bull. 35th Annual American Physical Society Meeting, November 1-5, 1993, St. Louis, Missouri, (Abstract) Vol. 38, 2061.
- Sauter, O., "Neoclassical Resistivity in Tokamak Geometry With Arbitrary Collisionalities," in Bull. 35th Annual American Physical Society Meeting, November 1-5, 1993, St. Louis, Missouri, (Abstract) Vol. 38, 2076.
- Schaffer, M.J., N.H. Brooks, J.W. Cuthbertson, S.I. Lippmann, M.A. Mahdavi, R. Maingi, M.M. Menon, K. Schaubel, M.R. Wade, and R.D. Wood, "Scrape-Off Layer Flow Enhancement With Divertor Pumping on DIII-D," in Bull. 35th Annual American Physical Society Meeting, November 1-5, 1993, St. Louis, Missouri, (Abstract) Vol. 38, 2058.

- Schaffer, M.J., S.L. Allen, N.H. Brooks, D. Buchenauer, R.B. Campbell, J.W. Cuthbertson, R. Ellis, T.E. Evans, D.F. Finkenthal, A.H. Futch, R.J. Groebner, G.H. Henkel, D.N. Hill, D.L. Hillis, F.L. Hinton, J.T. Hogan, M.A. Hollerbach, W.L. Hsu, A.W. Hyatt, G.L. Jackson, T.R. Jarboe, R. Jong, C.C. Klepper, A.W. Leonard, S.I. Lippmann, M.A. Mahdavi, R. Maingi, M.M. Menon, P.K. Mioduszewski, R.A. Moyer, T.H. Osborne, L.W. Owen, T.W. Petrie, G.D. Porter, M.E. Rensink, T.D. Rognlien, L. Schmitz, D.L. Sevier, J.P. Smith, G.M. Staebler, R.D. Stambaugh, T. Uckan, M.R. Wade, J.G. Watkins, W.P. West, and C.P.C. Wong, "Results From the DIII-D Advanced Divertor Program," in Proc. 9th IAEA Workshop on Stellarators, May 10-14, 1993, Garching, Germany; General Atomics Report GA-A21281 (1993).
- Schaffer, M.J., S. Yamaguchi, and Y. Kondoh, "Preliminary Oscillating Fluxes Current Drive Experiment in DIII-D Tokamak," submitted to Nucl. Fusion (1993); General Atomics Report GA-A20613 (1992).
- Schaffer, M.J., D. Buchenauer, J.W. Cuthbertson, R. Ellis, et al., "Edge Effects During DIII-D Divertor Biasing," General Atomics Report GA-A21060 (1992).
- Schaubel, K.M., C.B. Baxi, G.L. Campbell, G.J. Laughon, M.A. Mahdavi, M.M. Menon, C.C. Makariou, J.P. Smith, and M.J. Schaffer, "The Development of an In-Vessel Cryopump System for the DIII-D Tokamak," in Proc. of 1993 Cryogenic Engineering Conference, July 12-16, 1993, Albuquerque, New Mexico; General Atomics Report GA-A21349 (1993).
- Schaubel, K.M., G.J. Laughon, G.L. Campbell, A.R. Langhorn, N.C. Stevens, and M.L. Tupper, "The DIII-D Cryogenic System Upgrade," to be published in Proc. 15th Symp. on Fusion Engineering, IEEE (Hyannis, Massachusetts, October 11-15, 1993); General Atomics Report GA-A21444 (1993).
- Schissel, D.P., and The H-Mode Database Working Group, "Analysis of the ITER H-Mode Confinement Database," in Proc. 20th European Conference on Controlled Fusion and Plasma Heating, Lisbon, Portugal, 1993, (European Physical Society, Petit-Lancy, Switzerland, 1993) Vol. 17C, Part I, p. 103; General Atomics Report GA-A21310 (1993).
- Schissel, D.P., M.A. Mahdavi, J.C. DeBoo, R. Maingi, and M. Le, "Decoupling the Effect of Plasma Current and Plasma Density on H-Mode Energy Confinement in DIII-D," in Bull. 35th Annual American Physical Society Meeting, November 1-5, 1993, St. Louis, Missouri, (Abstract) Vol. 38, 1938.
- Scoville, B.G., M. Madruga, R.-M. Hong, and J.C. Phillips, "New Conditioning Procedure Derived from Operating Experience with the Common Long-Pulse Ion Source," to be published in Proc. 15th Symp. on Fusion Engineering, IEEE (Hyannis, Massachusetts, October 11-15, 1993); General Atomics Report GA-A21422 (1993).
- Scoville, J.T., and R.J. La Haye, "Locked Mode Beta Limits in Cryopumped DIII-D H-Mode Discharges," in Bull. 35th Annual American Physical Society Meeting, November 1-5, 1993, St. Louis, Missouri, (Abstract) Vol. 38, 2063.
- Seraydarian, R.P., K.H. Burrell, and R.J. Groebner, "Determination of the Absolute Spatial Location of Viewing Chords for a Multichord Spectroscopy Diagnostic by Spectroscopic Means," in Bull. 35th Annual American Physical Society Meeting, November 1-5, 1993, St. Louis, Missouri, (Abstract) Vol. 38, 2070.

- Simonen, T.C., "The Long Range DIII-D Plan," to be published in Proc. Fusion Power Association Annual Meeting, January 28-29, 1993. San Diego, California; General Atomics Report GA-A21213 (1993).
- Smith, J.P., K.M. Schaubel, C.B. Baxi, G.L. Campbell, A.W. Hyatt, A.R. Langhorn, M.A. Mahdavi, E.E. Reis, M.J. Schaffer, D.L. Sevier, and R.D. Stambaugh, "Installation and Initial Operation of the DIII-D Advanced Divertor Cryocondensation Pump," to be published in Proc. 15th Symp. on Fusion Engineering, IEEE (Hyannis, Massachusetts, October 11-15, 1993); General Atomics Report GA-A21396 (1993).
- Snider, R.T., R.J. La Haye, A. Turnbull, and D. Wroblewski, "Modification of the Sawtooth Crash Behavior During Large Error Field Experiments on the DIII-D Tokamak," to be published in Nucl. Fusion (1993); General Atomics Report GA-A21276 (1993).
- Snider, R.T., Y. Kamada, R.J. La Haye, and Y. Mirua, "The Effect of Plasma Rotation and Error Fields on Sawteeth," in Bull. 35th Annual American Physical Society Meeting, November 1-5, 1993, St. Louis, Missouri, (Abstract) Vol. 38, 2063.
- Squire, J.P., J. Lohr, S. Popov, V.M. Trukhin, and A. Vasileev, "High Count Rate X-Ray Spectrometers on DIII-D," in Bull. 35th Annual American Physical Society Meeting, November 1-5, 1993, St. Louis, Missouri, (Abstract) Vol. 38, 2070.
- Staebler, G.M., F.L. Hinton, J.C. Wiley, R.R. Dominguez, C.M. Greenfield, et al., "H- and VH-Modes from Energy, Particle, and Momentum Transport Models," accepted for publication in Phys. Fluids B; General Atomics Report GA-A21278 (1993).
- Staebler, G.M., F.L. Hinton, J.C. Wiley, R.R. Dominguez, C.M. Greenfield, T.H. Osborne, and T.K. Kurki-Suonio, "Theory of VH-Modes," in Bull. 35th Annual American Physical Society Meeting, November 1-5, 1993, St. Louis, Missouri, (Abstract) Vol. 38, 1937.
- St. John, H., J.R. Ferron, L.L. Lao, T.H. Osborne, S.J. Thompson, and D. Wroblewski, "Coupled MHD and Transport Analysis of Improved Confinement DIII-D Discharges," in Proc. 20th European Conference on Controlled Fusion and Plasma Heating, Lisbon, Portugal, 1993, (European Physical Society, Petit-Lancy, Switzerland, 1993) Vol. 17C, Part I, p. 99; General Atomics Report GA-A21309 (1993).
- St. John, H., D. Wroblewski, P.A. Politzer, and S.J. Thompson, "Long Time Evolution Simulation of High  $\beta_p$  Discharges in DIII-D Using MHD/Transport Coupled Calculations," in Bull. 35th Annual American Physical Society Meeting, November 1-5, 1993, St. Louis, Missouri, (Abstract) Vol. 38, 2066
- Strait, E.J., T.S. Taylor, A.D. Turnbull, M.S. Chu, J.R. Ferron, L.L. Lao, and T.H. Osborne, "Beta-Limiting Instabilities in DIII-D Discharges with Large Bootstrap Current," in Proc. 20th European Conference on Controlled Fusion and Plasma Heating, Lisbon, Portugal, 1993, (European Physical Society, Petit-Lancy, Switzerland, 1993) Vol. 17C, Part I, p. 211; General Atomics Report GA-A21301 (1993).
- Strait, E.J., W.W. Heidbrink, A.D. Turnbull, M.S. Chu, and H.H. Duong, "Stability of Neutral Beam-Driven TAE Modes in DIII-D," to be published in Nucl. Fusion; General Atomics Report GA-A21037 (1993).

- Strait, E.J., W.W. Heidbrink, and A.D. Turnbull, "Doppler Shift of the TAE Mode Frequency in DIII-D," to be published in *Plasma Physics and Controlled Fusion; General Atomics Report GA-A21200* (1993).
- Strait, E.J., "Stability of High Beta Tokamak Plasmas," in *Bull. 35th Annual American Physical Society Meeting, November 1-5, 1993, St. Louis, Missouri, (Abstract) Vol. 38, 2098*.
- Taylor, P.L., A.G. Kellman, K. Holtrop, R.L. Lee, and D.A. Humphreys, "DIII-D Disruption Experiments," in *Bull. 35th Annual American Physical Society Meeting, November 1-5, 1993, St. Louis, Missouri, (Abstract) Vol. 38, 2067*.
- Taylor, P.L., A.G. Kellman, and R.L. Lee, "Tritium in the DIII-D Carbon Tiles," in *Proc. International Atomic Energy Agency Technical Meeting on Development in Fusion Safety, June 7-11, 1993, Toronto, Canada; General Atomics Report GA-A21329* (1993).
- Taylor, T.S., A.D. Turnbull, Y.R. Lin-Liu, and H. St. John, "The Second Stable Core Advanced Tokamak Regime," to be submitted to *Phys. Fluids B; General Atomics Report GA-A21385* (1993).
- Taylor, T.S., "Optimized Profiles for Improved Confinement and Stability in Tokamak Discharges," in *Bull. 35th Annual American Physical Society Meeting, November 1-5, 1993, St. Louis, Missouri, (Abstract) Vol. 38, 1936*.
- Thomas, D.M., R.M. Patterson, K.L. Greene, and K.H. Burrell, "Local Studies of Edge Density Changes During the L to H Transition on DIII-D Using LIBEAM," in *Bull. 35th Annual American Physical Society Meeting, November 1-5, 1993, St. Louis, Missouri, (Abstract) Vol. 38, 2064*.
- Thompson, S.J., L.L. Lao, H.E. St. John, J.R. Ferron, T.S. Taylor, and D. Wroblewski, "Profile Analysis of High Performance Discharges in the DII-D Tokamak," in *Bull. 35th Annual American Physical Society Meeting, November 1-5, 1993, St. Louis, Missouri, (Abstract) Vol. 38, 2066*.
- Turnbull, A.D., "Stability Analysis of Advanced Tokamak Configurations," in *Bull. 35th Annual American Physical Society Meeting, November 1-5, 1993, St. Louis, Missouri, (Abstract) Vol. 38, 2065*.
- Turnbull, A.D., "Global Alfvén Modes: Theory and Experiment," *Phys. of Plasmas; General Atomics Report GA-A21138* (1993).
- Vanderlaan, J.F., "CAMAC Throughput of a New RISC-Based Data Acquisition Computer at the DIII-D Tokamak," to be published in *Proc. 15th Symp. on Fusion Engineering, IEEE (Hyannis, Massachusetts, October 11-15, 1993); General Atomics Report GA-A21416* (1993).
- Wade, M.R., D.L. Hillis, J.T. Hogan, D.F. Finkenthal, W.P. West, K.H. Burrell, and R.P. Seraydarian, "Dependence of Helium Transport on Plasma Current and ELM Frequency in H-Mode Discharges in DIII-D," in *Proc. 20th European Conference on Controlled Fusion and Plasma Heating, Lisbon, Portugal, 1993, (European Physical Society, Petit-Lancy, Switzerland, 1993) Vol. 17C, Part I, p. 63; General Atomics Report GA-A21305* (1993).

- Wade, M.R., D.L. Hillis, J.T. Hogan, D.F. Finkenthal, W.P. West, and K.H. Burrell, "Characterization of Helium Transport in ELMing H-Mode Discharge," in Bull. 35th Annual American Physical Society Meeting, November 1-5, 1993, St. Louis, Missouri, (Abstract) Vol. 38, 1936.
- Watkins, J.G., R.A. Moyer, K.H. Burrell, D.A. Buchenauer, J.W. Cuthbertson, T.N. Carlstrom, P. Gohil, D.N. Hill, and D.M. Thomas, "Scrape-Off Layer Scaling in DIII-D," in Bull. 35th Annual American Physical Society Meeting, November 1-5, 1993, St. Louis, Missouri, (Abstract) Vol. 38, 2059.
- Waltz, R.E., and A.H. Boozer, "Local Shear in General Magnetic Stellarator Geometry," Phys. Fluids B 5, 2201 (1993); General Atomics Report GA-A21071 (1993).
- West, W.P., T.W. Petrie, N.H. Brooks, A.M. Howald, D. Whyte, R.D. Wood, S.L. Allen, K. Krieger, S.I. Lippmann, D.N. Hill, "Impurity Containment in the Divertor of DIII-D," in Bull. 35th Annual American Physical Society Meeting, November 1-5, 1993, St. Louis, Missouri, (Abstract) Vol. 38, 2059.
- Whyte, D.G., W.P. West, S.I. Lippmann, W.R. Wade, R.D. Wood, "Core Transport Studies on DIII-D Using Impurity Injection," in Bull. 35th Annual American Physical Society Meeting, November 1-5, 1993, St. Louis, Missouri, (Abstract) Vol. 38, 2064.
- Wong, C.P.C., R.F. Bourue, C.B. Baxi, A.P. Colleraine, V. Del Bene, H. J. Grunloh, S.B. Inamati, D.D. Kapich, J.A. Kissinger, T. Lechtenberg, A.C. Lewis, J.A. Leuer, E.C. Miracle, J.L. Pickering, R. Rao, K. Redler, E.E. Reis, R.H. Ryder, R.W. Schleicher, R.F. Will, "A Robust Helium-Cooled Shield/Blanket Design for ITER," to be published in Proc. 15th Symp. on Fusion Engineering, IEEE (Hyannis, Massachusetts, October 11-15, 1993); General Atomics Report GA-A21485 (1993).
- Wood, R.D., S.I. Lippmann, W.P. West, and D.G. Whyte, "Impurity Measurements in the All Carbon DIII-D Tokamak Using the SPRED Spectrometer," in Bull. 35th Annual American Physical Society Meeting, November 1-5, 1993, St. Louis, Missouri, (Abstract) Vol. 38, 2064.
- Wright, A.L., J.C. Allen, W.P. Cary, and T.E. Harris, "Performance of the DIII-D 110 GHz ECH System During the First Year of Operations and Testing," to be published in Proc. 15th Symp. on Fusion Engineering, IEEE (Hyannis, Massachusetts, October 11-15, 1993); General Atomics Report GA-A21456 (1993).
- Wroblewski, D., and R.T. Snider, "Evidence of the Complete Magnetic Reconnection During an Internal Disruption in a Tokamak," Phys. Rev. Lett. 71, 859 (1993); General Atomics Report GA-A21197 (1993).
- Wroblewski, D., H. St. John, R.A. James, P. Gohil, and B.W. Stallard, "Modeling of the Current Density Profiles in DIII-D," in Bull. 35th Annual American Physical Society Meeting, November 1-5, 1993, St. Louis, Missouri, (Abstract) Vol. 38, 2066.

**DATE**

**FILMED**  
8/4/94

**END**

